AD_____

Award Number: DAMD17-03-1-0012

TITLE: Targeting Microvascular Pericytes in Angiogenic Vessels of Prostate Cancer

PRINCIPAL INVESTIGATOR: Ugur Ozerdem, M.D.

CONTRACTING ORGANIZATION: La Jolla Institute for Molecular Medicine
San Diego, CA 92121

REPORT DATE: April 2006

TYPE OF REPORT: Final

PREPARED FOR: U.S. Army Medical Research and Materiel Command
Fort Detrick, Maryland 21702-5012

REPORT DOCUMENTATION PAGE

Form Approved
OMB No. 0704-0188

1. REPORT DATE	2. REPORT TYPE	3. DATES COVERED
01-04-2006	Final	1 Apr 2003 – 31 Mar 2006

4. TITLE AND SUBTITLE

Targeting Microvascular Pericytes in Angiogenic Vessels of Prostate Cancer

5a. CONTRACT NUMBER

5b. GRANT NUMBER
DAMD17-03-1-0012

5c. PROGRAM ELEMENT NUMBER

6. AUTHOR(S)

Ugur Ozerdem, M.D.

5d. PROJECT NUMBER

5e. TASK NUMBER

5f. WORK UNIT NUMBER

7. PERFORMING ORGANIZATION NAME(S) AND ADDRESS(ES)

La Jolla Institute for Molecular Medicine
San Diego, CA 92121

8. PERFORMING ORGANIZATION REPORT NUMBER

9. SPONSORING / MONITORING AGENCY NAME(S) AND ADDRESS(ES)
U.S. Army Medical Research and Materiel Command
Fort Detrick, Maryland 21702-5012

10. SPONSOR/MONITOR'S ACRONYM(S)

11. SPONSOR/MONITOR'S REPORT NUMBER(S)

12. DISTRIBUTION / AVAILABILITY STATEMENT
Approved for Public Release; Distribution Unlimited

13. SUPPLEMENTARY NOTES
Original contains colored plates: ALL DTIC reproductions will be in black and white.

14. ABSTRACT

The walls of neovascular capillaries in prostate cancer are composed of endothelial cells and pericytes. Pericytes of postnatal pathological neovascularization have dual origin: They derive from bone marrow progenitors (vasculogenesis),or by sprouting from pre-existing vessels (angiogenesis). NG2+ nascent pericytes promote neovascularization and increase interstitial fluid pressure in tumors. The aims of this investigation are to determine whether therapeutic interference with pericyte-NG2 proteoglycan decreases prostate cancer neovascularization, and controls tumor growth. The anti-angiogenic effect of hydron pellets containing NG2 neutralizing antibody was quantified in intracorneal PC-3 and LNCaP xenografts. TRAMP and TRAMP-C1 tumors grafted in NG2 knockout mice represented intrinsic pericyte targeting. TRAMP and TRAMP-C1 grafts were analyzed with confocal microscope for microvascular density (MVD) and lymphatic vascular density (LVD). NG2 neutralizing antibody decreased corneal neovascularization in PC3 ($p<0.0001$), and LNCaP ($p=0.0079$) xenografts. Mean MVD in TRAMP and TRAMP-C1 tumors in NG2 knockout mice were 71% ($p=0.0006$) and 63% ($p=0.0011$) lower than wild type controls, respectively. Mean LVD in TRAMP and TRAMP-C1 tumors in NG2 knockout mice were 73% ($p=0.0003$) and 84% ($p<0.0001$) lower than wild type controls, respectively. Targeting of pericyte-NG2 decreases neovascularization , lymphangiogenesis and tumor progression in prostate cancer significantly.

15. SUBJECT TERMS
angiogenesis, lymphatics, mural cell, neovascularization, NG2, pericyte, prostate, cancer, interstitial fluid pressure, IFP, bone marrow-derived cells

16. SECURITY CLASSIFICATION OF:				18. NUMBER OF PAGES	19a. NAME OF RESPONSIBLE PERSON
					USAMRMC
a. REPORT	b. ABSTRACT	c. THIS PAGE			19b. TELEPHONE NUMBER *(include area code)*
U	U	U	UU	49	

Standard Form 298 (Rev. 8-98)
Prescribed by ANSI Std. Z39.18

Table of Contents

FINAL REPORT-DAMD 17-03-1-0012

This final report outlines the outcome of the research April 1, 2003 through March 31, 2006. All of the goals (specific aims) of the proposed research were successfully completed April 1, 2003 through March 31, 2006.

INTRODUCTION

Prostate cancer is the most common cancer diagnosed in men and is the second leading cause of cancer-related death among men in the United States (Jemal et al., 2005). American Cancer Society statistics project 232,090 new prostate cancer cases for 2005, and that 30,350 patients will die this year. It is therefore imperative to find new therapies for coping with this major health problem. Anti-angiogenic therapy offers an attractive option for the treatment, since tumor progression depends on angiogenesis.

Microvascular wall is composed of two cell types; endothelium and pericyte. The functional role of pericytes in angiogenesis and their potential as anti-angiogenic targets in prostate cancer have only recently drawn attention of investigators. Overall aim of our research supported by DAMD17-03-1-0012 is to establish pericyte and NG2 proteoglycan located on pericyte as novel anti-angiogenic target for treatment of prostate cancer. This overall aim is organized into 3 sub-divisions (tasks) for experimental testing:

1) Analysis of neovasculature in prostate cancer.
2) Demonstrate the feasibility of pericyte-based targeting by investigating the ability of NG2-neutralizing antibody to inhibit angiogenesis in LNCaP and PC-3 prostate cancers grown in nude mouse cornea.
3) Analysis of transgenic adenocarcinoma of mouse prostate (TRAMP) grown in NG2 knockout and wild type mice to elucidate the effect of intrinsic (genetic) targeting of NG2 proteoglycan on pericytes.

OUTCOME OF THE RESEARCH IN THE LIGHT OF THE STATEMENT OF WORK (SOW)

Task 1. Mapping the pericyte/endothelial cell relationship in prostate tumors

Task 1A was accomplished and reported already in a peer-reviewed journal (Ozerdem and Stallcup, 2003). The U.S. Department of Defense Prostate Cancer Research Program's support was accordingly acknowledged in the Acknowledgement section of the publication in the same Journal. Our results have shown extensive contribution of pericytes expressing NG2 and PDGF receptor β-positive pericytes (mural cells) forming the angiogenic sprouts in prostate cancer tissues in mouse models of prostate cancer.

Task 1B. Analysis of vasculature in prostate tumors: Vasculature in LNCaP and PC-3 tumor tissues along with TRAMP tissues were analyzed in more detail. We encountered lymphatic vessels in addition to blood vessels in prostate tumor tissues and therefore expanded the analysis of neovasculature to include lymphangiogenic vessels in Task 3. Immunohistochemical and confocal microscopic analysis of PC-3 and LNCaP, and TRAMP tumors revealed the following findings:

1) NG2+ and PDGF receptor-β+ pericytes invest the endothelium in neovasculature extensively in all three types of prostate tumors studied.
2) All three types of tumors have extensive lymphangiogenic vessels expressing LYVE-1 antigen. Since we encountered extensive lymphangiogenesis in Task 1B, we analyzed not only blood vessel microvascular density but lymphatic vessel density in Task 3 in TRAMP tumors grown in NG2 knockout and wild type mice. These findings were published in The Prostate journal (Ozerdem, 2006). The U.S. Department of Defense Prostate Cancer Research Program's support was accordingly acknowledged in the Acknowledgement section of the publication in the same journal.

Task 2. Anti-angiogenic effects of NG2 antibody on prostate cancer

Establishment of LNCaP and PC-3 prostate tumors in the cornea and analysis (quantification) of extrinsic targeting of pericyte-NG2 in PC-3 and LNCAP tumor xenografts grown in nude mouse cornea.

The cornea is a thin (400 microns), transparent, avascular tissue in which the growth of all new angiogenic vessels generated in response to implanting tumor xenografts can be quantified in a straightforward manner using a stereomicroscope (Kenyon et al., 1996) (Kenyon et al., 1997). In a modification of four established *in vivo* techniques (Muthukkaruppan and Auerbach, 1979) (Kenyon et al., 1996) (Kenyon et al., 1997) (Fernandez et al., 2001) (Ozerdem, 2004), pellets containing anti-NG2 antibody were tested for their ability to inhibit corneal angiogenesis induced by PC-3 or LNCAP tumor fragments. These tests were performed to reveal the extent to which NG2 blockage can slow the angiogenesis that occurs in response to prostate tumors implanted in six-week-old, male, outbred athymic mice (Crl:nu/nu) (Charles River Laboratories, Wilmington, MA).

The surgical procedures for inducing corneal angiogenesis in the mouse (Muthukkaruppan and Auerbach, 1979) (Kenyon et al., 1996) (Kenyon et al., 1997) (Fernandez et al., 2001) are modified to accommodate tumor xenografts and hydron pellets containing either rabbit anti-NG2, or isotype-matched non-immune globulin (control) by making a wider keratotomy incision and a deeper micropocket. Male nude athymic mice (Crl:nu/nu) were obtained from Charles River Laboratories, (Wilmington, MA). Male nude mice (Crl:nu/nu) were obtained from Charles River Laboratories, (Wilmington, MA) and used for inducing PC-3 and LNCAP prostate tumor xenografts.

Hydron pellets (0.4x0.4x0.2 mm) containing the NG2 antibody or control non-immune globulin, and tumor fragment (0.3x0.3x0.3 mm) were implanted in the corneal pocket in male nude mice (Crl:nu/nu). Tumor fragments were prepared from subcutaneous PC-3 or LNCAP prostate tumor xenografts grown in nude mice (total 4 donor mice). Slow-release polyhydroxyethyl methacrylate (hydron) (Hydro Med Sciences, Cranbury, NJ) pellets are formulated to contain 45μg sucrose aluminum sulfate (sucralfate) (Sigma, St.Louis, MO) plus one of two experimental additives: 0.8μg

affinity-purified rabbit anti-NG2 antibody (Ozerdem, 2004) (Ozerdem and Stallcup, 2004) (Ozerdem and Stallcup, 2003), or 0.8 µg isotype-matched non-immune globulin. Six-week-old mice were anesthetized with Avertin (0.015-0.017 ml/g body weight), and under an operating microscope, one pellet and tumor fragment were surgically implanted into the corneal stroma of one eye at a distance of 0.7 mm from the corneo-scleral limbus. Corneal stromal micropockets were created by using a modified von Graefe knife. Treatment pellet and matching control pellet eyes received the tumor fragment from the same donor. Twenty (20) eyes were operated for PC 3 tumor implantation. Ten (10) eyes were operated for LNCAP tumor implantation. On postoperative day 7, angiogenesis was quantified by determining the area of vascularization by using Olympus Stereoscope SZX 12 (Olympus USA, Melville, NY) as described previously (Kenyon et al., 1996) (Kenyon et al., 1997). Hydron pellets containing NG2 neutralizing antibody decreased corneal neovascularization induced by PC3 or LNCaP fragments xenografted in the cornea. Hydron pellets containing NG2 neutralizing antibody decreased significantly corneal neovascularization induced by PC3 tumor xenografts. Mean corneal neovascularization in the treated and control eyes were 0.5341 mm^2 and 2.789 mm^2, respectively (n=20 eyes, $p<0.0001$ Mann Whitney U test)**.** Hydron pellets containing NG2 neutralizing antibody also decreased significantly corneal neovascularization induced by LNCaP tumor xenografts. Mean corneal neovascularization in the treated and control eyes were 0.3393 mm^2 and 3.443 mm^2, respectively (n=10 eyes, p=0.0079 Mann Whitney U test)**.**

Task 3.Analysis of the TRAMP model of prostate cancer

TRAMP prostate tumor fragments and cell lines were verified previously to be transplantable and tumorigenic when implanted in mice with C57BL/6 genetic background (Foster et al., 1997) (Ozerdem and Stallcup, 2003). This tumor transplantation paradigm is similar to transplantation of mouse transgenic mammary tumor fragments in C57BL/6 mouse (Maglione et al., 2004) (Namba et al., 2004) (Ozerdem and Stallcup, 2003). Four, male, 24-week-old TRAMP mice carrying the transgene served as tumor donors for 6-week-old, male NG2 knockout and wild type mice. Four NG2 knockout and 4 wild type control mice were used as recipients. Following a 3-mm skin incision in the dorsum, a 2mm x 2mmx 2mm fragment of tumor was implanted subcutaneously. The skin incision was closed with LiquiVet tissue adhesive (American Health Service, Libertyville, IL). The mice were followed for 3 weeks then sacrificed for tumor retrieval. Seven NG2 knockout and 7 wild type control mice were used for TRAMP-C1 cell line inoculation. TRAMP-C1 cells (5×10^6 cells) were injected subcutaneously in the dorsum. The mice were followed for 3 weeks and sacrificed for tumor retrieval. Tumor tissues were fixed with paraformaldehyde 4% for 6 hours, and then weighed with a Sartorius B120S scale (Sartorius Corporation, Bohemia, NY).

Microscopic In Vivo Lymphangiography in TRAMP mouse

Four, male TRAMP mice (24 week old) carrying the transgene were used for lymphangiography. High molecular weight (two million daltons) dextran conjugated with fluorescein isothiocyanate (Sigma, St. Louis, Missouri) was dissolved in 0.9% saline at

37^{O} C, vortexed, and then centrifuged for 5 minutes until the solution cleared. A custom-made 32 gauge, 3/8 inch, Hamilton needle with a bevel angle of 12 degrees attached to a no.701 syringe (Hamilton, Reno, Nevada) was loaded with 5 µl FITC-dextran solution. Following anesthesia with avertin injection (0.017 ml/g body weight) an inverted Y shaped incision was made on abdominal wall, and the bladder was reflected anteriorly. The tumor mass in the pars dorsalis of prostate was brought into view under an Olympus Fluorescence Stereoscope SZX 12 (Olympus USA, Melville, NY). The needle was then advanced to the core of the tumor, the plunger of the syringe was pulled back transiently to avoid intravascular penetration and 5 µl FITC-dextran solution was injected into the intratumoral interstitium. The needle was withdrawn slowly 30 seconds after injection. The mice were kept alive for 60 minutes and the peritumoral and periaortic region was observed continuously for lymphatic drainage under the fluorescence steromicroscope. In order to keep the tissues humid and increase the quality of imaging, 2% hydroxypropylmethylcellulose in 0.9 % sterile saline solution and glass coverslips (24x50mm) were used to cover the tissue.

Immunohistochemistry, Confocal Microscopic Imaging, and Image Analysis

Tissues were fixed in 4% paraformaldehyde for 6 hours, cryoprotected in 20% sucrose overnight, and frozen in O.C.T. embedding compound (Miles, Inc., Elkhardt, IN). Cryostat sections (40 µm) were air-dried onto Superfrost slides (Fisher Scientific, Pittsburgh, PA). Blood vessel endothelial cells (BEC) were identified using a cocktail of rat antibodies against mouse endoglin (CD105), PECAM-1 (CD31), and VEGF receptor-2 (flk-1) (Pharmingen, San Diego, CA) (Chang et al., 2000) (Ozerdem and Stallcup, 2003) (Ozerdem and Stallcup, 2004) a strategy that was utilized previously to maximize labeling of all blood vessel endothelial cells. Lymphatic endothelium (LEC) was identified by immunolabeling with rabbit anti-mouse LYVE-1 antibody (a generous gift from Dr. Kari Alitalo) as described (Witmer et al., 2004) (Petrova et al., 2004). Pericytes were identified by labeling with rabbit PDGF β-receptor antibody, rabbit antibodies against the NG2 proteoglycan (Ozerdem and Stallcup, 2003) (Ozerdem and Stallcup, 2004; Rajantie et al., 2004), and Cy3-labeled mouse monoclonal (Clone 1A4) antibody against the α-isoform of smooth muscle actin (ASMA) (Catalog number C6198, Sigma, St. Louis, MO). Proliferation index of pericytes were quantified by using bromodeoxyuridine (BrdU) (Catalog number 16880 Sigma-Fluka, St. Louis, MO) assay with intraperitoneal injection of BrdU (80 µg/g body weight) in sterile saline 4 hours prior to sacrifice. Pericytes in S (synthesis) phase of the cell cycle were identified by means of double-immunostaining with sheep-anti BrdU antibody (Catalog number 20-BS17 Fitzgerald Industries, Concord,MA) (Dolbeare et al., 1983) (Dean et al., 1984) (Nowakowski et al., 1989) (Ozerdem and Stallcup, 2004), and ASMA antibody. Frozen sections were digested with 0.005% pepsin (Sigma, St. Louis, MO) in 0.01 HCl for 30 minutes at 37^{0}C followed by treatment with 4N HCl for 30 minutes at room temperature. Sections were then blocked by incubation in 5% goat serum in PBS for 30 minutes (Ezaki et al., 2001; Ozerdem and Stallcup, 2004) prior to incubation with antibody. Immunohistochemical detection of active caspase 3 is a highly specific method for in vivo evaluation of apoptosis (Inai et al., 2004) (Baluk et al., 2004) (Smitherman et al., 2003). Apoptosis index in pericytes was quantified by double-immunostaining with

rabbit polyclonal antibody to activated caspase 3 (Catalog number AF835, R&D Systems, Minneapolis, MN) (Inai et al., 2004) (Baluk et al., 2004) and Cy3-ASMA (Catalog number C6198, Sigma, St. Louis, MO). Following immunostaining slides were mounted with Vectashield (Catalog number 1200, Vector Laboratories, Burlingame, CA).

Following cryosectioning, 5 sections representing the entire thickness of the tumor tissue were selected from the numbered sections by using systematic random sampling (Dawson and Trapp, 2001). These histological sections (220 sections from TRAMP and TRAMP-C1 grafts) were analyzed with a multi-channel laser scanning confocal microscope for microvascular density (MVD) and lymphatic vascular density (LVD). Briefly, optical sections were obtained from the specimens using the Fluoview 1000 laser scanning confocal microscope (Olympus USA, Melville, NY) in the three-channel sequential scanning mode. Serial optical sections (1 μm each) across the entire thickness (40 μm) of the histological specimens were overlaid (Z-stack) to provide reconstructions of entire vessels. This allowed unambiguous identification of the spatial relationship between pericytes and endothelial cells in the vessel wall. The Volocity image analysis software (Openlab-Improvision Inc, Lexington MA) (serial # 88262001) was used for quantification of MVD and LVD. The classifier module of the Volocity software was used to automatically identify MVD or LVD following multi-channel scanning.

Statistical Analysis

Prism 4.0 software (GraphPad, San Diego,CA) was used for statistical analyses. Systematic random sampling of serial histological sections was carried out according to methods described previously (Dawson and Trapp, 2001) (Rajantie et al., 2004). Pericytes were NG2-negative and PDGF β-receptor-positive in NG2 knockout mice, and NG2-positive and PDGF receptor β-positive in the wild type mice in TRAMP and TRAMP-C1 grafts. Mean microvascular density (MVD) in TRAMP and TRAMP-C1 tumors in NG2 knockout mice was 71% ($p=0.0006$) and 63% ($p=0.0011$) lower than wild type controls, respectively.

The average BrdU uptake (proliferation index) by ASMA-positive pericytes in a 4-hour time window in TRAMP tumor grafts in NG2 knockout and wild type mice were 0.66% and 3.13%, respectively ($p=0.0286$). The average BrdU uptake (proliferation index) by ASMA-positive pericytes in a 4-hour time window in TRAMP-C1 tumor grafts in NG2 knockout and wild type mice were 0.50% and 3.46 %, respectively ($p=0.006$). This investigation shows diminished uptake of BrdU by pericytes in NG2 knockout mice in TRAMP and TRAMP-C1 grafts compared to pericytes in wild type mice in TRAMP and TRAMP-C1 grafts. The average apoptosis index in ASMA-positive pericytes in TRAMP tumor grafts in NG2 knockout and wild type mice were 5.07% and 1.57% respectively ($p=0.0571$).The average apoptosis index in ASMA-positive pericytes in TRAMP-C1 tumor grafts in NG2 knockout and wild type mice were 6.30% and 2.25% respectively ($p=0.0262$).

Since there are conflicting reports concerning lymphangiogenesis and prostate cancer (Trojan et al., 2004) (Kaushal et al., 2005) (Zeng et al., 2004), it was necessary to verify the presence of functional lymphatic vessels originating from prostate cancer

tumors, as well as lymphangiogenic potential of de novo tumors before immunohistochemical identification of lymphatic endothelial cells was undertaken in syngeneic TRAMP tumor grafts. In vivo lymphangiography showed evidence of functional lymphatics in prostate (TRAMP) tumor. Mean lymphatic vascular density (LVD) in TRAMP and TRAMP-C1 tumors in NG2 knockout mice was 73% ($p=0.0003$) and 84% ($p<0.0001$) lower than wild type controls, respectively. The TRAMP and TRAMP-C1 tumor grafts grown in NG2 knockout mice were smaller than the grafts grown in wild type mice. The average weight of TRAMP tumor grafts in NG2 knockout and wild type mice were 75.98 mg and 126.3 mg respectively ($p=0.0286$). The average weight of TRAMP-C1 tumor grafts in NG2 knockout and wild type mice were 123.2 mg and 198.4 mg respectively ($p=0.0175$).

KEY RESEARCH ACCOMPLISHMENTS

- We have shown that the contribution of pericytes to neovascular vessels in prostate cancer xenografts and syngeneic grafts is extensive.
- We have shown that genetic (intrinsic) or pharmacological (extrinsic) targeting of pericyte-NG2 proteoglycan decreases neovascularization, lymphangiogenesis and tumor growth in prostate cancer significantly.
- We have shown that pericyte and NG2 proteoglycan are significant targets for prostate cancer therapy.

REPORTABLE OUTCOMES

Targeting of pericytes through NG2 proteoglycan has a significant anti-angiogenic and anti-lymphangiogenic effect in prostate cancer. This effect is mediated by increased apoptosis and decreased proliferation in vascular precursors recruited to prostate cancer stroma.

CONCLUSIONS

This research project, supported by DAMD17-03-1-0012, has shown a significant therapeutic effect of inhibition of pericytes and NG2 proteoglycan in prostate cancer.

REFERENCES

Baluk P, Lee CG, Link H, Ator E, Haskell A, Elias JA, McDonald DM. 2004. Regulated angiogenesis and vascular regression in mice overexpressing vascular endothelial growth factor in airways. Am J Pathol 165:1071-1085.

Chang YS, di Tomaso E, McDonald DM, Jones R, Jain RK, Munn LL. 2000. Mosaic blood vessels in tumors: frequency of cancer cells in contact with flowing blood. Proc Natl Acad Sci U S A 97:14608-14613.

Dawson B, Trapp RG. 2001. Basic and clinical biostatistics. New York: McGraw-Hill. 69-72 pp.

Dean PN, Dolbeare F, Gratzner H, Rice GC, Gray JW. 1984. Cell-cycle analysis using a monoclonal antibody to BrdUrd. Cell Tissue Kinet 17:427-436.

Dolbeare F, Gratzner H, Pallavicini MG, Gray JW. 1983. Flow cytometric measurement of total DNA content and incorporated bromodeoxyuridine. Proc Natl Acad Sci U S A 80:5573-5577.

Ezaki T, Baluk P, Thurston G, La Barbara A, Woo C, McDonald DM. 2001. Time course of endothelial cell proliferation and microvascular remodeling in chronic inflammation. Am J Pathol 158:2043-2055.

Fernandez A, Udagawa T, Schwesinger C, Beecken W, Achilles-Gerte E, McDonnell T, D'Amato R. 2001. Angiogenic potential of prostate carcinoma cells overexpressing bcl-2. J Natl Cancer Inst 93:208-213.

Foster BA, Gingrich JR, Kwon ED, Madias C, Greenberg NM. 1997. Characterization of prostatic epithelial cell lines derived from transgenic adenocarcinoma of the mouse prostate (TRAMP) model. Cancer Res 57:3325-3330.

Inai T, Mancuso M, Hashizume H, Baffert F, Haskell A, Baluk P, Hu-Lowe DD, Shalinsky DR, Thurston G, Yancopoulos GD, McDonald DM. 2004. Inhibition of vascular endothelial growth factor (VEGF) signaling in cancer causes loss of endothelial fenestrations, regression of tumor vessels, and appearance of basement membrane ghosts. Am J Pathol 165:35-52.

Jemal A, Murray T, Ward E, Samuels A, Tiwari RC, Ghafoor A, Feuer EJ, Thun MJ. 2005. Cancer statistics, 2005. CA Cancer J Clin 55:10-30.

Kaushal V, Mukunyadzi P, Dennis RA, Siegel ER, Johnson DE, Kohli M. 2005. Stage-specific characterization of the vascular endothelial growth factor axis in prostate cancer: expression of lymphangiogenic markers is associated with advanced-stage disease. Clin Cancer Res 11:584-593.

Kenyon BM, Browne F, D'Amato RJ. 1997. Effects of thalidomide and related metabolites in a mouse corneal model of neovascularization. Exp Eye Res 64:971-978.

Kenyon BM, Voest EE, Chen CC, Flynn E, Folkman J, D'Amato RJ. 1996. A model of angiogenesis in the mouse cornea. Invest Ophthalmol Vis Sci 37:1625-1632.

Maglione JE, McGoldrick ET, Young LJ, Namba R, Gregg JP, Liu L, Moghanaki D, Ellies LG, Borowsky AD, Cardiff RD, MacLeod CL. 2004. Polyomavirus middle T-induced mammary intraepithelial neoplasia outgrowths: single origin, divergent evolution, and multiple outcomes. Mol Cancer Ther 3:941-953.

Muthukkaruppan V, Auerbach R. 1979. Angiogenesis in the mouse cornea. Science 205:1416-1418.

Namba R, Maglione JE, Young LJ, Borowsky AD, Cardiff RD, MacLeod CL, Gregg JP. 2004. Molecular characterization of the transition to malignancy in a genetically engineered mouse-based model of ductal carcinoma in situ. Mol Cancer Res 2:453-463.

Nowakowski RS, Lewin SB, Miller MW. 1989. Bromodeoxyuridine immunohistochemical determination of the lengths of the cell cycle and the DNA-synthetic phase for an anatomically defined population. J Neurocytol 18:311-318.

Ozerdem U. 2004. Targeting neovascular pericytes in neurofibromatosis type 1. Angiogenesis 7:307-311.

Ozerdem U. 2006. Targeting of pericytes diminishes neovascularization and lymphangiogenesis in prostate cancer. Prostate 66:294-304.

Ozerdem U, Stallcup WB. 2003. Early contribution of pericytes to angiogenic sprouting and tube formation. Angiogenesis 6:241-249.

Ozerdem U, Stallcup WB. 2004. Pathological angiogenesis is reduced by targeting pericytes via the NG2 proteoglycan. Angiogenesis 7:269-276.

Petrova TV, Karpanen T, Norrmen C, Mellor R, Tamakoshi T, Finegold D, Ferrell R, Kerjaschki D, Mortimer P, Yla-Herttuala S, Miura N, Alitalo K. 2004. Defective valves and abnormal mural cell recruitment underlie lymphatic vascular failure in lymphedema distichiasis. Nat Med 10:974-981.

Rajantie I, Ilmonen M, Alminaite A, Ozerdem U, Alitalo K, Salven P. 2004. Adult bone marrow-derived cells recruited during angiogenesis comprise precursors for periendothelial vascular mural cells. Blood 104:2084-2086.

Smitherman AB, Gregory CW, Mohler JL. 2003. Apoptosis levels increase after castration in the CWR22 human prostate cancer xenograft. Prostate 57:24-31.

Trojan L, Michel MS, Rensch F, Jackson DG, Alken P, Grobholz R. 2004. Lymph and blood vessel architecture in benign and malignant prostatic tissue: lack of lymphangiogenesis in prostate carcinoma assessed with novel lymphatic marker lymphatic vessel endothelial hyaluronan receptor (LYVE-1). J Urol 172:103-107.

Witmer AN, Van Blijswijk BC, Van Noorden CJ, Vrensen GF, Schlingemann RO. 2004. In vivo angiogenic phenotype of endothelial cells and pericytes induced by vascular endothelial growth factor-a. J Histochem Cytochem 52:39-52.

Zeng Y, Opeskin K, Baldwin ME, Horvath LG, Achen MG, Stacker SA, Sutherland RL, Williams ED. 2004. Expression of vascular endothelial growth factor receptor-3 by lymphatic endothelial cells is associated with lymph node metastasis in prostate cancer. Clin Cancer Res 10:5137-5144.

APPENDIX

The appendix includes 5 papers (articles) published in the peer-reviewed journals by the principal investigator of the project supported by DAMD17-03-1-0012. The U.S. Department of Defense Prostate Cancer Research Program's support was acknowledged in the acknowledgement section of each publication.

Targeting of Pericytes Diminishes Neovascularization and Lymphangiogenesis in Prostate Cancer

Ugur Ozerdem*

La Jolla Institute for Molecular Medicine, San Diego, California

BACKGROUND. The walls of capillaries in prostate cancer are composed of endothelial cells, and pericytes. NG2 is a transmembrane proteoglycan on nascent pericytes with a functional role in neovascularization.

METHODS. The anti-angiogenic effect of hydron pellets containing NG2 neutralizing antibody was quantified in intracorneal PC-3 and LNCaP xenografts. TRAMP and TRAMP-C1 tumors grafted in NG2 knockout mice represented intrinsic pericyte targeting. TRAMP and TRAMP-C1 grafts were analyzed with confocal microscope for microvascular density (MVD) and lymphatic vascular density (LVD).

RESULTS. NG2 neutralizing antibody decreased corneal neovascularization in PC3 ($P < 0.0001$), and LNCaP ($P = 0.0079$) xenografts. Mean MVD in TRAMP and TRAMP-C1 tumors in NG2 knockout mice were 71% ($P = 0.0006$) and 63% ($P = 0.0011$) lower than wild type controls, respectively. Mean LVD in TRAMP and TRAMP-C1 tumors in NG2 knockout mice were 73% ($P = 0.0003$) and 84% ($P < 0.0001$) lower than wild type controls, respectively.

CONCLUSIONS. Targeting of pericyte-NG2 decreases neovascularization and lymphangiogenesis in prostate cancer significantly. *Prostate 66: 294–304, 2006.* © 2005 Wiley-Liss, Inc.

INTRODUCTION

Prostate cancer is the most common cancer diagnosed in men and is the second leading cause of cancer-related death among men in the United States [1]. American Cancer Society statistics project 232,090 new prostate cancer cases for 2005, and that 30,350 patients will die this year. It is, therefore, imperative to explore novel adjunctive therapies for coping with this major health problem.

Neoplastic progression depends upon the development of neovasculature in and around the tumor [2,3]. The progression of tumor neovascularization is critical to continued tumor progression [4–6]. Anti-neovascular therapy offers an attractive option for treatment of prostate cancer. The potential clinical importance of neovascularization (NV) for prostate cancer patients lies mainly in two areas: (1) prognostic applications based on quantification of microvascular density (MVD) and (2) therapeutic applications based on anti-neovascular therapy [7]. As a prognostic factor, MVD correlates with the clinical, and pathological stage of prostate cancer. MVD is, therefore, a significant predictor of tumor progression and survival following therapy [8–14].

The value of anti-neovascular therapy lies in its ability to target the tumor's circulation. Anti-neovascular therapy may also provide a solution to the problem of drug resistance, a major obstacle to systemic therapies for disseminated cancer. Only a few tumor types are significantly sensitive to chemotherapy [15]. Although a variety of resistance circumvention approaches have

Grant sponsor: US Department of Defense Prostate Cancer Research Program/Congressionally Directed Medical Research New Investigator Award; Grant number: PC020822; Grant sponsor: NIH (National Institute of Child Health and Human Development); Grant number: RO3 HD044783; Grant sponsor: University of California Tobacco-Related Disease Research Program Idea Award (to UO); Grant number: TRDRP 13IT-0067.

*Correspondence to: Ugur Ozerdem, MD, Assistant Professor, La Jolla Institute for Molecular Medicine, 4570 Executive Drive, Suite 100, San Diego, California 92121. E-mail: ozerdem@ljimm.org

Received 24 May 2005; Accepted 9 August 2005
DOI 10.1002/pros.20346
Published online 21 October 2005 in Wiley InterScience (www.interscience.wiley.com).

been attempted, highly effective strategies have yet to be found [15]. One advantage of anti-neovascular drugs for cancer therapy is that their targets may be less susceptible to the mechanisms of acquired drug resistance. The extensive genetic instability and molecular heterogeneity of cancer cells are major driving forces for the evolution of drug-resistance. The overall goals of anti-neovascular therapy, combined with conventional chemotherapy, surgery, radiotherapy, will be to reduce the incidence of drug resistance, minimize the adverse effects of treatment, and increase the overall efficacy of anti-cancer therapy [16,17].

In spite of the promise of anti-neovascular therapy, the limited success of endothelial cell-based strategies to date indicates that targeting of the endothelium alone is insufficient to arrest prostatic tumor growth. This suggests that development of strategies aimed at multiple targets is necessary to maximize the efficacy of anti-neovascular treatment. In this respect, it is critical to note that the walls of neovascular blood vessel capillaries are composed of two principal cell types: vascular endothelial cells (VEC), and Rouget cells [18]. Rouget cells, also known as mural cells or pericytes (*peri* = around, *cyte* = cell) form an outer sheath [19–21] surrounding the endothelial cells on the outer aspect of microvessels [22].

The functional role of vascular pericytes in the formation of neovasculature and tumor stroma is a neglected topic in vascular biology in general and prostate cancer in particular. A recent search of the *PUBMED* database at http://www.ncbi.nlm.nih.gov/ reveals only four papers referring to pericytes in the microvasculature of prostate cancer [23–26]. The functional role of pericytes and their early contribution to proliferation and growth of nascent microvascular sprouts in prostate cancer has been recently investigated [23]. The benefits of targeting pericytes in pathologies involving neovascularization are just beginning to be explored [27–33]. Recent investigations using receptor tyrosine kinase inhibitors revealed promising results to inhibit prostate cancer progression by means of targeting parenchymal, and stromal cells including pericytes [34–37]. Stromal compartment of prostate cancer is, therefore, an important source of cellular therapeutic targets such as pericytes [24,25], VEC, and lymphatic endothelial cells [38].

In this respect, identification of molecules important for the function of pericytes during neovascularization may serve as potential targets for clinical intervention in cases in which vascularization determines the progression of disease. The aims of this investigation are to determine whether therapeutic interference with the function of a key pericyte component, NG2 proteoglycan, inhibits prostate cancer neovascularization, and to examine the angiogenic and lymphangiogenic consequences of NG2 deficiency in prostate cancer vasculature. The effects of NG2 on pericyte function during pathological neovascularization will be examined using two separate mechanisms. The genetic ablation of NG2 in knockout mice represents an ''intrinsic'' pericyte target, whereas the use of anti-NG2 neutralizing antibodies serves as an ''extrinsic'' or pharmacological method of interfering with pericyte-NG2. Both types of studies demonstrate the functional importance of NG2 during neovascularization, establishing the potential value of the proteoglycan as a pericyte-specific target for anti-neovascular and anti-lymphangiogenic therapy in prostate cancer.

MATERIALS AND METHODS

Experimental Animals

NG2 null mice [29,39] were generated via a conventional homologous recombination approach [40,41]. The mice were back-crossed onto a C57BL/6 genetic background and NG2+/− heterozygotes were mated to establish separate male NG2 knockout (NG2−/−) and wild type (NG2+/+) colonies. Decreased neovascularization of the cornea and retina occurs in NG2 knockout mice when challenged with angiogenic growth factors or ischemia, respectively [29]. Breeding pairs of TRAMP (*tr*ansgenic *a*denocarcinoma of *m*ouse *p*rostate) C57BL/6-TgN (TRAMP) 8247Ng mice were obtained from the National Cancer Institute, Mouse Models of Human Cancers Consortium (MMHCC catalog number 01XC6, Frederick, MD). For genotyping, genomic DNA from tail was isolated, and the transgene was identified by PCR as described previously [42]. The mice had been back-crossed at least 10 generations onto the C57BL/6 background at the time of these experiments. Male nude athymic mice (Crl:nu/nu) were obtained from Charles River Laboratories, (Wilmington, MA) and used for inducing PC-3 and LNCaP prostate tumor xenografts.

Cell Lines

LNCaP [43,44] and PC-3 [45] human prostate cancer cell lines, and TRAMP-C1 mouse transgenic adenocarcinoma of prostate cell line derived from C57BL/6-TgN (TRAMP)8247Ng mouse [46] were obtained from American Type Culture Collection (ATCC, Manassas, VA), and cultured in accordance with the manufacturer's suggested cell culture protocols.

Animal Models

All animal studies were performed in accordance with National Institutes of Health Office of Laboratory

Animal Welfare (OLAW) guidelines, and were approved by the La Jolla Institute For Molecular Medicine animal research committee.

Extrinsic targeting of pericyte-NG2 in PC-3 and LNCaP tumor xenografts grown in nude mouse cornea. The cornea is a thin (400 μm), transparent, avascular tissue in which the growth of all new angiogenic vessels generated in response to implanting tumor xenografts can be quantified in a straightforward manner using a stereomicroscope [47,48]. In a modification of four established in vivo techniques [28,29,47–50], pellets containing anti-NG2 antibody were tested for their ability to inhibit corneal angiogenesis induced by PC-3 or LNCaP tumor fragments. These tests were performed to reveal the extent to which NG2 inhibition can slow the neovascularization that occurs in response to prostate tumors implanted in 6-week-old, male, outbred athymic mice (Crl:nu/nu) (Charles River Laboratories).

The surgical procedures for inducing corneal angiogenesis in the mouse were modified in this investigation to accommodate tumor xenografts and hydron pellets containing either rabbit anti-NG2, or isotype-matched non-immune globulin (control) by making a wider keratotomy incision and a deeper micropocket. Hydron pellets ($0.4 \times 0.4 \times 0.2$ mm) containing the NG2 antibody or control non-immune globulin, plus a tumor fragment ($0.3 \times 0.3 \times 0.3$ mm) were implanted in the corneal pocket in male nude mice (Crl:nu/nu). Tumor fragments were prepared from subcutaneous PC-3 or LNCaP prostate tumor xenografts grown in nude mice (total of four donor mice). Slow-release polyhydroxyethyl methacrylate (hydron) (Hydro Med Sciences, Cranbury, NJ) pellets were formulated to contain 45 μg sucrose aluminum sulfate (sucralfate) (Sigma, St. Louis, MO) plus one of two experimental additives: 0.8 μg affinity-purified rabbit anti-NG2 antibody [23,28,29,51,52], or 0.8 μg non-immune globulin. Six-week-old male mice were anesthetized with avertin (0.015–0.017 ml/g body weight), and under an operating microscope, one pellet and tumor fragment were surgically implanted into the corneal stroma of one eye at a distance of 0.7 mm from the corneo-scleral limbus. Corneal stromal micropockets were created by using a modified von Graefe knife. Eyes receiving either the treatment pellet or the matching control pellet were implanted with tumor fragments from the same donor. The eyes of 20 mice received PC-3 tumor implants, and 10 mouse eyes received LNCaP tumor implants. On postoperative day 7, angiogenesis was quantified by determining the area of vascularization using an Olympus Stereoscope SZX 12 (Olympus USA, Melville, NY) as described previously [47,48].

Intrinsic targeting of pericyte-NG2: TRAMP tumor fragment implantation or TRAMP-C1 cell line inoculation in NG2 knockout and wild type mice. TRAMP prostate tumor fragments and cell lines were verified previously to be transplantable and tumorigenic when implanted in mice with C57BL/6 genetic background [23,46]. This tumor transplantation paradigm is similar to transplantation of mouse transgenic mammary tumor fragments in C57BL/6 mouse [23,53,54]. Four, male, 24-week-old TRAMP mice carrying the transgene served as tumor donors for 6-week-old, male NG2 knockout and wild type mice. Four NG2 knockout and four wild type control mice were used as recipients. Following a 3-mm skin incision in the dorsum, a $2 \times 2 \times 2$ mm fragment of tumor was implanted subcutaneously. The skin incision was closed with LiquiVet tissue adhesive (American Health Service, Libertyville, IL). The mice were followed for 3 weeks then sacrificed for tumor retrieval. Seven NG2 knockout and seven wild type control mice were used for TRAMP-C1 cell line inoculation. TRAMP-C1 cells (5×10^6 cells) were injected subcutaneously in the dorsum. The mice were followed for 3 weeks and sacrificed for tumor retrieval. Tumor tissues were fixed with paraformaldehyde 4% for 6 hr, and then weighed with a Sartorius B120S scale (Sartorius Corporation, Bohemia, NY).

Microscopic in vivo lymphangiography in TRAMP mouse. Four, male TRAMP mice (24 week old) carrying the transgene were used for lymphangiography. High-molecular weight (two million Daltons) dextran conjugated with fluorescein isothiocyanate (Sigma) was dissolved in 0.9% saline at 37°C, vortexed, and then centrifuged for 5 min until the solution cleared. A custom-made 32 G, 3/8 inch, Hamilton needle with a bevel angle of 12° attached to a no. 701 syringe (Hamilton, Reno, NV) was loaded with 5 μl FITC-dextran solution. Following anesthesia with avertin injection (0.017 ml/g body weight), an inverted Y shaped incision was made on abdominal wall, and the bladder was reflected anteriorly. The tumor mass in the pars dorsalis of prostate was brought into view under an Olympus Fluorescence Stereoscope SZX 12 (Olympus USA). The needle was then advanced to the core of the tumor, the plunger of the syringe was pulled back transiently to avoid intravascular penetration and 5 μl FITC-dextran solution was injected into the intratumoral interstitium. The needle was withdrawn slowly 30 sec after injection. The mice were kept alive for 60 min and the peritumoral and periaortic region was observed continuously for lymphatic drainage under the fluorescence steromicroscope. In order to keep the tissues humid and increase the quality of imaging, 2% hydroxypropylmethylcellulose in 0.9%

sterile saline solution and glass coverslips (24 × 50 mm) were used to cover the tissue.

Immunohistochemistry, Confocal Microscopic Imaging, and Image Analysis

Tissues were fixed in 4% paraformaldehyde for 6 hr, cryoprotected in 20% sucrose overnight, and frozen in O.C.T. embedding compound (Miles, Inc., Elkhardt, IN). Cryostat sections (40 μm) were air-dried onto Superfrost slides (Fisher Scientific, Pittsburgh, PA). Blood vessel endothelial cells (BEC) were identified using a cocktail of rat antibodies against mouse endoglin (CD105), PECAM-1 (CD31), and VEGF receptor-2 (flk-1) (Pharmingen, San Diego, CA) [23,29,55] a strategy that was utilized previously to maximize labeling of all blood vessel endothelial cells. Lymphatic endothelium (LEC) was identified by immunolabeling with rabbit anti-mouse LYVE-1 antibody (a generous gift from Dr. Kari Alitalo) as described [56,57]. Pericytes were identified by labeling with rabbit PDGF β-receptor antibody, rabbit antibodies against the NG2 proteoglycan [23,28,29], and Cy3-labeled mouse monoclonal (Clone 1A4) antibody against the α-isoform of smooth muscle actin (ASMA) (Catalog number C6198, Sigma). Proliferation index of pericytes were quantified by using bromodeoxyuridine (BrdU) (Catalog number 16880 Sigma-Fluka) assay with intraperitoneal injection of BrdU (80 μg/g body weight) in sterile saline 4 hr prior to sacrifice. Pericytes in S (synthesis) phase of the cell cycle were identified by means of double-immunostaining with sheep-anti BrdU antibody (Catalog number 20-BS17 Fitzgerald Industries, Concord, MA) [29,58–60], and ASMA antibody. Frozen sections were digested with 0.005% pepsin (Sigma) in 0.01 HCl for 30 min at 37°C followed by treatment with 4 N HCl for 30 min at room temperature. Sections were then blocked by incubation in 5% goat serum in PBS for 30 min [29,61] prior to incubation with antibody. Immunohistochemical detection of active caspase 3 is a highly specific method for in vivo evaluation of apoptosis [62–64]. Apoptosis index in pericytes was quantified by double-immunostaining with rabbit polyclonal antibody to activated caspase 3 (Catalog number AF835, R&D Systems, Minneapolis, MN) [62,63] and Cy3-ASMA (Catalog number C6198, Sigma). Following immunostaining slides were mounted with Vectashield (Catalog number 1200, Vector Laboratories, Burlingame, CA).

Following cryosectioning, five sections representing the entire thickness of the tumor tissue were selected from the numbered sections by using systematic random sampling [65]. These histological sections (220 sections from TRAMP and TRAMP-C1 grafts) were analyzed with a multi-channel laser scanning confocal microscope for MVD and lymphatic vascular density (LVD). Briefly, optical sections were obtained from the specimens using the Fluoview 1000 laser scanning confocal microscope (Olympus USA) in the three-channel sequential scanning mode. Serial optical sections (1 μm each) across the entire thickness (40 μm) of the histological specimens were overlaid (Z-stack) to provide reconstructions of entire vessels. This allowed unambiguous identification of the spatial relationship between pericytes and endothelial cells in the vessel wall. The Volocity image analysis software (Openlab-Improvision, Inc, Lexington, MA) (serial no. 88262001) was used for quantification of MVD and LVD. The classifier module of the Volocity software was used to automatically identify MVD or LVD following multi-channel scanning.

Statistical Analysis

Prism 4.0 software (GraphPad, San Diego, CA) was used for statistical analyses. Systematic random sampling of serial histological sections was carried out according to methods described previously [28,65].

RESULTS

Extrinsic Targeting of Pericyte-NG2 Decreases Neovascularization in PC-3 and LNCaP Tumor Xenografts Grown in Nude Mouse Cornea

Hydron pellets containing NG2 neutralizing antibody decreased significantly corneal neovascularization induced by PC3 tumor xenografts. Mean corneal neovascularization in the treated and control eyes were 0.5341 and 2.789 mm^2, respectively ($n = 20$ eyes, $P < 0.0001$ Mann–Whitney *U*-test) (Fig. 1A–C). Hydron pellets containing NG2 neutralizing antibody also decreased significantly corneal neovascularization induced by LNCaP tumor xenografts. Mean corneal neovascularization in the treated and control eyes were 0.3393 and 3.443 mm^2, respectively ($n = 10$ eyes, $P = 0.0079$ Mann–Whitney *U*-test) (Fig. 1D–F).

Intrinsic Targeting of Pericyte-NG2 Decreases Neovascularization and Lymphangiogenesis in TRAMP Tumor Grafts in NG2 Knockout Mouse

Pericytes were NG2-negative and PDGF β-receptor-positive in NG2 knockout mice, and NG2-positive and PDGF receptor β-positive in the wild type mice in TRAMP and TRAMP-C1 grafts. Mean MVD in TRAMP (Fig. 2A–C) and TRAMP-C1 (Fig. 2D–F) tumors in NG2 knockout mice was 71% ($P = 0.0006$) (Fig. 2C) and 63% ($P = 0.0011$) (Fig. 2F) lower than wild type controls, respectively.

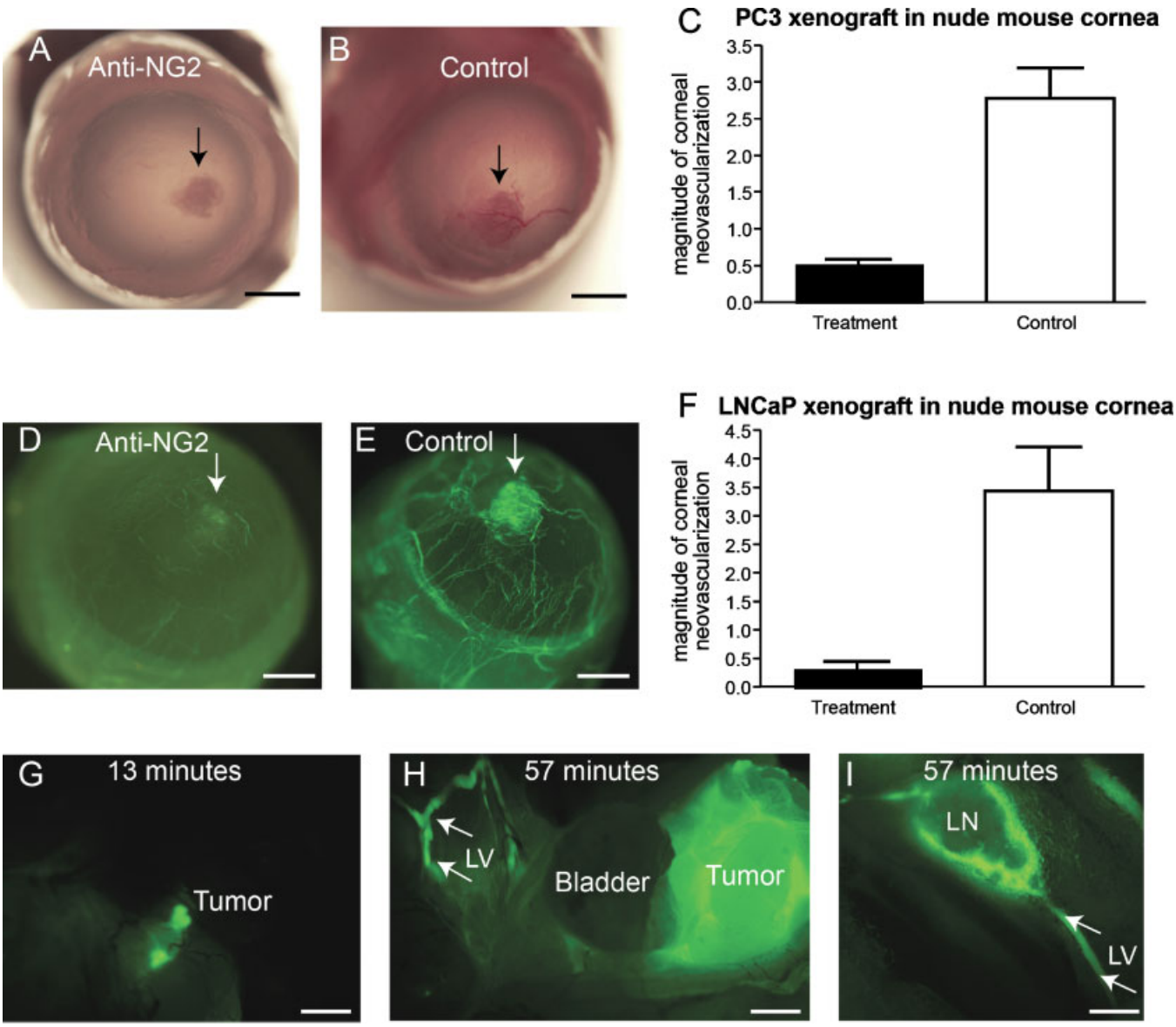

Fig. 1. Hydron pellet containing neutralizing anti-NG2 antibody (**A**) decreases the neovascularization induced by PC-3 tumor fragment compared to hydron pellet containing non-immune globulin (control) (**B**). Mean corneal neovascularization in the treated eyes and control eyes were 0.5341 and 2.789 mm^2, respectively ($n = 20$ eyes, $P < 0.0001$ Mann–Whitney *U*-test) (**C**). Arrows indicate the location of hydron pellet and tumor fragment implanted in the cornea in (A) and (B). Hydron pellet containing neutralizing anti-NG2 antibody (**D**) decreases the neovascularization induced by LNCaP tumor fragment compared to hydron pellet containing non-immune globulin control (**E**). Blood vessels containing FITC-dextran feed the LNCaP fragment more extensively in the control (E). Blood vessels in cornea in (D) and (E) are visualized with fluorescence stereomicroscope following intracardiac (left ventricular) injection of high-molecular weight FITC-dextran and corneal angiography. Mean corneal neovascularization in the treated eyes and control eyes were 0.3393 and 3.443 mm^2, respectively ($n = 10$ eyes, $P = 0.0079$ Mann–Whitney *U*-test) (**F**). In vivo lymphangiography showing evidence of functional lymphatics in prostate (TRAMP) tumor (**G**–**I**). Solution of high-molecular weight (two million Daltons) dextran conjugated with FITC (5 μl) is injected into the core of the tumor. FITC becomes visible in 13 min on the surface of the tumor (G). Within 1 hr FITC becomes visible within lymphatics (LV) and peri-aortic lymph node (LN) (H–I). Arrows in (H) and (I) indicate lymphatic vessel (LV). Scale bars indicate 500 μm in (A, B; D–E), 1 mm in (G–H), and 250 μm in (I) [Color figure can be viewed in the online issue, which is available at www.interscience.wiley.com.].

The average BrdU uptake (proliferation index) by ASMA-positive pericytes in a 4-hr time window in TRAMP tumor grafts in NG2 knockout and wild type mice were 0.66% and 3.13%, respectively ($P = 0.0286$). The average BrdU uptake (proliferation index) by ASMA-positive pericytes in a 4-hr time window in TRAMP-C1 tumor grafts in NG2 knockout and wild type mice were 0.50% and 3.46%, respectively ($P = 0.006$). Figure 3 shows diminished uptake of BrdU by pericytes in NG2 knockout mice in TRAMP (Fig. 3A)

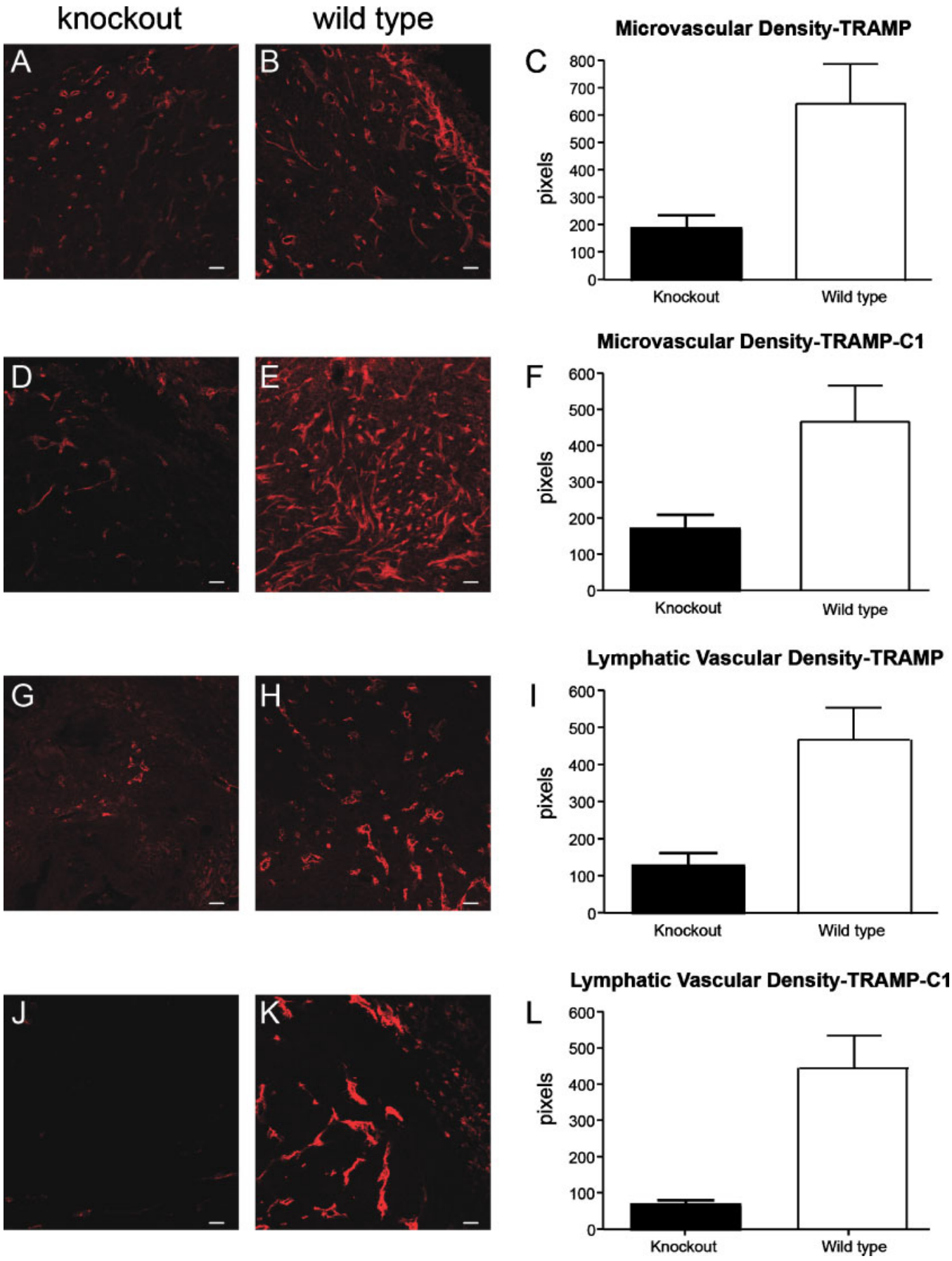
knockout
wild type
A
B
C
Microvascular Density-TRAMP
pixels
800
700
600
500
400
300
200
100
0
Knockout
Wild type
D
E
F
Microvascular Density-TRAMP-C1
pixels
600
500
400
300
200
100
0
Knockout
Wild type
G
H
I
Lymphatic Vascular Density-TRAMP
pixels
600
500
400
300
200
100
0
Knockout
Wild type
J
K
L
Lymphatic Vascular Density-TRAMP-C1
pixels
600
500
400
300
200
100
0
Knockout
Wild type

Fig. 2.

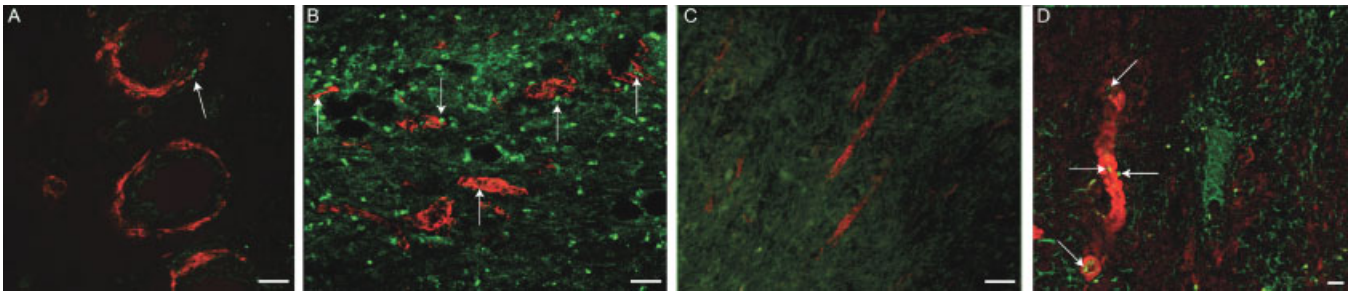

Fig. 3. Bromodeoxyuridine (BrdU) uptake (seen in green) by ASMA-positive pericytes (seen in red) in TRAMP tumor grafts was diminished in NG2 knockout mice (**A**) compared to wild type controls (**B**). The average BrdU uptake (proliferation index) by ASMA-positive pericytes in a 4-hr time window in TRAMP tumor grafts in NG2 knockout and wild type mice were 0.66% and 3.13%, respectively ($P = 0.0286$). Bromodeoxyuridine (BrdU) uptake (seen in green) by ASMA-positive pericytes (seen in red) in TRAMP-CI tumor grafts was diminished in NG2 knockout mice (**C**) compared to wild type controls (**D**). The average BrdU uptake (proliferation index) by ASMA-positive pericytes in a 4-hr time window in TRAMP-CI tumor grafts in NG2 knockout and wild type mice were 0.50% and 3.46%, respectively ($P = 0.006$). Arrows indicate BrdU-positive pericytes immunostained with Cy-3 labeled ASMA antibody. Scale bars indicate 20 μm. [Color figure can be viewed in the online issue, which is available at www.interscience.wiley.com.]

and TRAMP-C1 (Fig. 3C) grafts compared to pericytes in wild type mice in TRAMP (Fig. 3B) and TRAMP-C1 (Fig. 3D) grafts. Arrows in Fig. 3 indicate BrdU-positive/ASMA-positive pericytes. The average apoptosis index in ASMA-positive pericytes in TRAMP tumor grafts in NG2 knockout and wild type mice were 5.07% and 1.57% respectively ($P = 0.0571$).The average apoptosis index in ASMA-positive pericytes in TRAMP-C1 tumor grafts in NG2 knockout and wild type mice were 6.30% and 2.25%, respectively ($P = 0.0262$).

Since there are conflicting reports concerning lymphangiogenesis and prostate cancer [66–68], it was necessary to verify the presence of functional lymphatic vessels originating from prostate cancer tumors, as well as lymphangiogenic potential of *de novo* tumors before immunohistochemical identification of lymphatic endothelial cells was undertaken in syngeneic TRAMP tumor grafts. In vivo lymphangiography showed evidence of functional lymphatics in prostate (TRAMP) tumor (Fig. 1G–I). Mean LVD in TRAMP (Fig. 2G) and TRAMP-C1 (Fig. 2J) tumors in NG2 knockout mice was 73% ($P = 0.0003$) (Fig. 1I) and 84% ($P < 0.0001$) (Fig. 1L) lower than wild type controls (Fig. 2H,K), respectively. The TRAMP and TRAMP-C1 tumor grafts grown in NG2 knockout mice were smaller than the grafts grown in wild type mice. The average weight of TRAMP tumor grafts in NG2 knockout and wild type mice were 75.98 and 126.3 mg, respectively ($P = 0.0286$). The average weight of TRAMP-C1 tumor grafts in NG2 knockout and wild type mice were 123.2 and 198.4 mg, respectively ($P = 0.0175$).

DISCUSSION AND CONCLUSIONS

Therapeutic strategies targeting multiple cell types such as, pericytes, endothelial cells, and tumor cells maximize the efficacy of the anti-tumor treatment [28–31]. Recent investigations using receptor tyrosine kinase inhibitors against multiple cell types and multiple receptors revealed promising results to inhibit prostate cancer progression by targeting stromal and parenchymal cells [34,36,37,69]. Stromal compartment of prostate cancer is, therefore, an important source of cellular therapeutic targets such as pericytes [24,25], VEC, and lymphatic endothelial cells [38]. The results of this study in which hydron pellets were used to target pericyte-NG2 proteoglycan on PC3 and LNCaP tumor xenografts suggest a significant role for pericytes and NG2 proteoglycan in prostate cancer neovascularization, and consequently, as potential therapeutic targets. Given that endothelial cells and pericytes from

Fig. 2. (*Overleaf*) Decreased neovascularization and lymphangiogenesis in TRAMP and TRAMP-CI grafts in the presence of intrinsic inhibition of NG2 proteoglycan. Histological sections of TRAMP and TRAMP-CI tumor grafts grown in NG2 knockout and wild type mouse are immunostained and imaged with scanning laser confocal microscope. Blood vessel endothelium is identified using a cocktail of antibodies against endoglin (CDI05), PECAM-1 (CD31), and VEGF receptor-2 (flk-1) (**A**,**B**,**D**,**E**). Lymphatic endothelium is identified using LYVE-1 antibody (**G**,**H**,**J**,**K**). TRAMP tumor grown in knockout mouse shows decreased neovascular blood vessels (A) and lymphatic vessels (G) compared to wild type control (B) and (H). TRAMP-CI tumor grown in knockout mouse shows decreased neovascular blood vessels (D) and lymphatic vessels (J) compared to wild type control (E) and (K). Intrinsic targeting of NG2 in NG2 knockout mouse decreased microvascular density (MVD) by 71% in TRAMP grafts ($P = 0.0006$ Mann–Whitney *U*-test) (C), and 63% in TRAMP-CI grafts ($P = 0.0011$ Mann–Whitney *U*-test) (**F**). Intrinsic targeting of NG2 in NG2 knockout mouse decreased lymphatic vascular density (LVD) by 73% in TRAMP grafts ($P = 0.0003$ Mann–Whitney *U*-test) (**I**), and 84% in TRAMP-CI grafts ($P < 0.0001$ Mann–Whitney *U* test) (**L**). Scale bars indicate 20 μm. [Color figure can be viewed in the online issue, which is available at www.interscience.wiley.com.]

different tissues and pathological processes are functionally heterogeneous, and diverse in origin as a result of microenvironmental influences [26,70,71], it is likely that the supporting mural cells in prostate cancer are equally diverse in their response to environmental cues. Hence, the prostate tumors inoculated in the cornea [50] and subcutaneous space [72] may partially simulate the neovascularization response that occurs in the prostate gland.

NG2, a membrane-spanning chondroitin sulfate proteoglycan associated with mitotically active, nascent pericytes (PC), exhibits several properties which suggest it is a functional player in neovascularization [23,28,29,51,52,73] and interstitial fluid pressure [74]. NG2 appears to serve as a co-receptor for both bFGF (basic fibroblast growth factor) and PDGF (platelet-derived growth factor) [75,76]. Pericyte-NG2 chondroitin sulfate proteoglycan binds to extracellular matrix components such as type VI, type V, and type II collagen, tenascin, and laminin in the extracellular matrix [77,78]. Biochemical data also demonstrate the involvement of both galectin-3 and $\alpha 3\beta 1$ integrin in the BEC response to pericyte-NG2, and show that NG2, galectin-3, and $\alpha 3\beta 1$ form a complex on the cell surface promoting cell motility [79]. Recent investigations have revealed decreased neovascularization following intrinsic (NG2 knockout mice) or extrinsic (hydron polymer pellets containing NG2 neutralizing antibody) targeting of NG2 proteoglycan in retinal ischemia (retinopathy of prematurity), neurofibromatosis type 1 (NF1), and in bFGF-induced neovascularization in cornea [28,29]. The results of the current study suggest a decreased prostate tumor growth in NG2 knockout mice. Decreased tumor growth is possibly facilitated by decreased MVD induced by decreased pericyte proliferation, and increased pericyte apoptosis in the tumor stroma. Decreased BrdU uptake by NG2-null pericytes in the current study also corroborates a previous study showing diminished BrdU uptake by NG2-null pericytes compared to NG2-wild type controls in retinal neovascularization [29]. In the current study, we use a single intraperitoneal BrdU injection 4 hr prior to tissue retrieval whereas in the retinal neovascularization study [29] we used BrdU injections every day for 4 days prior to tissue retrieval.

Presence of NG2-negative but PDGF β-receptor-positive pericytes in TRAMP and TRAMP-C1 tumors grown in NG2 knockout mice suggest that nascent pericytes in prostate tumor derive from the host tissue (tumor stroma) but not from the tumor parenchyma. This finding corroborates previous investigations elucidating the host origin of pericytes in tumor grafts [23,80,81]. Neovascular pericytes in the host are derived from two sources: pericytes around pre-existing capillaries, and from circulating bone marrow precursors of pericytes (bone marrow hematopoietic and bone marrow mesenchymal progenitor cells) [73]. Inhibition of pericytes through genetic (intrinsic) ablation (i.e., NG2 knockout mouse) in all tissues, including pre-existing capillaries and bone marrow precursors of pericytes, decreases neovascularization significantly. Thus, pericytes and NG2 proteoglycan are potential cellular and molecular anti-neovascular therapeutic targets in prostate cancer.

One intriguing observation is the decreased lymphangiogenesis in TRAMP and TRAMP-C1 tumors grown in NG2 knockout mice. Homing of lymphangiogenic precursors to interstitial tissues and then to lymphangiogenic vessel walls from the blood circulation is open to speculation. Two potential mechanisms that merit further investigation include: attachment between lymphatic precursors and blood vessel wall followed by transmigration of these progenitor cells into the lymphangiogenic vessel wall, or the transdifferentiation of pericytes into lymphatic endothelial cells. Decreased lymphangiogenesis may also be secondary to changes in the extracellular matrix-pericyte interactions that lead to decreased interstitial fluid pressure (IFP). Further studies are warranted to elucidate these possibilities.

In summary, the contribution of pericytes to neovascular vessels in prostate cancer xenografts and syngeneic grafts is extensive. Genetic (intrinsic) or pharmacological (extrinsic) targeting of pericyte-NG2 proteoglycan decreases neovascularization and lymphangiogenesis in prostate cancer significantly. As an adjunct to existing conventional therapeutic modalities, multiple targeting strategies taking pericytes and NG2 proteoglycan into consideration may be useful not only to decrease neovascularization but also modify the stroma of prostate cancer to increase the effectiveness of conventional chemotherapy in refractory tumors.

ACKNOWLEDGMENTS

The author is indebted to NCI Mouse Models of Human Cancers Consortium for providing C57BL/6-TgN (TRAMP) 8247Ng mouse breeders, and Dr. Kari Alitalo for providing LYVE-1 antibody.

REFERENCES

1. Jemal A, Murray T, Ward E, Samuels A, Tiwari RC, Ghafoor A, Feuer EJ, Thun MJ. Cancer statistics, 2005. CA Cancer J Clin 2005;55(1):10–30.
2. Fidler IJ, Ellis LM. The implications of angiogenesis for the biology and therapy of cancer metastasis. Cell 1994;79(2):185–188.
3. Folkman J. How is blood vessel growth regulated in normal and neoplastic tissue? G.H.A. Clowes Memorial Award Lecture. Cancer Res 1986;46(2):467–473.

4. Folkman J. Tumor angiogensis: Role in regulation of tumor growth. Symp Soc Dev Biol 1974;30:43–52.
5. Folkman J, Watson K, Ingber D, Hanahan D. Induction of angiogenesis during the transition from hyperplasia to neoplasia. Nature 1989;339(6219):58–61.
6. Hanahan D, Weinberg RA. The hallmarks of cancer. Cell 2000; 100(1):57–70.
7. Lissbrant IF, Lissbrant E, Damber JE, Bergh A. Blood vessels are regulators of growth, diagnostic markers, and therapeutic targets in prostate cancer. Scand J Urol Nephrol 2001;35(6): 437–452.
8. Brawer MK, Bigler SA, Deering RE. Quantitative morphometric analysis of the microcirculation in prostate carcinoma. J Cell Biochem Suppl 1992:62–64.
9. Brawer MK, Deering RE, Brown M, Preston SD, Bigler SA. Predictors of pathologic stage in prostatic carcinoma. The role of neovascularity. Cancer 1994;73(3):678–687.
10. Weidner N, Carroll PR, Flax J, Blumenfeld W, Folkman J. Tumor angiogenesis correlates with metastasis in invasive prostate carcinoma. Am J Pathol 1993;143(2):401–409.
11. Borre M, Offersen BV, Nerstrom B, Overgaard J. Microvessel density predicts survival in prostate cancer patients subjected to watchful waiting. Br J Cancer 1998;78(7):940–944.
12. Mehta R, Kyshtoobayeva A, Kurosaki T, Small EJ, Kim H, Stroup R, McLaren CE, Li KT, Fruehauf JP. Independent association of angiogenesis index with outcome in prostate cancer. Clin Cancer Res 2001;7(1):81–88.
13. Choy M, Rafii S. Role of angiogenesis in the progression and treatment of prostate cancer. Cancer Invest 2001;19(2): 181–191.
14. Izawa JI, Dinney CP. The role of angiogenesis in prostate and other urologic cancers: A review. CMAJ 2001;164(5):662–670.
15. Goldie JH. Drug resistance in cancer: A perspective. Cancer Metastasis Rev 2001;20(1–2):63–68.
16. Folkman J. Angiogenesis research: From laboratory to clinic. Forum (Genova) 1999;9(3 Suppl 3):59–62.
17. Campbell SC. Advances in angiogenesis research: Relevance to urological oncology. J Urol 1997;158(5):1663–1674.
18. Rouget CMB. Sur la contractilité capillaires sanguins. CR Acad Sci 1879;88:916–918.
19. Sims DE. Recent advances in pericyte biology—implications for health and disease. Can J Cardiol 1991;7(10):431–443.
20. Risau W. Mechanisms of angiogenesis. Nature 1997;386(6626): 671–674.
21. Nehls V, Denzer K, Drenckhahn D. Pericyte involvement in capillary sprouting during angiogenesis in situ. Cell Tissue Res 1992;270(3):469–474.
22. Rhodin JA. Ultrastructure of mammalian venous capillaries, venules, and small collecting veins. J Ultrastruct Res 1968;25(5): 452–500.
23. Ozerdem U, Stallcup WB. Early contribution of pericytes to angiogenic sprouting and tube formation. Angiogenesis 2003; 6(3):241–249.
24. Tuxhorn JA, McAlhany SJ, Dang TD, Ayala GE, Rowley DR. Stromal cells promote angiogenesis and growth of human prostate tumors in a differential reactive stroma (DRS) xenograft model. Cancer Res 2002;62(11):3298–3307.
25. McAlhany SJ, Ressler SJ, Larsen M, Tuxhorn JA, Yang F, Dang TD, Rowley DR. Promotion of angiogenesis by ps20 in the differential reactive stroma prostate cancer xenograft model. Cancer Res 2003;63(18):5859–5865.
26. Eberhard A, Kahlert S, Goede V, Hemmerlein B, Plate KH, Augustin HG. Heterogeneity of angiogenesis and blood vessel maturation in human tumors: Implications for antiangiogenic tumor therapies. Cancer Res 2000;60(5):1388–1393.
27. Baluk P, Hashizume H, McDonald DM. Cellular abnormalities of blood vessels as targets in cancer. Curr Opin Genet Dev 2005; 15(1):102–111.
28. Ozerdem U. Targeting neovascular pericytes in neurofibromatosis type 1. Angiogenesis 2004;7(4):307–311.
29. Ozerdem U, Stallcup WB. Pathological angiogenesis is reduced by targeting pericytes via the NG2 proteoglycan. Angiogenesis 2004;7(3):269–276.
30. Pietras K, Hanahan D. A multitargeted, metronomic, and maximum-tolerated dose ''Chemo-Switch'' regimen is antiangiogenic, producing objective responses and survival benefit in a mouse model of cancer. J Clin Oncol 2005;23(5):939–952.
31. Saharinen P, Alitalo K. Double target for tumor mass destruction. J Clin Invest 2003;111(9):1277–1280.
32. Bergers G, Song S, Meyer-Morse N, Bergsland E, Hanahan D. Benefits of targeting both pericytes and endothelial cells in the tumor vasculature with kinase inhibitors. J Clin Invest 2003; 111(9):1287–1295.
33. Pasqualini R, Arap W, McDonald DM. Probing the structural and molecular diversity of tumor vasculature. Trends Mol Med 2002;8(12):563–571.
34. Kim SJ, Uehara H, Yazici S, Langley RR, He J, Tsan R, Fan D, Killion JJ, Fidler IJ. Simultaneous blockade of platelet-derived growth factor-receptor and epidermal growth factor-receptor signaling and systemic administration of paclitaxel as therapy for human prostate cancer metastasis in bone of nude mice. Cancer Res 2004;64(12):4201–4208.
35. Mathew P, Fidler IJ, Logothetis CJ. Combination docetaxel and platelet-derived growth factor receptor inhibition with imatinib mesylate in prostate cancer. Semin Oncol 2004;31(2 Suppl 6): 24–29.
36. Uehara H, Kim SJ, Karashima T, Shepherd DL, Fan D, Tsan R, Killion JJ, Logothetis C, Mathew P, Fidler IJ. Effects of blocking platelet-derived growth factor-receptor signaling in a mouse model of experimental prostate cancer bone metastases. J Natl Cancer Inst 2003;95(6):458–470.
37. Yazici S, Kim SJ, Busby JE, He J, Thaker P, Yokoi K, Fan D, Fidler IJ. Dual inhibition of the epidermal growth factor and vascular endothelial growth factor phosphorylation for antivascular therapy of human prostate cancer in the prostate of nude mice. Prostate 2005; (in press).
38. Soh S, Ishii T, Sato E, Akishima Y, Ito K, Baba S. Topographic distribution of lymphatic vessels in the normal human prostate. Prostate 2005;63(4):330–335.
39. Grako KA, Ochiya T, Barritt D, Nishiyama A, Stallcup WB. PDGF (alpha)-receptor is unresponsive to PDGF-AA in aortic smooth muscle cells from the NG2 knockout mouse. J Cell Sci 1999;112(Pt 6):905–915.
40. Mansour SL, Thomas KR, Capecchi MR. Disruption of the proto-oncogene int-2 in mouse embryo-derived stem cells: A general strategy for targeting mutations to non-selectable genes. Nature 1988;336(6197):348–352.
41. Capecchi MR. Altering the genome by homologous recombination. Science 1989;244(4910):1288–1292.
42. Greenberg NM, DeMayo F, Finegold MJ, Medina D, Tilley WD, Aspinall JO, Cunha GR, Donjacour AA, Matusik RJ, Rosen JM. Prostate cancer in a transgenic mouse. Proc Natl Acad Sci USA 1995;92(8):3439–3443.

43. Horoszewicz JS, Leong SS, Chu TM, Wajsman ZL, Friedman M, Papsidero L, Kim U, Chai LS, Kakati S, Arya SK, Sandberg AA. The LNCaP cell line–a new model for studies on human prostatic carcinoma. Prog Clin Biol Res 1980;37:115–132.
44. Horoszewicz JS, Leong SS, Kawinski E, Karr JP, Rosenthal H, Chu TM, Mirand EA, Murphy GP. LNCaP model of human prostatic carcinoma. Cancer Res 1983;43(4):1809–1818.
45. Kaighn ME, Narayan KS, Ohnuki Y, Lechner JF, Jones LW. Establishment and characterization of a human prostatic carcinoma cell line (PC-3). Invest Urol 1979;17(1):16–23.
46. Foster BA, Gingrich JR, Kwon ED, Madias C, Greenberg NM. Characterization of prostatic epithelial cell lines derived from transgenic adenocarcinoma of the mouse prostate (TRAMP) model. Cancer Res 1997;57(16):3325–3330.
47. Kenyon BM, Voest EE, Chen CC, Flynn E, Folkman J, D'Amato RJ. A model of angiogenesis in the mouse cornea. Invest Ophthalmol Vis Sci 1996;37(8):1625–1632.
48. Kenyon BM, Browne F, D'Amato RJ. Effects of thalidomide and related metabolites in a mouse corneal model of neovascularization. Exp Eye Res 1997;64(6):971–978.
49. Muthukkaruppan V, Auerbach R. Angiogenesis in the mouse cornea. Science 1979;205(4413):1416–1418.
50. Fernandez A, Udagawa T, Schwesinger C, Beecken W, Achilles-Gerte E, McDonnell T, D'Amato R. Angiogenic potential of prostate carcinoma cells overexpressing bcl-2. J Natl Cancer Inst 2001;93(3):208–213.
51. Ozerdem U, Monosov E, Stallcup WB. NG2 proteoglycan expression by pericytes in pathological microvasculature. Microvasc Res 2002;63(1):129–134.
52. Ozerdem U, Grako KA, Dahlin-Huppe K, Monosov E, Stallcup WB. NG2 proteoglycan is expressed exclusively by mural cells during vascular morphogenesis. Dev Dyn 2001;222(2):218–227.
53. Maglione JE, McGoldrick ET, Young LJ, Namba R, Gregg JP, Liu L, Moghanaki D, Ellies LG, Borowsky AD, Cardiff RD, MacLeod CL. Polyomavirus middle T-induced mammary intraepithelial neoplasia outgrowths: Single origin, divergent evolution, and multiple outcomes. Mol Cancer Ther 2004;3(8):941–953.
54. Namba R, Maglione JE, Young LJ, Borowsky AD, Cardiff RD, MacLeod CL, Gregg JP. Molecular characterization of the transition to malignancy in a genetically engineered mouse-based model of ductal carcinoma in situ. Mol Cancer Res 2004;2(8): 453–463.
55. Chang YS, di Tomaso E, McDonald DM, Jones R, Jain RK, Munn LL. Mosaic blood vessels in tumors: Frequency of cancer cells in contact with flowing blood. Proc Natl Acad Sci USA 2000; 97(26):14608–14613.
56. Witmer AN, Van Blijswijk BC, Van Noorden CJ, Vrensen GF, Schlingemann RO. In vivo angiogenic phenotype of endothelial cells and pericytes induced by vascular endothelial growth factor-α. J Histochem Cytochem 2004;52(1):39–52.
57. Petrova TV, Karpanen T, Norrmen C, Mellor R, Tamakoshi T, Finegold D, Ferrell R, Kerjaschki D, Mortimer P, Yla-Herttuala S, Miura N, Alitalo K. Defective valves and abnormal mural cell recruitment underlie lymphatic vascular failure in lymphedema distichiasis. Nat Med 2004;10(9):974–981.
58. Dolbeare F, Gratzner H, Pallavicini MG, Gray JW. Flow cytometric measurement of total DNA content and incorporated bromodeoxyuridine. Proc Natl Acad Sci USA 1983;80(18):5573–5577.
59. Dean PN, Dolbeare F, Gratzner H, Rice GC, Gray JW. Cell-cycle analysis using a monoclonal antibody to BrdUrd. Cell Tissue Kinet 1984;17(4):427–436.
60. Nowakowski RS, Lewin SB, Miller MW. Bromodeoxyuridine immunohistochemical determination of the lengths of the cell cycle and the DNA-synthetic phase for an anatomically defined population. J Neurocytol 1989;18(3):311–318.
61. Ezaki T, Baluk P, Thurston G, La Barbara A, Woo C, McDonald DM. Time course of endothelial cell proliferation and microvascular remodeling in chronic inflammation. Am J Pathol 2001;158(6):2043–2055.
62. Baffert F, Thurston G, Rochon-Duck M, Le T, Brekken R, McDonald DM. Age-related changes in vascular endothelial growth factor dependency and angiopoietin-1-induced plasticity of adult blood vessels. Circ Res 2004;94(7):984–992.
63. Baluk P, Lee CG, Link H, Ator E, Haskell A, Elias JA, McDonald DM. Regulated angiogenesis and vascular regression in mice overexpressing vascular endothelial growth factor in airways. Am J Pathol 2004;165(4):1071–1085.
64. Smitherman AB, Gregory CW, Mohler JL. Apoptosis levels increase after castration in the CWR22 human prostate cancer xenograft. Prostate 2003;57(1):24–31.
65. Dawson B, Trapp RG. Basic and clinical biostatistics. 3rd edition. New York: McGraw-Hill; 2001. pp 69–72.
66. Trojan L, Michel MS, Rensch F, Jackson DG, Alken P, Grobholz R. Lymph and blood vessel architecture in benign and malignant prostatic tissue: Lack of lymphangiogenesis in prostate carcinoma assessed with novel lymphatic marker lymphatic vessel endothelial hyaluronan receptor (LYVE-1). J Urol 2004;172(1): 103–107.
67. Kaushal V, Mukunyadzi P, Dennis RA, Siegel ER, Johnson DE, Kohli M. Stage-specific characterization of the vascular endothelial growth factor axis in prostate cancer: Expression of lymphangiogenic markers is associated with advanced-stage disease. Clin Cancer Res 2005;11(2 Pt 1):584–593.
68. Zeng Y, Opeskin K, Baldwin ME, Horvath LG, Achen MG, Stacker SA, Sutherland RL, Williams ED. Expression of vascular endothelial growth factor receptor-3 by lymphatic endothelial cells is associated with lymph node metastasis in prostate cancer. Clin Cancer Res 2004;10(15):5137–5144.
69. Mathew P, Thall PF, Jones D, Perez C, Bucana C, Troncoso P, Kim SJ, Fidler IJ, Logothetis C. Platelet-derived growth factor receptor inhibitor imatinib mesylate and docetaxel: A modular phase I trial in androgen-independent prostate cancer. J Clin Oncol 2004;22(16):3323–3329.
70. Lacorre DA, Baekkevold ES, Garrido I, Brandtzaeg P, Haraldsen G, Amalric F, Girard JP. Plasticity of endothelial cells: Rapid dedifferentiation of freshly isolated high endothelial venule endothelial cells outside the lymphoid tissue microenvironment. Blood 2004;103(11):4164–4172.
71. Rajantie I, Ilmonen M, Alminaite A, Ozerdem U, Alitalo K, Salven P. Adult bone marrow-derived cells recruited during angiogenesis comprise precursors for periendothelial vascular mural cells. Blood 2004;104(7):2084–2086.
72. Waters DJ, Janovitz EB, Chan TC. Spontaneous metastasis of PC-3 cells in athymic mice after implantation in orthotopic or ectopic microenvironments. Prostate 1995;26(5):227–234.
73. Ozerdem U, Alitalo K, Salven P, Li A. Contribution of bone marrow-derived pericyte precursor cells to corneal vasculogenesis. Invest Ophthalmol Vis Sci 2005; MS# 05-0309 (in press).
74. Ozerdem U, Hargens AR. A simple method for measuring interstitial fluid pressure in cancer tissues. Microvasc Res 2005; (in press).
75. Goretzki L, Burg MA, Grako KA, Stallcup WB. High-affinity binding of basic fibroblast growth factor and platelet-derived

growth factor-AA to the core protein of the NG2 proteoglycan. J Biol Chem 1999;274(24):16831–16837.

76. Grako KA, Stallcup WB. Participation of the NG2 proteoglycan in rat aortic smooth muscle cell responses to platelet-derived growth factor. Exp Cell Res 1995;221(1):231–240.
77. Tillet E, Ruggiero F, Nishiyama A, Stallcup WB. The membrane-spanning proteoglycan NG2 binds to collagens V and VI through the central nonglobular domain of its core protein. J Biol Chem 1997;272(16):10769–10776.
78. Burg MA, Tillet E, Timpl R, Stallcup WB. Binding of the NG2 proteoglycan to type VI collagen and other extracellular matrix molecules. J Biol Chem 1996;271(42):26110–26116.
79. Fukushi J, Makagiansar IT, Stallcup WB. NG2 proteoglycan promotes endothelial cell motility and angiogenesis via engagement of galectin-3 and alpha3beta1 integrin. Mol Biol Cell 2004;15(8):3580–3590.
80. Abramsson A, Berlin O, Papayan H, Paulin D, Shani M, Betsholtz C. Analysis of mural cell recruitment to tumor vessels. Circulation 2002;105(1):112–117.
81. Yang M, Baranov E, Wang JW, Jiang P, Wang X, Sun FX, Bouvet M, Moossa AR, Penman S, Hoffman RM. Direct external imaging of nascent cancer, tumor progression, angiogenesis, and metastasis on internal organs in the fluorescent orthotopic model. Proc Natl Acad Sci USA 2002;99(6):3824–3829.

Available online at www.sciencedirect.com

SCIENCE DIRECT

Microvascular Research 70 (2005) 116 – 120

Microvascular Research

www.elsevier.com/locate/ymvre

Short Communication

A simple method for measuring interstitial fluid pressure in cancer tissues

Ugur Ozerdem[a,*], Alan R. Hargens[b]

[a]La Jolla Institute for Molecular Medicine, 4570 Executive Drive, Suite 100, San Diego, California 92121, USA
[b]Orthopaedic Surgery, University of California San Diego, USA

Received 27 May 2005; revised 27 June 2005; accepted 15 July 2005
Available online 31 August 2005

Abstract

A novel procedure using a polyurethane transducer-tipped catheter (Millar) is described that allows reliable measurement of interstitial fluid pressure (IFP) in cancer tissues. Before and after each use, the transducer is calibrated at 37°C by a water column. After calibration, the transducer is passed through the lumen of a surgical needle. The sensor is kept in the lumen of the needle during penetration into the tumor. The sensor tip is then introduced into the center core of the tumor as the needle sleeve is withdrawn from the tumor surface. Our new technique is simple and provides IFPs equal to those provided by the well-established, wick-in-needle technique. Using our new technique, we compared IFP in skin melanoma grafts in NG2 knockout and wild–type mice. Knocking out NG2 proteoglycan on vasculogenic and angiogenic pericytes reduced interstitial fluid pressure in melanoma from +4.9 cm H_2O to −0.4 cm H_2O ($P = 0.0054$ Mann–Whitney U test).

Keywords: Cancer; Pericyte; NG2; Interstitial; Fluid; Pressure; Targeting; Wick-in-needle

Introduction

When a piece of bark is peeled off a transpiring tree and a cut is made in the xylem, no sap runs out; in fact, a drop of water placed on the cut is drawn in for the sap is under negative pressure. Similarly, when the subcutaneous tissue of an animal is exposed, fluid does not seep out since the interstitial fluid is under negative pressure. In normal subcutaneous tissue, the interstitial fluid pressure (IFP) is negative (Scholander et al., 1968). By contrast, IFP is often increased in tumor tissue (Young et al., 1950) and forms a barrier against efficient drug delivery into the tumor (Jain, 1987a,b). There are several techniques described for IFP measurements, all of which require experience to use ramified instrumentation and surgical procedures. They include: wick catheter (Scholander et al., 1968; Hargens, 1981; Mubarak and Hargens, 1981), modified wick technique (wick-in-needle technique) (Fadnes et al., 1977; Wiig et al., 1987), servo-micropipette (Wiederhielm et al., 1964) for acute studies of IFP, and subcutaneous capsule implantation for 4–6 weeks (Guyton, 1963) allowing chronic tests of IFP.

Here, we describe a simplified procedure using a transducer-tipped catheter and a precision glide needle that allows reliable measurement of IFP in tumor tissues. We believe this technique will allow the researchers in the vascular biology field and clinicians in the oncology field to apply IFP measurement easily as a useful tool in research.

Materials and methods

In order to compare and validate the pressures obtained with the miniature pressure transducer with a well-established, conventional method (0.6 mm wick-in-needle) (Fadnes et al., 1977; Wiig et al., 1987), we simultaneously compared a needle-guided Millar SPC 320, 2F Mikro-Tip sensor (http://www.millarinstruments.com) and wick-in-needle probes side-by-side in a pilot study in two mice (C57BL/6) bearing B16F1 skin tumor grafts. For wick-in-needle technique, a 0.6 mm needle was provided with a 2-mm-long side hole 2 mm from the tip. The edges of the side

* Corresponding author. Fax: +1 858 587 6742.
E-mail address: ozerdem@LJIMM.org (U. Ozerdem).

0026-2862/$ - see front matter © 2005 Elsevier Inc. All rights reserved.
doi:10.1016/j.mvr.2005.07.003

Fig. 1. Interstitial fluid pressure measurement with ultraminiature pressure transducer. (A) The ultraminiature transducer (arrow) is introduced percutaneously 1 mm through the tumor capsule into the superficial tumor in a protective metal guide (18-gauge needle) (arrowhead). (B) The metal guide is withdrawn slowly, while the sensor is introduced into the center of the tumor. The location of the center of the tumor is estimated by dividing the caliper-measured diameter of tumor in half. The transducer can be marked for millimeter gradation using standard fine point pens (not shown in this picture). (C) Handling of the needle guide and transducer is very easy during microsurgical procedures on mice. Scale bar = 600 μm.

hole were polished with a sharpening stone. Strands of nylon fibers were pulled into the needle. The needle was connected to a P23XL pressure transducer (serial number 10153923, Spectramed, Oxnard, CA) by means of a polyethylene tube. The P23XL transducer was connected to a Windograf Model 40-8474 amplifier (serial number 1463, Gould Inc., Valley View, OH). The polyethylene tube and needle were filled with 0.9% saline through another port on the side of the Plexiglas dome of the transducer. Care was taken to prevent air bubbles within the entire system. Zero reference pressure was obtained after placing the needle at the level of needle insertion. Following anesthesia, the needle-guided miniature transducer and wick-in-needle were introduced parallel into the tumor 3 mm apart from one another. The averages of two simultaneous readings for miniature transducer and wick-in-needle were comparable and 9.2 and 9.0 cm H_2O, respectively.

We used an ultraminiature transducer-tipped catheter in which the sensor is side-mounted at the tip: SPC-320 transducer (2 French size, 0.66 mm in diameter) and an 18-gauge, 1.5-in. precision glide needle (Fig. 1). Ultraminiature transducer tipped catheter, TC-510 Control unit, adapter cables, and TAM-D amplifier modules were purchased from Harvard Apparatus (Holliston, MA). All animal studies were performed in accordance with National Institutes of Health Office of Laboratory Animal Welfare (OLAW) guidelines and were approved by the La Jolla Institute For Molecular Medicine animal research committee. NG2 null mice (Grako et al., 1999) were generated via a conventional homologous recombination approach (Mansour et al., 1988; Capecchi, 1989). The mice were back-crossed onto a C57BL/6 genetic background and NG2+/− heterozygotes were mated to establish separate male NG2 knockout (NG2−/−) and wild type (NG2+/+) colonies (Ozerdem and Stallcup, 2004). B16F1 mouse melanoma cells (American Type Culture Collection, Manassas, VA) (5×10^6 cells) were inoculated subcutaneously in the dorsum. The mice were followed for 2 weeks. Following anesthesia with intraperitoneal avertin injection (0.017 ml/g body weight), the size of the tumor in mouse is measured with a caliper. Then, the distance between the skin surface and the center core of the tumor is estimated. Before each use, the transducer is calibrated for accuracy by using a distilled water column at 37°C (Fig. 2A). Calibration in the water column (Fig. 2A) (before and after IFP measurements in tumors) revealed a positive and linear correlation between the transducer output (mV) and pressure (cm H_2O) of the miniature transducer (Fig. 2B). After calibration, the trans-

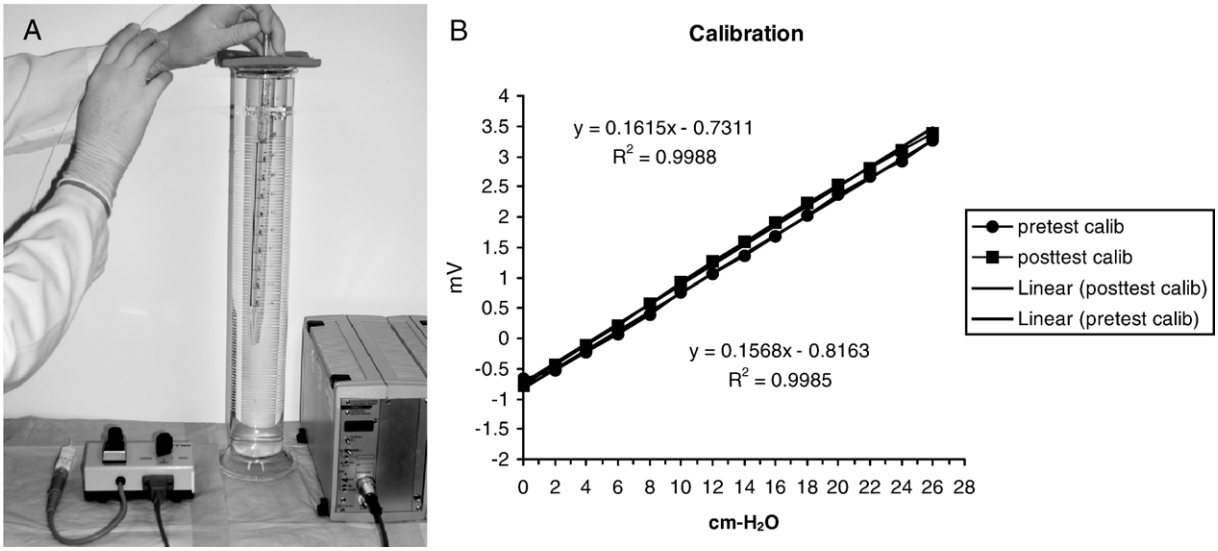

Fig. 2. Calibration of the miniature transducer. The miniature transducer is calibrated in distilled water column at 37°C (A). Calibration curves both before (pretest) and after (posttest) in vivo measurements show a linear correlation between the depth of water column (pressure in cm H_2O) and transducer output (mV) (B).

ducer is passed through the lumen of a Becton-Dickinson 18-gauge, 1.5-in. precision glide needle (Franklin Lakes, NJ). The sensor is kept in the lumen of the needle during penetration into the surface of the tumor. The sensor tip is introduced into the core of the tumor as the needle guide is withdrawn from the tumor surface. Tumor pressure (IFP) is read by means of TAM-D module after 15 s.

Results

Polyurethane ultraminiature pressure transducers, recognized for impeccable accuracy in the pressure range between −50 mm Hg to +300 mm Hg, provide a simple, accurate, and thromboresistant method of measuring the pressure at the source (Zimmer and Millar, 1998). Entire procedure of calibration of the sensor, introduction of the sensor into the tumor, and IFP reading does not take more than 10 min and can be performed with ease by anyone who can perform a subcutaneous injection. Our preliminary studies using this technique to measure IFP in subcutaneous B16F1 melanoma in NG2 knockout and wild type mice 2 weeks following grafting revealed an average core IFP of −0.4 cm H_2O and +4.9 cm H_2O in NG2 proteoglycan knockout and wild type mice, respectively. The difference was statistically significant (n = 24, P = 0.0054 Mann–Whitney U test) (Fig. 3).

Discussion

The interstitial fluid pressure within a tumor is actively regulated through interactions between cells and extracellular matrix molecules. Many anticancer drugs and antibodies used for treating patients with cancer are transported from the circulatory system through the interstitial space by convection (i.e. by streaming of a flowing fluid) rather than by diffusion. Increased tumor IFP causes inefficient uptake of therapeutic agents by decreasing convection. Cancer cells are therefore exposed to a lower effective concentration of therapeutic agents than normal cells, reducing treatment efficiency. Decreasing tumor IFP can thus improve convection of cancer chemotherapeutics into the tumor (Jain, 1987a,b; Heldin et al., 2004).

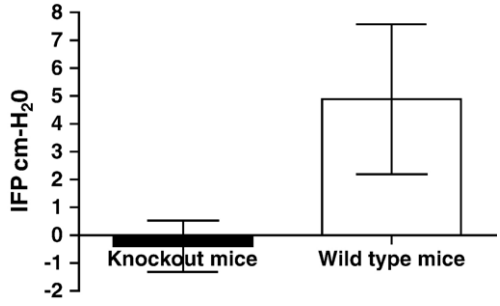

Fig. 3. Targeting NG2 proteoglycan on neovascular pericytes reduces interstitial hypertension in skin melanoma in mice. IFP measurements were performed 2 weeks following subcutaneous tumor grafting. Intrinsic (genetic) inhibition of NG2 proteoglycan decreases IFP in B16F1 melanoma grafts in NG2 knockout mice (average core IFP of −0.4 cm H_2O) compared to B16F1 melanoma grafts in wild type controls (average core IFP of +4.9 cm H_2O) (n = 24, P = 0.0054 Mann–Whitney U test).

In this respect, it is also noteworthy that pericytes are known to control interstitial pressure (IFP) by regulating their attachment to a collagen/microfibrillar network, which in turn restrains a proteoglycan/hyaluronan gel from retaining water (Pietras et al., 2001; Heldin et al., 2004; Rodt et al., 1996). In addition, signaling through PDGF β-receptors on pericytes increases IFP, whereas its inhibition reduces IFP (Pietras et al., 2001). Hence, IFP is a dynamic parameter that can potentially be controlled by regulating pericyte activity and their interaction with the extracellular matrix (Pietras et al., 2001). Our results reveal decreased IFP levels in tumors grown in NG2 knockout mice and suggest that NG2 chondroitin sulfate proteoglycan on pericytes has a role on IFP through its interaction with extracellular matrix components. Pericyte–NG2 chondroitin sulfate proteoglycan binds to extracellular matrix components such as type V, type VI, and type II collagen, tenascin, and laminin (Tillet et al., 1997; Burg et al., 1996). Biochemical data also demonstrate the involvement of both galectin-3 and α3β1 integrin in the EC response to pericyte–NG2 and show that NG2, galectin-3, and α3β1 form a complex on the cell surface promoting cell motility (Fukushi et al., 2004). Our recent findings revealed decreased neovascularization following intrinsic (NG2 knockout mice) or extrinsic (hydron polymer pellets containing NG2 neutralizing antibody) targeting of NG2 proteoglycan (Ozerdem, 2004; Ozerdem and Stallcup, 2004). Lowering tumor IFP by targeting NG2 proteoglycan on pericytes may be a useful approach in improving anticancer drug (conventional chemotherapy) efficacy.

This study also demonstrates that IFP is elevated in skin melanoma, corroborating previous studies showing elevated IFP in human melanoma (Boucher et al., 1991), human melanoma xenografts in mice (Kristensen et al., 1996; Tufto et al., 1996), and hamster melanomas (Leunig et al., 1992, 1994).

Critique of four IFP measurement techniques

The micropuncture (0.1 μm glass micropipette) technique does not allow for measurements in deep tissues; usually recordings can only be made down to about 1 mm from the surface (Wiederhielm, 1981; Adair et al., 1983). Furthermore, the glass micropipette breaks very easily during tissue penetration and from the slightest motion of the mouse. The wick catheter technique (Scholander et al., 1968) is vulnerable to clotting if there is extravasated blood within the tissue (Wiederhielm, 1981; Adair et al., 1983). The wick-in-needle technique requires custom-made needles with optimum-size side ports (Wiederhielm, 1981; Adair

et al., 1983). Chronic implantation of the 15-mm capsule is not practical and involves considerable tissue distortion, trauma, and wound healing response (Wiederhielm, 1981; Adair et al., 1983). Capsule implantation is not applicable for human use. In a comparison of two acute (micropipettes and wick-in-needle) and two chronic methods (perforated and porous capsules) in dog skin/subcutis, Wiig et al. (1987) found that transient pressure differences recorded by acute versus chronic methods during changes in hydration result from different physical properties of the capsule lining compared with that of the surrounding skin, in addition to a possible osmometer effect of the capsule lining. Therefore, we chose the wick-in-needle as the best standard by which to compare with Millar SPC-320, 2F Mikro-Tip with side port sensor. One possible disadvantage of this transducer-tipped catheter for IFP measurement is that the transducer may be susceptible to solid tissue pressure artifacts. However, in our pilot studies in tumors with positive pressure, this was found not to be the case, and the values obtained by the Millar probe were essentially equivalent to those obtained by the wick-in-needle technique.

The simplified IFP measurement procedure described in this report will allow the basic researchers and clinicians to apply IFP measurement easily and widely as a useful tool in their research.

Acknowledgments

This brief report is dedicated to P.F. Scholander, M.D., Ph.D. (1905–1980) who made pioneering contributions to the wealth of knowledge in the field of interstitial tissue fluid pressure. This work has been supported by grants from NIH (National Institute of Child Health and Human Development) RO3 HD044783, the U.S. Department of Defense Prostate Cancer Research Program New Investigator Award PC020822, and University of California, Tobacco-Related Disease Research Program Idea Award (TRDRP 13IT-0067) to Dr. Ugur Ozerdem. Dr. Alan R. Hargens is supported by grants from NASA Johnson Space Center NAG9-1425 and NASA #2004-0270. The authors thank Laura Gay, Adnan Cutuk, and Brandon Macias for their assistance.

References

Adair, T.H., Hogan, R.D., Hargens, A.R., Guyton, A.C., 1983. Techniques in Measurement of Tissue Fluid Pressures and Lymph Flow. Elsevier, County Clare, Ireland.

Boucher, Y., Kirkwood, J.M., Opacic, D., Desantis, M., Jain, R.K., 1991. Interstitial hypertension in superficial metastatic melanomas in humans. Cancer Res. 51 (24), 6691–6694.

Burg, M.A., Tillet, E., Timpl, R., Stallcup, W.B., 1996. Binding of the NG2 proteoglycan to type VI collagen and other extracellular matrix molecules. J. Biol. Chem. 271 (42), 26110–26116.

Capecchi, M.R., 1989. Altering the genome by homologous recombination. Science 244 (4910), 1288–1292.

Fadnes, H.O., Reed, R.K., Aukland, K., 1977. Interstitial fluid pressure in rats measured with a modified wick technique. Microvasc. Res. 14 (1), 27–36.

Fukushi, J., Makagiansar, I.T., Stallcup, W.B., 2004. NG2 proteoglycan promotes endothelial cell motility and angiogenesis via engagement of galectin-3 and alpha3beta1 integrin. Mol. Biol. Cell 15 (8), 3580–3590.

Grako, K.A., Ochiya, T., Barritt, D., Nishiyama, A., Stallcup, W.B., 1999. PDGF (alpha)-receptor is unresponsive to PDGF-AA in aortic smooth muscle cells from the NG2 knockout mouse. J. Cell Sci. 112 (Pt. 6), 905–915.

Guyton, A.C., 1963. A concept of negative interstitial pressure based on pressures in implanted perforated capsules. Circ. Res. 12, 399–414.

Hargens, A.R., 1981. Introduction and historical perspectives. In: Hargens, A.R. (Ed.), Tissue Fluid Pressure and Composition. Williams and Wilkins, Baltimore, pp. 1–10.

Heldin, C.H., Rubin, K., Pietras, K., Ostman, A., 2004. High interstitial fluid pressure—An obstacle in cancer therapy. Nat. Rev. Cancer 4 (10), 806–813.

Jain, R.K., 1987. Transport of molecules in the tumor interstitium: a review. Cancer Res. 47 (12), 3039–3051.

Jain, R.K., 1987. Transport of molecules across tumor vasculature. Cancer Metastasis Rev. 6 (4), 559–593.

Kristensen, C.A., Nozue, M., Boucher, Y., Jain, R.K., 1996. Reduction of interstitial fluid pressure after TNF-alpha treatment of three human melanoma xenografts. Br. J. Cancer 74 (4), 533–536.

Leunig, M., Goetz, A.E., Dellian, M., Zetterer, G., Gamarra, F., Jain, R.K., et al., 1992. Interstitial fluid pressure in solid tumors following hyperthermia: possible correlation with therapeutic response. Cancer Res. 52 (2), 487–490.

Leunig, M., Goetz, A.E., Gamarra, F., Zetterer, G., Messmer, K., Jain, R.K., 1994. Photodynamic therapy-induced alterations in interstitial fluid pressure, volume and water content of an amelanotic melanoma in the hamster. Br. J. Cancer 69 (1), 101–103.

Mansour, S.L., Thomas, K.R., Capecchi, M.R., 1988. Disruption of the proto-oncogene int-2 in mouse embryo-derived stem cells: a general strategy for targeting mutations to non-selectable genes. Nature 336 (6197), 348–352.

Mubarak, S.J., Hargens, A.R., 1981. Clinical use of the wick catheter technique. In: Hargens, A.R. (Ed.), Tissue Fluid Pressure and Composition. Williams and Wilkins, Baltimore, pp. 261–268.

Ozerdem, U., 2004. Targeting neovascular pericytes in neurofibromatosis type 1. Angiogenesis 7 (4), 307–311.

Ozerdem, U., Stallcup, W.B., 2004. Pathological angiogenesis is reduced by targeting pericytes via the NG2 proteoglycan. Angiogenesis 7 (3), 269–276.

Pietras, K., Ostman, A., Sjoquist, M., Buchdunger, E., Reed, R.K., Heldin, C.H., et al., 2001. Inhibition of platelet-derived growth factor receptors reduces interstitial hypertension and increases transcapillary transport in tumors. Cancer Res. 61 (7), 2929–2934.

Rodt, S.A., Ahlen, K., Berg, A., Rubin, K., Reed, R.K., 1996. A novel physiological function for platelet-derived growth factor-BB in rat dermis. J. Physiol. 495 (Pt 1), 193–200.

Scholander, P.F., Hargens, A.R., Miller, S.L., 1968. Negative pressure in the interstitial fluid of animals. Fluid tensions are spectacular in plants; in animals they are elusively small, but just as vital. Science 161 (839), 321–328.

Tillet, E., Ruggiero, F., Nishiyama, A., Stallcup, W.B., 1997. The membrane-spanning proteoglycan NG2 binds to collagens V and VI through the central nonglobular domain of its core protein. J. Biol. Chem. 272 (16), 10769–10776.

Tufto, I., Lyng, H., Rofstad, E.K., 1996. Interstitial fluid pressure, perfusion rate and oxygen tension in human melanoma xenografts. Br. J. Cancer, Suppl. 27, S252–S255.

Wiederhielm, C.A., 1981. The tissue pressure controversy, a semantic dilemma. In: Hargens, A.R. (Ed.), Tissue Fluid Pressure and Composition. Williams and Wilkins, Baltimore, pp. 21–333

Wiederhielm, C.A., Woodbury, J.W., Kirk, S., Rushmer, R.F., 1964. Pulsatile pressures in the microcirculation of frog's mesentery. Am. J. Physiol. 207, 173–176.

Wiig, H., Reed, R.K., Aukland, K., 1987. Measurement of interstitial fluid pressure in dogs: evaluation of methods. Am. J. Physiol. 253 (2 Pt. 2), H283–H290.

Young, J.S., Lumsden, C.E., Stalker, A.L., 1950. The significance of the tissue pressure of normal testicular and of neoplastic (Brown–Pearce carcinoma) tissue in the rabbit. J. Pathol. Bacteriol. 62 (3), 313–333.

Zimmer, H.G., Millar, H.D., 1998. Technology and application of ultraminiature catheter pressure transducers. Can J. Cardiol. 14 (10), 1259–1266.

Contribution of Bone Marrow–Derived Pericyte Precursor Cells to Corneal Vasculogenesis

Ugur Ozerdem,[1] *Kari Alitalo,*[2] *Petri Salven,*[3] *and Andrew Li*[4]

Purpose. Bone-marrow (BM)–derived hematopoietic precursor cells are thought to participate in the growth of blood vessels during postnatal vasculogenesis. In this investigation, multichannel laser scanning confocal microscopy and quantitative image analysis were used to study the fate of BM-derived hematopoietic precursor cells in corneal neovascularization.

Methods. A BM-reconstituted mouse model was used in which the BM from enhanced green fluorescent protein (GFP)–positive mice was transplanted into C57BL/6 mice. Basic fibroblast growth factor (bFGF) was used to induce corneal neovascularization in mice. The vasculogenic potential of adult BM-derived cells and their progeny were tested in this in vivo model. Seventy-two histologic sections selected by systematic random sampling from four mice were immunostained and imaged with a confocal microscope and analyzed with image-analysis software.

Results. BM-derived endothelial cells did not contribute to bFGF-induced neovascularization in the cornea. BM-derived periendothelial vascular mural cells (pericytes) were detected at sites of neovascularization, whereas endothelial cells of blood vessels originated from preexisting blood vessels in limbal capillaries. Fifty three percent of all neovascular pericytes originated from BM, and 47% of them originated from preexisting corneoscleral limbus capillaries. Ninety-six percent and 92% of BM-derived pericytes also expressed CD45 and CD11b, respectively, suggesting their hematopoietic origin from the BM.

Conclusions. Pericytes of new corneal vessels have a dual source: BM and preexisting limbal capillaries. These findings establish BM as a significant effector organ in corneal disorders associated with neovascularization. (*Invest Ophthalmol Vis Sci.* 2005;46:3502–3506) DOI:10.1167/iovs.05-0309

The neovascularization of tissues is accomplished by two distinct processes: vasculogenesis (V) and angiogenesis (A).[1–6] During angiogenesis, preexisting blood vessels form neovascular sprouts. In vasculogenesis, blood vessels develop from progenitor cells that coalesce and differentiate to form vessels. The walls of neovascular blood vessel capillaries are composed of two principal cell types: vascular endothelial cells (VECs), and Rouget cells.[7] Rouget cells, also known as mural cells or pericytes, form an outer sheath[6,8,9] surrounding the endothelial cells on the outer aspect of microvessels.[10]

Reports about pericyte or endothelial differentiation from bone-marrow hematopoietic cells in various neovascularization models[11–18] are controversial. Two reports have suggested that adult bone-marrow (BM)–derived precursors give rise to pericytes but not to VECs,[11,12] and numerous other reports have suggested that BM-derived precursors give rise to VECs.[14–18] Differences in tissues, disease models, and neovascularization models may be a reason for this controversy. Difficulty in identifying pericytes, which are in very close spatial proximity to endothelial cells, may be another factor resulting in this controversy.

The normal mammalian cornea is one of the few tissues that is devoid of preexisting lymphatics and blood vessels. Therefore, the presence of any blood and lymphatic vessels in the cornea always signifies a pathologic process. The actual in vivo differentiation capacity of adult BM-derived hematopoietic precursors cells into pericytes or endothelial cells in corneal neovascularization remains unclear, as do the contribution of vasculogenesis and angiogenesis of new vessels (i.e., the vessels formed by BM-derived precursor cells [vasculogenesis] and the vessels formed by the cells sprouting from preexisting vessels [angiogenesis]).

Whereas endothelial cells have been studied extensively, much less is known about pericytes. As the name indicates, pericytes surround the endothelial cells on the abluminal aspect of microvessels.[10] A recent search of the PubMed database (http://www.ncbi.nlm.nih.gov/ National Institutes of Health, Bethesda, MD) revealed a 109-fold difference between the number of papers published on these two vascular cell types. Because the cellular processes and the role of circulating BM-derived progenitor cells underlying neovascular sprout formation remain incompletely understood,[11,19,20] increased attention to pericytes and their interaction with endothelial cells will yield a better understanding of the role of BM in corneal disorders associated with neovascularization.

We used a BM-reconstituted mouse model in which the BM from enhanced green fluorescent protein $(GFP)^+$ mice was transplanted into normal C57BL/6 mice. Using this mouse model, we set out to test the neovascular potential of adult BM-derived hematopoietic progenitor cells and their progeny in vivo. We used the basic fibroblast growth factor (bFGF)-induced mouse corneal neovascularization model to quantify vasculogenesis and angiogenesis. In addition, we differentiated quantitatively BM-derived pericytes from angiogenic pericytes derived from preexisting vessels.

We showed that BM-derived vascular precursors contributed only to the formation of pericytes but not VECs in corneal neovascularization. This investigation revealed that a significant fraction of neovascular pericytes in the cornea derive from BM-derived hematopoietic progenitor cells rather than from preexisting vessels, suggesting an extensive role for BM and vasculogenesis in corneal neovascularization. We also showed that a small fraction of lymphatic endothelial cells (LECs) in lymphangiogenic vessel walls in the cornea are from

From the [1]La Jolla Institute for Molecular Medicine, La Jolla, California; [2]Biomedicum Helsinki, [3]University of Helsinki, Helsinki, Finland; [4]University of California San Diego, La Jolla, California.

Supported by Grant R03 HD044783 from the National Institute of Child Health and Human Development, a U.S. Department of Defense Prostate Cancer Research Program New Investigator Award PC020822, and Grant TRDRP 13IT-0067 from the Tobacco-Related Disease Research Program of the University of California Idea Award (UO).

Submitted for publication March 11, 2005; revised April 22, 2005; accepted July 29, 2005.

Disclosure: **U. Ozerdem**, None; **K. Alitalo**, None; **P. Salven**, None; **A. Li**, None

The publication costs of this article were defrayed in part by page charge payment. This article must therefore be marked "*advertisement*" in accordance with 18 U.S.C. §1734 solely to indicate this fact.

Corresponding author: Ugur Ozerdem, Assistant Professor, La Jolla Institute for Molecular Medicine, 4570 Executive Drive, Suite 100, San Diego, CA 92121; ozerdem@ljimm.org.

Investigative Ophthalmology & Visual Science, October 2005, Vol. 46, No. 10

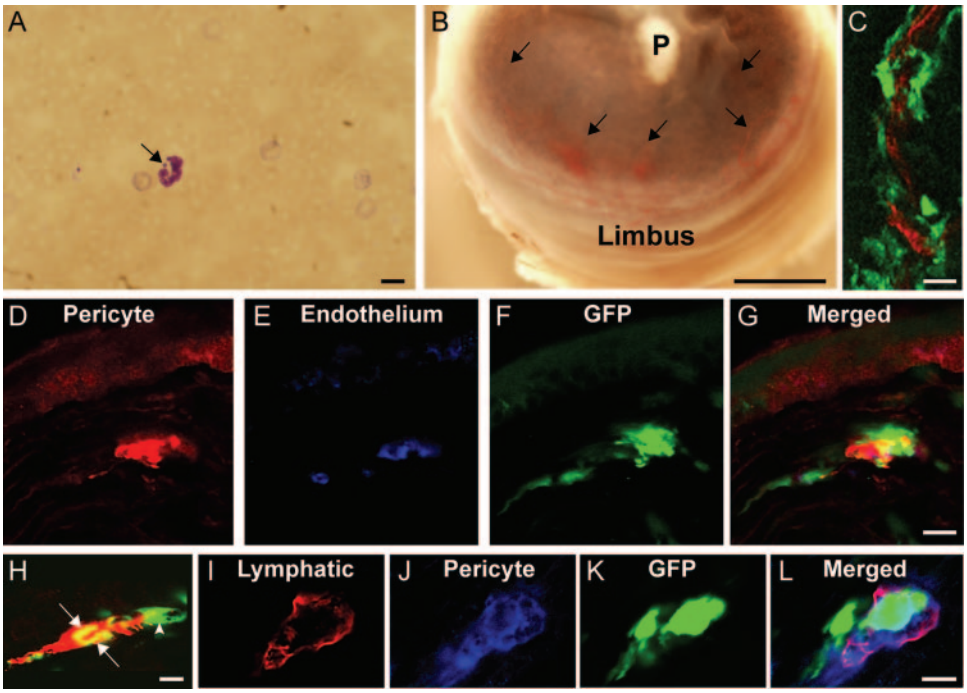

FIGURE 1. (**A**) Peripheral blood smear stained with May-Grunwald shows a polymorphonuclear leukocyte with Barr body chromatin in the form of drumstick (*arrow*) in a BM recipient male mouse. Scale bar, 10 μm. (**B**) Polymer (hydron) pellet (P) containing 90 ng of bFGF implanted into the corneal stroma of BM-recipient mouse. *Arrows*: neovasculature penetrating the cornea from the corneoscleral limbus 7 days after pellet implantation. Scale bar, 300 μm. (**C**) Frozen section of neovascularized cornea (as seen in **B**) obtained from a C57BL/6 mouse in which the BM was reconstituted with enhanced GFP^+ BM via transplantation. Blood vessel endothelial cells (*red*) were identified by using confocal microscopy in conjunction with combined immunohistochemical staining for CD31, CD105, and flk-1. Donor-derived GFP^+ pericytes formed perivascular sleeves (*green*) around GFP-negative blood vessel endothelium (*red*). Scale bar, 10 μm. (**D–G**) Frozen section of neovascularized cornea stained using immunohistochemistry to identify pericytes (NG2, *red* in **D**) and blood vessel endothelium (combined CD31 + CD105 + flk-1; *blue* in **E**). (**F**, **G**) BM-derived cells expressing GFP (*green*). (**G**) Merger of images (**D–F**) shows both GFP^+ and GFP^- (limbus-derived) pericytes investing the GFP^- blood vessel endothelium (*blue*). (**H**) Frozen section of neovascularized cornea stained using immunohistochemistry to identify lymphangiogenic endothelium with LYVE-1 (*red*). A lymphangiogenic sprout in the cornea shows both LYVE-1^+ and GFP^- cells (*red*) and LYVE-1^+ and GFP^+ cells (*yellow*) as indicated by *arrows*. *Arrowhead*: perivascular cell investing the lymphatic wall like a sleeve. (**I–L**) Frozen section of neovascularized cornea immunostained for LYVE-1 (**I**, *red*) and NG2 (**J**, *blue*) for identification of lymphatic endothelium and pericytes, respectively. Bone-marrow–derived cells are identified by their GFP expression (**K**, *green*). Perivascular cells (*blue*) show discontinuous investment of the lymphatic capillary wall (*red*). Both BM-derived (*green*) and non-BM–derived perivascular cells (*blue*) support the lymphatic capillary wall (images **I**, **J**, and **K** merged in **L**). Scale bar: (**A**, **D–G**, **H**) 10 μm; (**B**) 300 μm; (**I–L**) 5 μm.

BM-derived hematopoietic precursor cells, whereas most lymphatic capillaries originate from preexisting limbal lymphatics.

METHODS

All animal studies were performed in accordance with The National Institutes of Health Office of Laboratory Animal Welfare (OLAW) guidelines and the ARVO Statement for the Use of Animals in Research and were approved by the La Jolla Institute for Molecular Medicine animal research committee.

Animals and BM Transplantations

Mice reconstituted with enhanced GFP^+ syngeneic BM cells were created to study the behavior of BM cells in vivo. Briefly, BM cells were collected by flushing the femurs and tibias of female C57BL/6 TgN(ACTbEGFP)1Osb mice (Jackson Laboratory, Bar Harbor, ME) with ice-cold phosphate-buffered saline (PBS) via a 25-gauge needle. After the lysis of red blood cells, BM progenitor cells were resuspended in PBS. After counting, the cells were spun down and resuspended at a concentration of 3×10^6 cells/100 μL. The recipient male mice (four mice) were irradiated by a lethal dosage of 1000 rads (10 Gy). Three days before the irradiation, the animals were housed in sterilized cages and fed standard chow that has been irradiated. The mice drank water containing the antibiotic sulfamethoxazole/trimethoprim to reduce the risk of opportunistic infections. The animals were housed in sterile cages and fed sterile food throughout the procedure. Three hours after irradiation, 3×10^6 cells were injected retro-orbitally via the ophthalmic venous plexus in the right orbit. We found previously that this procedure is much more effective than using the tail vein injections. It takes, on average, less than 30 seconds to inject 100 mL of cells versus several minutes to vasodilate the vessels in the mouse before trying to inject the cells via the tail vein, many times unsuccessfully. In addition, the animals are less stressed when this ophthalmic venous plexus injection procedure is used. Flow cytometry (FACScan; BD Biosciences, Franklin Lakes, NJ) showed that peripheral blood cells of the recipients were reconstituted with GFP^+ cells 4 weeks after transplantation. Peripheral blood smears stained with May-Grunwald revealed Barr body chromatin (the inactivated X chromosome seen in females) in recipient male mice corroborating the reconstitution of BM after transplantation (Fig. 1A). More than 95% reconstitution of the BM by GFP^+ donor-derived cells is previously reported with similar BM transplantation techniques.[11,21]

Basic Fibroblast Growth Factor–Induced Corneal Neovascularization Model

Basic fibroblast growth (bFGF) is known to be a potent stimulus for angiogenesis and lymphangiogenesis.[22] Implantation of hydron pellets containing bFGF (90 ng) induces both neovascularization and lymphangiogenesis in the mouse cornea.[23–25] The mouse corneal micropocket assay, a noninflammatory neovascularization assay, was performed as previously described.[23] Previous studies using this in vivo model have shown the contribution of pericytes coexpressing NG2 proteoglycan and platelet-derived growth factor (PDGF) β-receptor to neovascular vessel walls as the new vessels spread into the cornea.[26,27] Slow-release polyhydroxyethyl methacrylate (hydron) pellets ($0.4 \times 0.4 \times 0.2$ mm) were formulated to contain 90 ng recombinant basic fibroblast growth factor (bFGF; Invitrogen-Gibco, Grand Island, NY) and 45 μg sucrose aluminum sulfate (sucralfate; Sigma-Aldrich, St. Louis, MO). The mice reconstituted with enhanced GFP^+ syngeneic BM cells were anesthetized with Avertin (0.015–0.017 mL/g body weight), and a single hydron pellet was surgically implanted into the corneal stroma of the left eye, 0.7 mm from the corneoscleral limbus (Fig. 1B). On postoperative day 7, mice were killed and their eyes enucleated.

Immunohistochemistry, Confocal Microscopic Imaging, and Image Analysis

Enucleated eyes were fixed in 4% paraformaldehyde for 6 hours, cryoprotected in 20% sucrose overnight, and frozen in optimal cutting temperature (OCT) embedding compound (Miles, Inc., Elkhardt, IN). Cryostat sections (40 μm) were air-dried onto coated slides (Superfrost; Fisher Scientific, Pittsburgh, PA). Pericytes were identified by labeling with rabbit, or rat antibodies against the NG2 proteoglycan, or rabbit PDGF β-receptor antibody.[11,26–30] Both NG2 and PDGF β-receptors are regarded as specific markers for pericytes.[31,32]

Lymphatic endothelium was identified by immunolabeling with rabbit anti-mouse LYVE-1 antibody, as described elsewhere.[33,34] Blood vessel endothelial cells were identified with a cocktail of rat antibodies against mouse endoglin (CD105), platelet-endothelial cell adhesion molecule (PECAM-1; CD31), and VEGF receptor-2 (flk-1; BD-Pharmingen, San Diego, CA),[27,29,35] a strategy that has been used to maximize labeling of all blood vessel endothelial cells. Immunohistochemical identification of hematopoietic cells was made using rat anti-mouse CD45 (LCA, Ly-5; BD-Pharmingen), and rat anti-mouse CD11b (Mac-1α) antibodies (BD-Pharmingen), as previously described.[11]

Alexa-647 and Alexa-594-labeled goat anti-rat secondary antibodies were obtained from Molecular Probes (Eugene, OR), and rhodamine red X (RRX)-labeled goat anti-rabbit secondary antibodies were obtained from Jackson ImmunoResearch Laboratories (West Grove, PA). Slides were mounted with antifade medium (Vectashield; Vector Laboratories, Burlingame, CA).

After cryosectioning, sections representing the entire thickness of the cornea were selected from the numbered sections (180 sections from four mice) by using systematic random sampling.[36] The sampled histologic sections (72 sections) were analyzed with a multichannel laser scanning confocal microscope. Briefly, optical sections were obtained from the specimens using the microscope (Fluoview 1000; Olympus USA, Melville, NY) in the three-channel sequential scanning mode. Serial optical sections (1 μm each) across the entire thickness (40 μm) of the histologic specimens were overlaid (z-stack) to provide reconstructions of entire vessels. This allowed unambiguous identification of the spatial relationship between pericytes and endothelial cells in the vessel wall.

Image analysis software (Volocity; Openlab-Improvision, Inc., Lexington, MA) was used for differential quantification of pericytes, VECs, and LECs for GFP, CD45, and CD11b expression.

Results

Contribution of Bone-Marrow–Derived Pericyte Precursors to Neovascularization

Confocal microscopic examination of histologic sections (Figs. 1C–G) revealed evidence of donor-derived (GFP^+) and host (limbal capillary)-derived (GFP-negative) $NG2^+$ and PDGF β-$receptor^+$ periendothelial cells (pericytes) forming sleeves around GFP-negative blood vessel endothelium. We were unable to find evidence of BM-derived blood vessel endothelial cells in corneal neovasculature. This suggests that neovascular blood vessel endothelium in cornea originates from corneoscleral limbal blood vessel capillaries, whereas pericytes have a dual origin: corneoscleral limbus vasculature and bone-marrow hematopoietic cells. In 22 histologic slides from four mice, 53% of all neovascular pericytes ($NG2^+$ periendothelial cells) were GFP^+ and 47% $\pm$ 3.7% (SEM) of them were GFP negative. Quantification based on 40 histologic slides revealed that 96% $\pm$ 0.7% (SEM) of $GFP^+/NG2^+$ pericytes also expressed CD45, whereas 92% $\pm$ 1.7% of $GFP^+/NG2^+$ pericytes expressed CD11b. This suggests a hematopoietic origin from BM of these pericytes.

Contribution of Bone Marrow to Lymphangiogenic Endothelium

Lymphangiogenic sprouts in the cornea showed both $LYVE\text{-}1^+$ and GFP^-, and $LYVE^+$ and GFP^+ endothelium (Fig. 1H, arrows). Of 10 histologic slides examined, eight percent of $LYVE\text{-}1^+$ cells were GFP^+, whereas 92% of $LYVE\text{-}1^+$ cells were GFP^-, suggesting that BM-derived progenitors contribute minimally to lymphangiogenesis in cornea. Lymphangiogenic vessel walls in the cornea showed discontinuous investment of lymphatic endothelium by $NG2^+$ and PDGFβ-receptor–positive periendothelial cells (which are GFP^+) in the form of incomplete sleeves (Fig. 1H–L). Quiescent lymphatic capillaries in the corneoscleral limbus where no intervention was performed revealed no pericytes on the lymphatic capillary wall.

Discussion

Three observations presented in our study seem especially noteworthy. First, pericytes of the corneal new vessels have a dual source: BM (vasculogenesis) and preexisting limbal capillaries (angiogenesis). More pericytes originate from BM than preexisting limbal capillaries by a factor of 1.12. Our results also suggest that although most BM-derived pericytes in corneal neovascularization derive from hematopoietic precursor cells, a small fraction (4%–8%) of BM-derived pericytes in the cornea derive from nonhematopoietic BM precursor cells. These nonhematopoietic progenitor cells may represent BM stromal or mesenchymal stem cells.[37–41] These findings establish BM with its hematopoietic and nonhematopoietic elements as a significant effector organ in corneal disorders associated with neovascularization.

Second, the diverse origin of pericytes and their spatial proximity to each other in the neovascular sprouts raise the possibility of a neovascularization mechanism composed of both angiogenesis and vasculogenesis. By definition, angiogenesis and vasculogenesis refer to the formation of blood vessels from prexisting blood vessels and stem cells, respectively. This suggests the possibility of a synergy or overlap of two mechanisms operating simultaneously in the same neovascular sprouts, rather than independent progression of angiogenesis from vasculogenesis. Further studies are warranted to elucidate the homing mechanisms of circulating BM-derived pericyte precursors through the preexisting endothelium and pericyte layer (barrier) at neovascular sprouts. This homing process may involve extensive pericyte–endothelium and pericyte–pericyte adhesion and extravasation (emigration) processes, along with weakening of the junctional complexes between these cell types. Our findings, coupled with our previous reports,[11,26,28,29] also corroborate the findings of other investigators, revealing the participation of nascent pericytes during the earliest stages of neovascularization.[9,31,42–46] Although pericytes are widely regarded to be the microvascular equivalent of smooth muscle cells, the origin, development, and function of these cells appear to be variable and complex.[47–49] Our ability to detect the precocious contribution of pericytes to microvascular development depends heavily on the use of NG2 proteoglycan and PDGF β-receptor as markers for these cells at an early stage of their development.[31,32] NG2 proteoglycan on pericytes is a functional player in angiogenesis, and its extrinsic (pharmacological) or intrinsic (genetic) inhibition is associated with a significant decrease in angiogenesis and decreased pericyte-endothelium investment ratios in neovascularization.[27,30] NG2, a membrane-spanning chondroitin sulfate proteoglycan associated with mitotically active, nascent pericytes, exhibits several properties that suggest it is a functional player in neovascularization.[26–30] NG2 appears to serve as a

coreceptor for both bFGF and PDGF.[50,51] Pericyte-NG2 chondroitin sulfate proteoglycan binds to extracellular matrix components such as types V, VI, and II collagen; tenascin; and laminin.[52,53] Biochemical data also demonstrate the involvement of both galectin-3 and $\alpha 3\beta 1$ integrin in the VEC response to pericyte-NG2 and show that NG2, galectin-3, and $\alpha 3\beta 1$ form a complex on the cell surface promoting cell motility.[54] Our recent findings revealed decreased neovascularization after intrinsic (NG2 knockout mice) or extrinsic (hydron polymer pellets containing NG2 neutralizing antibody) targeting of NG2 proteoglycan in ischemia, neurofibromatosis type 1 (NF1), and the corneal bFGF-induced neovascularization model.[27,30] In the retinal vessels of NG2-knockout mice, proliferation of both pericytes and endothelial cells after ischemia is significantly reduced, and the pericyte-endothelial cell ratio declines from the wild-type value of 0.86 to 0.24.[27] When pericyte NG2 proteoglycan is targeted, a 53% reduction in tumor neovascularization is possible in NF1-derived malignant peripheral nerve sheath tumor (MPNST).[30] One of the traditional markers for pericyte identification has been the expression of α-SMA. However, a growing body of evidence suggests that α-SMA is a late marker for differentiated pericytes and therefore may be poorly expressed in developing angiogenic microvasculature.[31,32] Because only a fraction of developing pericytes can be identified on the basis of α-SMA expression,[9,32,55–58] we used NG2 and PDGF β-receptor immunohistochemistry to identify pericytes.[29,31,32,59]

Third, our investigations also identified discontinuous investment of lymphangiogenic capillary walls by BM-derived periendothelial cells in lymphangiogenesis induced by bFGF. These pericytes may provide the capillary wall with some temporary physical support until the lymphatic endothelium establishes direct connection with the extracellular matrix. The same cells may also represent a transitional stage of BM-derived precursors before they transdifferentiate into lymphatic endothelium. In our studies so far, we have not identified pericytes in quiescent lymphatic capillary walls.

Recent studies suggest that dual targeting of pericytes and endothelial cells improves the efficacy of treatments aimed at inhibiting neovascular vessels.[27,30,60–62] Clearly, the design of improved targeting strategies aimed at pericytes and lymphatic endothelial cells that derive from hematopoietic precursors depends on further understanding of the role of pericytes in neovascularization. Our study provides evidence that BM-derived pericytes contribute to the early phases of neovascular sprout formation during pathologic neovascularization and lymphangiogenesis. As significant players in neovascularization, BM-derived precursors represent an additional target for treatments designed to downregulate neovascularization in cornea.

References

1. Folkman J. Angiogenesis in cancer, vascular, rheumatoid and other disease. *Nat Med*. 1995;1:27–31.
2. D'Amore PA. Mechanisms of retinal and choroidal neovascularization. *Invest Ophthalmol Vis Sci*. 1994;35:3974–3979.
3. Campochiaro PA. Retinal and choroidal neovascularization. *J Cell Physiol*. 2000;184:301–310.
4. Folkman J, Shing Y. Angiogenesis. *J Biol Chem*. 1992;267:10931–10934.
5. Risau W, Flamme I. Vasculogenesis. *Annu Rev Cell Dev Biol*. 1995;11:73–91.
6. Risau W. Mechanisms of angiogenesis. *Nature*. 1997;386:671–674.
7. Rouget CMB. Sur la contractilité capillaires sanguins. *Comptes Rendus de l'Académie des Sciences.* 1879;88:916–918.
8. Sims DE. Recent advances in pericyte biology: implications for health and disease. *Can J Cardiol*. 1991;7:431–43.
9. Nehls V, Denzer K, Drenckhahn D. Pericyte involvement in capillary sprouting during angiogenesis in situ. *Cell Tissue Res*. 1992;270:469–474.
10. Rhodin JA. Ultrastructure of mammalian venous capillaries, venules, and small collecting veins. *J Ultrastruct Res*. 1968;25:452–500.
11. Rajantie I, Ilmonen M, Alminaite A, Ozerdem U, Alitalo K, Salven P. Adult bone marrow-derived cells recruited during angiogenesis comprise precursors for periendothelial vascular mural cells. *Blood*. 2004;104:2084–2086.
12. Ziegelhoeffer T, Fernandez B, Kostin S, et al. Bone marrow-derived cells do not incorporate into the adult growing vasculature. *Circ Res*. 2004;94:230–238.
13. Heil M, Ziegelhoeffer T, Mees B, Schaper W. A different outlook on the role of bone marrow stem cells in vascular growth: bone marrow delivers software not hardware. *Circ Res*. 2004;94:573–574.
14. Asahara T, Masuda H, Takahashi T, et al. Bone marrow origin of endothelial progenitor cells responsible for postnatal vasculogenesis in physiological and pathological neovascularization. *Circ Res*. 1999;85:221–228.
15. Asahara T, Kawamoto A. Endothelial progenitor cells for postnatal vasculogenesis. *Am J Physiol.* 2004;287:C572–C579.
16. Asahara T, Isner JM. Endothelial progenitor cells for vascular regeneration. *J Hematother Stem Cell Res*. 2002;11:171–178.
17. Asahara T. Endothelial progenitor cells for neovascularization. *Ernst Schering Res Found Workshop*. 2003;43:211–216.
18. Shirakawa K, Furuhata S, Watanabe I, et al. Induction of vasculogenesis in breast cancer models. *Br J Cancer*. 2002;87:1454–1461.
19. Bergers G, Benjamin LE. Tumorigenesis and the angiogenic switch. *Nat Rev Cancer*. 2003;3:401–410.
20. Darland DC, D'Amore PA. Blood vessel maturation: vascular development comes of age. *J Clin Invest*. 1999;103:157–158.
21. Galimi F, Summers RG, van Praag H, Verma IM, Gage FH. A role for bone marrow-derived cells in the vasculature of noninjured CNS. *Blood*. 2005;105:2400–2402.
22. Cao R, Eriksson A, Kubo H, Alitalo K, Cao Y, Thyberg J. Comparative evaluation of FGF-2-, VEGF-A-, and VEGF-C-induced angiogenesis, lymphangiogenesis, vascular fenestrations, and permeability. *Circ Res*. 2004;94:664–670.
23. Kenyon BM, Voest EE, Chen CC, Flynn E, Folkman J, D'Amato RJ. A model of angiogenesis in the mouse cornea. *Invest Ophthalmol Vis Sci*. 1996;37:1625–1632.
24. Kenyon BM, Browne F, D'Amato RJ. Effects of thalidomide and related metabolites in a mouse corneal model of neovascularization. *Exp Eye Res*. 1997;64:971–978.
25. Chang LK, Garcia-Cardena G, Farnebo F, et al. Dose-dependent response of FGF-2 for lymphangiogenesis. *Proc Natl Acad Sci USA*. 2004;101:11658–11663.
26. Ozerdem U, Monosov E, Stallcup WB. NG2 proteoglycan expression by pericytes in pathological microvasculature. *Microvasc Res*. 2002;63:129–134.
27. Ozerdem U, Stallcup WB. Pathological angiogenesis is reduced by targeting pericytes via the NG2 proteoglycan. *Angiogenesis*. 2004;7:269–276.
28. Ozerdem U, Grako KA, Dahlin-Huppe K, Monosov E, Stallcup WB. NG2 proteoglycan is expressed exclusively by mural cells during vascular morphogenesis. *Dev Dyn*. 2001;222:218–227.
29. Ozerdem U, Stallcup WB. Early contribution of pericytes to angiogenic sprouting and tube formation. *Angiogenesis*. 2003;6:241–249.
30. Ozerdem U. Targeting neovascular pericytes in neurofibromatosis type 1. *Angiogenesis*. 2004;7:307–311.
31. Gerhardt H, Betsholtz C. Endothelial-pericyte interactions in angiogenesis. *Cell Tissue Res*. 2003;314:15–23.
32. McDonald DM, Choyke PL. Imaging of angiogenesis: from microscope to clinic. *Nat Med*. 2003;9:713–725.
33. Witmer AN, Van Blijswijk BC, Van Noorden CJ, Vrensen GF, Schlingemann RO. In vivo angiogenic phenotype of endothelial cells and pericytes induced by vascular endothelial growth factor-a. *J Histochem Cytochem*. 2004;52:39–52.

34. Petrova TV, Karpanen T, Norrmen C, et al. Defective valves and abnormal mural cell recruitment underlie lymphatic vascular failure in lymphedema distichiasis. *Nat Med*. 2004;10:974–981.
35. Chang YS, di Tomaso E, McDonald DM, Jones R, Jain RK, Munn LL. Mosaic blood vessels in tumors: frequency of cancer cells in contact with flowing blood. *Proc Natl Acad Sci USA*. 2000;97: 14608–14613.
36. Dawson B, Trapp RG. *Basic and Clinical Biostatistics.* 3rd ed. New York: McGraw-Hill; 2001.
37. Prockop DJ. Marrow stromal cells as stem cells for nonhematopoietic tissues. *Science*. 1997;276:71–74.
38. Jiang Y, Henderson D, Blackstad M, Chen A, Miller RF, Verfaillie CM. Neuroectodermal differentiation from mouse multipotent adult progenitor cells. *Proc Natl Acad Sci*. 2003;100(Suppl 1): 11854–11860.
39. Pittenger MF, Mackay AM, Beck SC, et al. Multilineage potential of adult human mesenchymal stem cells. *Science*. 1999;284:143–147.
40. Jiang Y, Jahagirdar BN, Reinhardt RL, et al. Pluripotency of mesenchymal stem cells derived from adult marrow. *Nature*. 2002; 418(6893):41–49.
41. Nakamura T, Ishikawa F, Sonoda KH, et al. Characterization and distribution of bone marrow-derived cells in mouse cornea. *Invest Ophthalmol Vis Sci*. 2005;46:497–503.
42. Schlingemann RO, Rietveld FJ, de Waal RM, Ferrone S, Ruiter DJ. Expression of the high molecular weight melanoma-associated antigen by pericytes during angiogenesis in tumors and in healing wounds. *Am J Pathol*. 1990;136:1393–1405.
43. Schlingemann RO, Oosterwijk E, Wesseling P, Rietveld FJ, Ruiter DJ. Aminopeptidase a is a constituent of activated pericytes in angiogenesis. *J Pathol*. 1996;179:436–442.
44. Wesseling P, Schlingemann RO, Rietveld FJ, Link M, Burger PC, Ruiter DJ. Early and extensive contribution of pericytes/vascular smooth muscle cells to microvascular proliferation in glioblastoma multiforme: an immuno-light and immuno-electron microscopic study. *J Neuropathol Exp Neurol*. 1995;54:304–310.
45. Amselgruber WM, Schafer M, Sinowatz F. Angiogenesis in the bovine corpus luteum: an immunocytochemical and ultrastructural study. *Anat Histol Embryol*. 1999;28:157–166.
46. Redmer DA, Doraiswamy V, Bortnem BJ, et al. Evidence for a role of capillary pericytes in vascular growth of the developing ovine corpus luteum. *Biol Reprod*. 2001;65:879–889.
47. Le Lievre CS, Le Douarin NM. Mesenchymal derivatives of the neural crest: analysis of chimaeric quail and chick embryos. *J Embryol Exp Morphol*. 1975;34:125–154.
48. Sims DE. The pericyte–a review. *Tissue Cell*. 1986;18:153–174.
49. Allt G, Lawrenson JG. Pericytes: cell biology and pathology. *Cells Tissues Organs*. 2001;169:1–11.
50. Goretzki L, Burg MA, Grako KA, Stallcup WB. High-affinity binding of basic fibroblast growth factor and platelet-derived growth factor-AA to the core protein of the NG2 proteoglycan. *J Biol Chem*. 1999;274:16831–16837.
51. Grako KA, Stallcup WB. Participation of the NG2 proteoglycan in rat aortic smooth muscle cell responses to platelet-derived growth factor. *Exp Cell Res*. 1995;221:231–240.
52. Tillet E, Ruggiero F, Nishiyama A, Stallcup WB. The membrane-spanning proteoglycan NG2 binds to collagens V and VI through the central nonglobular domain of its core protein. *J Biol Chem*. 1997;272:10769–10776.
53. Burg MA, Tillet E, Timpl R, Stallcup WB. Binding of the NG2 proteoglycan to type VI collagen and other extracellular matrix molecules. *J Biol Chem*. 1996;271:26110–26116.
54. Fukushi J, Makagiansar IT, Stallcup WB. NG2 proteoglycan promotes endothelial cell motility and angiogenesis via engagement of galectin-3 and alpha3beta1 integrin. *Mol Biol Cell*. 2004;15:3580–3590.
55. Nehls V, Drenckhahn D. Heterogeneity of microvascular pericytes for smooth muscle type alpha- actin. *J Cell Biol*. 1991;113:147–154.
56. Balabanov R, Dore-Duffy P. Role of the CNS microvascular pericyte in the blood-brain barrier. *J Neurosci Res*. 1998;53:637–644.
57. Boado RJ, Pardridge WM. Differential expression of alpha-actin mRNA and immunoreactive protein in brain microvascular pericytes and smooth muscle cells. *J Neurosci Res*. 1994;39:430–435.
58. Alliot F, Rutin J, Leenen PJ, Pessac B. Pericytes and periendothelial cells of brain parenchyma vessels co-express aminopeptidase N, aminopeptidase A, and nestin. *J Neurosci Res*. 1999;58:367–378.
59. Sundberg C, Ljungstrom M, Lindmark G, Gerdin B, Rubin K. Microvascular pericytes express platelet-derived growth factor-beta receptors in human healing wounds and colorectal adenocarcinoma. *Am J Pathol*. 1993;143:1377–1388.
60. Pietras K, Hanahan D. A multitargeted, metronomic, and maximum-tolerated dose "chemo-switch" regimen is antiangiogenic, producing objective responses and survival benefit in a mouse model of cancer. *J Clin Oncol*. In press.
61. Bergers G, Song S, Meyer-Morse N, Bergsland E, Hanahan D. Benefits of targeting both pericytes and endothelial cells in the tumor vasculature with kinase inhibitors. *J Clin Invest*. 2003;111:1287–1295.
62. Saharinen P, Alitalo K. Double target for tumor mass destruction. *J Clin Invest*. 2003;111:1277–1280.

Angiogenesis **6**: 241–249, 2003.

Early contribution of pericytes to angiogenic sprouting and tube formation*

Ugur Ozerdem[1] & William B. Stallcup[2]
[1]*La Jolla Institute for Molecular Medicine, Vascular Biology Division, La Jolla, California, USA;* [2]*The Burnham Institute, Neurobiology Program, La Jolla, California, USA*

Received 7 August 2003; accepted in revised form 30 November 2003

Key words: angiogenesis, endothelium, neovascularization, NG2, PDGF β-receptor, pericyte, sprout, tube, tumor, transplantation

Abstract

Immunostaining with endothelial and pericyte markers was used to evaluate the cellular composition of angiogenic sprouts in several types of tumors and in the developing retina. Confocal microscopy revealed that, in addition to conventional endothelial tubes heavily invested by pericytes, all tissues contained small populations of endothelium-free pericyte tubes in which nerve/glial antigen 2 (NG2) positive, platelet-derived growth factor beta (PDGF β) receptor-positive perivascular cells formed the lumen of the microvessel. Perfusion of tumor-bearing mice with FITC-dextran, followed by immunohistochemical staining of tumor vasculature, demonstrated direct apposition of pericytes to FITC-dextran in the lumen, confirming functional connection of the pericyte tube to the circulation. Transplantation of prostate and mammary tumor fragments into NG2-null mice led to the formation of tumor microvasculature that was invariably NG2-negative, demonstrating that pericytes associated with tumor microvessels are derived from the host rather than from the conversion of tumor cells to a pericyte phenotype. The existence of pericyte tubes reflects the early participation of pericytes in the process of angiogenic sprouting. The ability to study these precocious contributions of pericytes to neovascularization depends heavily on the use of NG2 and PDGF β-receptor as reliable early markers for activated pericytes.

Abbreviations: BrdU – bromodeoxyuridine; CD31 – PECAM-1; CD105 – endoglin; flk 1 – VEGF receptor-2; LNCaP – prostatic carcinoma cell line derived from a supraclavicular lymph node metastasis; NG2 – nerve/glial antigen 2; PBS – phosphate-buffered saline; PC-3 – prostatic carcinoma cell line derived from a bone metastasis of a patient; PDGF β-receptor – platelet-derived growth factor beta receptor; α-SMA – alpha isoform of smooth muscle actin; TRAMP – transgenic adenocarcinoma of mouse prostate

Introduction

Angiogenesis is essential for almost all aspects of normal development, as well as for many pathological processes, including tumor growth and metastasis [1, 2]. The walls of typical angiogenic microvessels are composed of two principal cell types: endothelial cells, which form the inner lining of the vascular tube, and pericytes (mural cells) which form an outer sheath around the endothelium [2–4]. While endothelial cells have been studied extensively, much less is known about the pericyte, a name ('peri' around and 'cyto' cell) that denotes the cell's periendothelial location at the abluminal aspect of microvessels [5]. A recent search of the PUBMED database at http://www.ncbi.nlm.nih.gov reveals a 118-fold difference between the number of papers published on these two vascular cell types. Since the cellular processes underlying neovascular sprout formation remain incompletely understood [6, 7], increased attention to pericytes and their interaction with endothelial cells will be required not only to attain a better understanding of vascular biology, but also to realize the full potential of anti-angiogenic therapy in oncology.

The relationship between endothelial cells and pericytes varies from tissue to tissue. As one example, the density of pericyte investment of the microvascular endothelium is quite high in the developing central nervous system, but very low in skeletal muscle [8, 9]. In tumor neovasculature this relationship may be even more variable. Underscoring the heterogeneity of tumor vasculature, as many as nine distinct angiogenic vessel classes have been described in neoplasms, based on both morphology and the cellular composition of the vessel

* Presented in part at the vascular biology symposium of Federation of American Societies for Experimental Biology (FASEB), 2003, Annual Meeting in San Diego, California, USA.

Correspondence to: Ugur Ozerdem, MD, Assistant Professor, La Jolla Institute for Molecular Medicine, Vascular Biology Division, 4570 Executive Drive, Suite 100, La Jolla, CA 92121, USA. Tel: +1-858-587-8788; Fax: +1-858-587-6742; E-mail: ozerdem@ljimm.org

Table 1. The varieties and classification of blood vessels in the substance of neoplasm. (From Warren BA [10]).

Class 1. Arteries and arterioles
Class 2. Capillaries
Class 3. Capillary sprouts
Class 4. Sinusoidal vessels
Class 5. Blood channels without endothelial lining
Class 6. Giant capillaries
Class 7. Capillaries with fenestrated endothelium
Class 8. Venules and veins
Class 9. Arterio-venous anastomoses

wall (Table 1) [10]. One of these vessel classes (class 5) describes vascular walls in which the endothelium is discontinuous. Examples of class-5 vessels have recently become more numerous with the description of mosaic vessels [11, 12] and the phenomenon of vasculogenic mimicry [13–15].

These vessel types call to mind a recent suggestion from our studies that vascular pericytes can contribute to the heterogeneous nature of microvessels, even in non-tumor situations. In a model of corneal angiogenesis, we found endothelial cell-free segments of microvessels in which pericytes appeared to comprise the lumen of the microvascular tube [16]. In the current study we further analyze the ontogeny, morphology, and functional properties of pericyte tubes in normal retinal vasculature and in several types of tumors (melanoma, mammary, prostate, lung, glioma). This study expands our understanding of the contribution of pericytes to the process of angiogenic sprouting, demonstrating the early participation of these perivascular cells in microvascular tube formation.

Materials and methods

Tumors

Lewis lung carcinoma [17] and B16F1 melanoma [18] tumors resulted from subcutaneous injection of 5×10^6 cells into C57Bl/6 mice. Human prostatic carcinoma cell line derived from a bone metastasis of a patient (PC-3) prostate [19], protatic carcinoma cell line derived from a supraclavicular lymph node (LNCaP) prostate [20] and U87MG glioma tumors [21] were grown subcutaneously in athymic (Crl nu:nu) mice. Mammary tumors were obtained from female MMTV/PyMT mice, which spontaneously develop neoplasms due to activation of the polyoma middle T oncogene (MT) under control of the mouse mammary tumor virus (MMTV) promoter [22]. Prostate tumors were obtained from transgenic adenoma of prostate (TRAMP) mice [23].

Retinal vascular development

Vascular development in the retina progresses from the optic nerve head, extending peripherally along the inner retinal surface and finally invading the outer retinal layers. The laminar anatomy of the retina and the fact that vascularization largely occurs postnatally make this tissue a very useful model for the study of neovascular sprouting [24, 25]. Eyes were taken from postnatal days 2 and 7 (P2 and P7) C57Bl/6 mice following daily intraperitoneal bromodeoxyuridine (BrdU) (Sigma, St. Louis, Missouri) injections (80 μg/g body weight) to allow subsequent identification of proliferating vascular cells. Eyes were sectioned in a plane oriented sagitally to the optic nerve, so that each section represented a slice of the entire eyeball and retina. Immunostaining was then used to identify the tips of the most peripheral blood vessels in the primary vascular plexus, marking the transition between the vascular and avascular retinal tissue.

Transplantation of transgenic prostate and breast tumors

Breast and prostate tumors, respectively, were dissected from sacrificed MMTV/PyMT and TRAMP mice, both of which have an nerve/glial antigen 2 (NG2)+/+, C57Bl/6 genetic background. As described below, tumor fragments were transplanted into C57Bl/6, NG2-/- (NG2 knockout) mice [26] to determine whether the pericytes in tumor neovasculature are host or tumor-derived.

For mammary tumor transplantation, female NG2 knockout mice were anesthetized with Avertin, and an inverted Y-shaped incision was made through the abdominal skin [27]. The number-four mammary fat pads were exposed by a blunt dissection, and a small incision (1 mm) was made in each fat pad to accommodate 1 mm^3 PyMT tumor fragments. The incision was closed using metal clips, and the mice were followed for 3 months to allow tumors to grow to a size of 1 cm^3.

The cornea is a transparent, avascular tissue which enables real-time identification of new pathologic vessels that form as a result of implantation of tumor fragments [28]. NG2 knockout mice were anesthetized with Avertin, and tumor fragments (0.027 mm^3) from 8-month-old TRAMP mice were implanted into corneal stromal micropockets created using a modified von Graefe knife [29]. The mice were monitored by biomicroscopic examination for two weeks to follow the progress of tumor vascularization within the corneal stroma.

Immunohistochemistry and vascular imaging

Following fixation of all tissues in 4% paraformaldehyde, cryopreservation in 20% sucrose in phosphate-buffered saline (PBS) at 4 °C, embedding in O.C.T. compound (Sakura Inc., Torrance, California), and snap-freezing, frozen histologic sections (40–80 μm) were cut using a Reichert cryostat (Reichert Inc., Buffalo, New York).

Endothelial cells have been shown to express different cell surface markers as a function of developmental age [30]. We therefore identified endothelial cells using a cocktail of antibodies against endoglin (CD105),

PECAM-1 (CD31), and VEGF receptor-2 (flk-1) (Pharmingen, San Diego, California), a strategy that has been previously utilized to maximize labeling of all vascular endothelial cells, both immature and mature [11]. Pericytes were identified by labeling with affinity-purified rabbit polyclonal antibodies prepared in our laboratory against the NG2 proteoglycan or the platelet-derived growth factor beta receptor (PDGF β-receptor) [9, 16]. Both NG2 and PDGF β-receptor are regarded as specific markers for pericytes [12, 31]. Proliferative pericyte and endothelial cell populations were identified immunohistochemically using anti-BrdU antibody (Fitzgerald Industries, Concord, Massachusetts) [32–34]. Briefly, frozen sections were digested with 0.005% pepsin (Sigma, St. Louis, Missouri) in 0.01 HCl for 30 min at 37 °C followed by treatment with 4N HCl for 30 min at room temperature. Sections were then blocked by incubation in 5% goat serum in PBS for 30 min [35] prior to incubation with antibody.

Confocal microscopic imaging of combined endothelial (CD31 + CD105 + VEGF receptor-2, flk1) [11, 30] and pericyte markers (NG2 or PDGF β-receptor) was performed as described previously [9, 16, 36]. Briefly, optical sections were obtained from the specimens using the Bio-Rad MRC-1024MP confocal microscope. Serial optical sections (1 μm each) across the entire thickness (40–80 μm) of the histological specimens were overlaid (Z-stack) to provide reconstructions of entire vessels. This allowed unambiguous identification of the spatial relationship between pericytes and endothelial cells in the vessel wall. In order to estimate the frequency of vessels in any given tissue that contained endothelium-free segments (pericyte tubes), we performed systematic random sampling [37] to obtain 10 histologic sections for each tissue type to represent the corresponding frozen tissue block. Following immunohistochemistry, we counted the number of such endothelium-free segments (pericyte tubes) by microscopy, and divided the number of pericyte tubes by the total number of vessels in immunostained sections.

Fluorescein microangiography integrated with immunohistochemistry

To determine the functionality of pericyte tubes in a subcutaneous B16F1 melanoma, we performed fluorescein angiography using high molecular weight (two million daltons) dextran conjugated with fluorescein isothiocyanate (Sigma, St. Louis, Missouri). Since FITC-dextran remains completely within the vascular lumen without diffusion or decay [38], this procedure identifies only those vessels that are actively perfused by the circulation. FITC-dextran-perfused tissues were sectioned and immunostained for PDGF β-receptor or NG2 (red fluorochrome) to identify vessel walls in which pericytes interface directly with the intraluminal FITC-dextran.

Results

Pericyte tubes in early angiogenic sprouts

Examination of sections taken from spontaneous mammary tumors in female MMTV-PyMT mice reveals that a subpopulation of angiogenic tumor microvessels (1%) contain endothelium-free segments in which the vascular lumen is formed by a pericyte tube (Figures 1a–c). This phenomenon is remarkably similar to that observed in our corneal angiogenesis studies [16]. The Z-stack overlay demonstrates the absence of endothelial markers associated with the pericyte tube across the entire extent of the vessel in question (arrows and Δ in panel c). In the more typical vessels containing endothelial elements, we consistently noted extensive pericyte investment of the endothelium (panel c). Since it has been proposed that activated pericytes may be involved in creating/marking pathways for invading endothelial cells [4, 39], we wondered if pericyte tubes might represent an early developmental stage of microvessel development at which formation of the vascular endothelium is not complete. To test this possibility, we examined much younger (12 days old) tumors produced by subcutaneous grafts of mouse Lewis lung carcinoma cells in C57Bl/6 mice. Sections of these tumors contain even more striking examples in which entire vessels appear to be composed of pericyte tubes (Figures 1d–f). As before, the Z-stack demonstrates that these tubes are devoid of endothelial markers across their entire width. Even younger tumors (7 days) produced by subcutaneous xenografts of human PC-3 prostate tumor cells into athymic male mice (Figures 1g–i) contain examples not only of endothelium-free pericyte tubes (arrows and Δ in panel i), but also large numbers of individual pericytes invading the tumor in the absence of endothelial cells. TRAMP, LNCaP, and U87MG glioma tumors were also examined and found to contain populations of pericyte tubes (data not shown).

To investigate the occurrence of pericyte tubes in normally developing microvasculature, we examined the mouse retina, in which a primary vascular plexus develops postnatally at the interface between the retina and vitreous. In addition to comparing endothelial and pericyte-specific markers, we also evaluated these samples for cell proliferation by immunohistochemical staining for BrdU incorporation. The sagital orientation of the sections made it possible to identify the tips of angiogenic sprouts growing toward more peripheral regions of the retina (arrow in Figure 2a). We used Nomarski interference microscopy (as in Figure 2c) to help choose sections that appeared to contain intact sprout tips. Between postnatal days 2 and 7 it is clear that pericytes and endothelial cells are both present at the growing tip of the vascular sprout. Using confocal microscopy, we found examples of endothelium-free segments of growing sprouts that appeared to be formed by pericytes (Δ in panel b), demonstrating the occurrence of pericyte tubes in normal as well as pathological

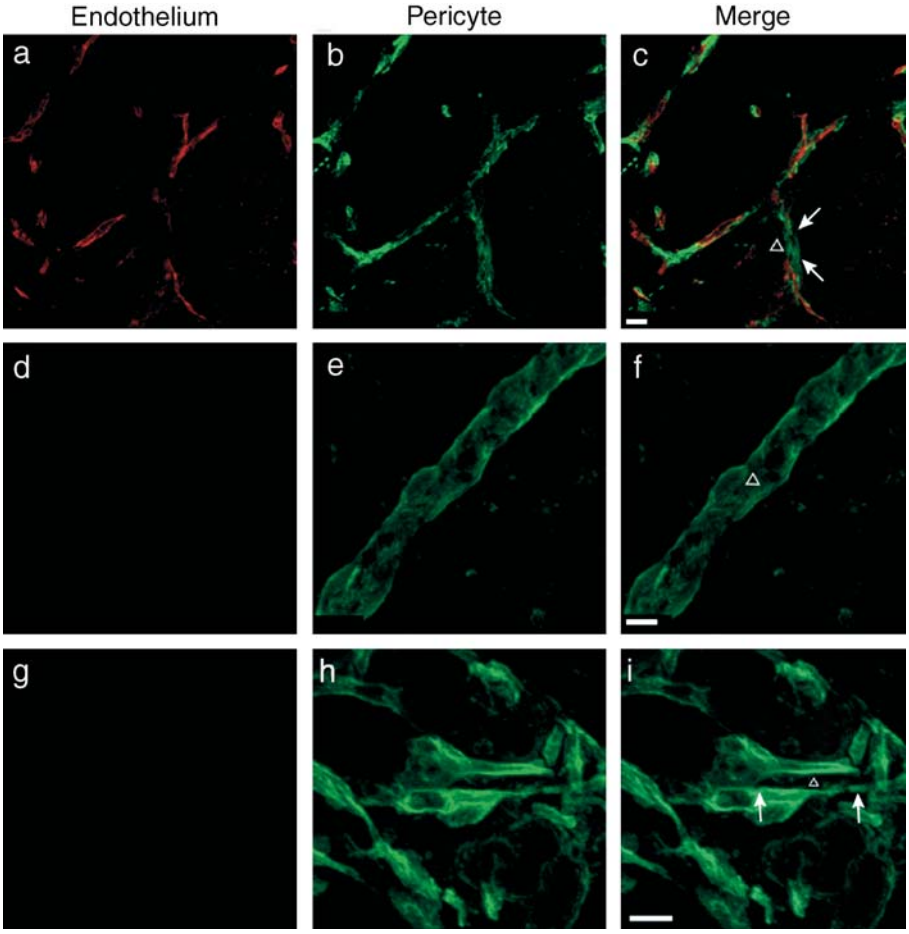

Figure 1. Pericyte tubes are a component of tumor microvasculature. Frozen sections were taken from spontaneous MMTV-PyMT breast carcinoma (a–c), subcutaneous Lewis lung carcinoma (d–f), and subcutaneous PC-3 prostate tumor (g–i). Vascular endothelial elements (red) are identified by combined immunohistochemical staining for CD31, CD105, and flk-1. Pericytes (green) are identified by staining for NG2 proteoglycan. All panels are Z-stack confocal images. All three tumor types contain endothelium-free pericyte tubes, labeled by Δ in the merged images of panels c, f and i. The margins of complete pericyte tubes are indicated with arrows in c and i. In f the entire segment is a pure pericyte tube. Note the absence of endothelium (a, d, g and c, f, i) in regions that contain pericyte tubes (b, e, h). Scale bars indicate 10 μm.

microvasculature. The frequency of pericyte tubes in retinal microvasculature was similar to that seen in the various tumor models (1%). Strikingly, both endothelial cells (arrows) and pericytes (arrowheads) in growing retinal vessel tips have nuclei that are BrdU-positive. The pericyte nucleus characteristically fills almost the entire soma of the cell and bulges away from the lumen of the microvessel [8]. These factors explain why some pericyte nuclei in Figure 2b occupy an extreme peripheral position relative to the vessel. It is clear from the accompanying Nomarski image (Figure 2c) however, that these nuclei belong to pericytes that are closely associated with the microvessel. The presence of these BrdU-labeled nuclei is consistent with the nascent character of the vessel and shows that both cell populations are mitotically active at this stage. In microvessels such as these that contain both pericytes and endothelial cells, we always noted extensive investment of the endothelium by PDGF β-receptor-positive, NG2-positive pericytes. This is a general characteristic of microvessels in the central nervous system [3, 8, 31].

Pericyte tubes are perfused by the tumor circulation

Sections of a subcutaneous B16F1 melanoma tumor perfused with FITC-dextran were examined to evaluate whether pericyte tubes are a functional component of the circulation. In 1% of the angiogenic vessels in these specimens, we observed a direct interface (Figure 3c) between pericytes (Figure 3a) and luminal FITC-dextran (Figure 3b), indicative of patency of the pericyte tube. This phenomenon was seen using either PDGF β-receptor immunostaining (Figure 3) or NG2 immunostaining (not shown) to identify pericytes. Since FITC-dextran does not leak and diffuse from blood vessels, the only way for a pericyte tube to be filled with the dye is to be connected to the active circulation.

Pericytes in transplanted tumor microvessels are of host origin

Just as it has been suggested that tumor cells can display endothelial markers and contribute to forming the

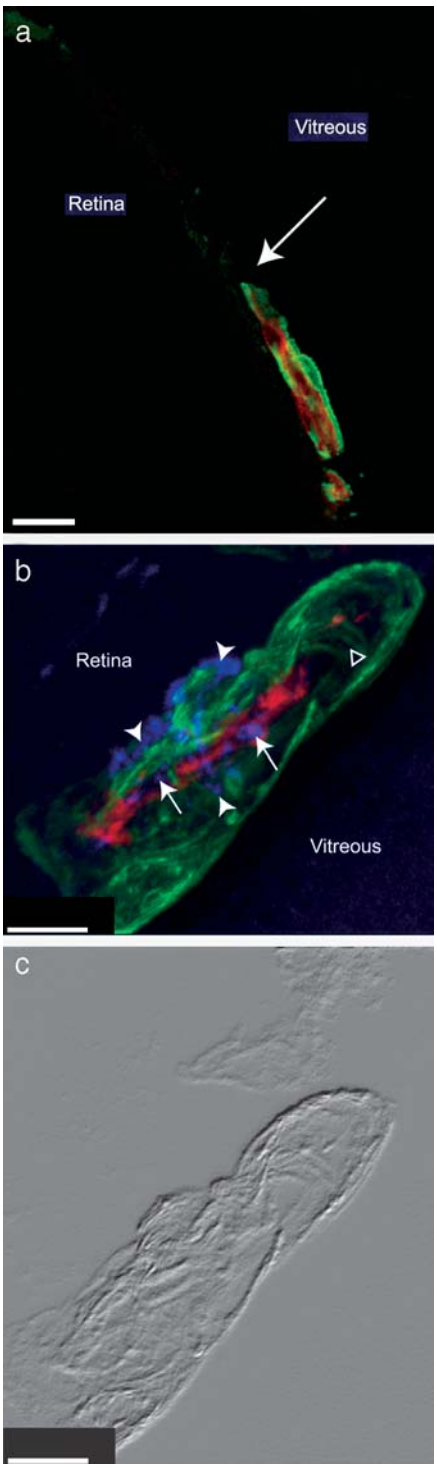

Figure 2. Early pericyte association with angiogenic microvessels in newborn mouse retina. Frozen sections of P2 (a) and P7 (b and c) mouse retina were processed by immunohistochemistry to identify the vascular endothelium (combined CD31 + CD105 + flk-1, red), pericytes (NG2, green), and nuclei of mitotic cells (BrdU, purple, panel b). Z-stack confocal images show that vascular pericytes extensively invest the angiogenic sprouts at both ages. Arrow in panel a indicates the tip of the growing angiogenic sprout at the vascular/avascular junction in the P2 peripheral retina. At P7 (panels b and c) both pericytes (arrowheads) and endothelial cells (arrows) contain BrdU-positive nuclei. Δ marks an endothelium free, pericyte tube-containing region of the angiogenic sprout. Panel c is the Nomarski image of a single focal plane from the specimen shown in panel b. Scale bars indicate 20 μm (a) and 5 μm (b, c).

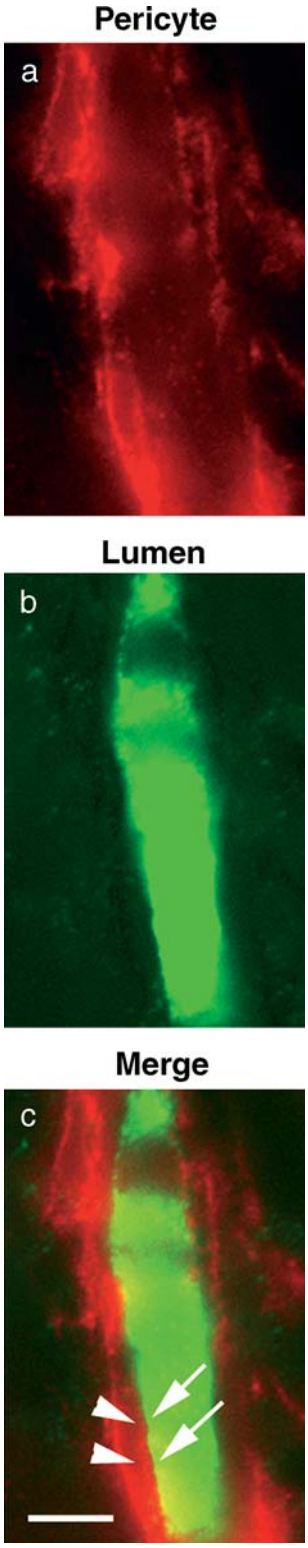

Figure 3. Functional (perfused) pericyte tube. In sections obtained from a subcutaneous B16F1 melanoma perfused with FITC-dextran, a pericyte tube immunostained (red) for PDGF β-receptor (a), is in direct contact with the vascular lumen filled with FITC-dextran (green) (b). In the merged image (c), arrowheads identify pericytes forming the vessel wall. Arrows indicate FITC-dextran in the lumen of the pericyte tube. The direct interface between these two labels precludes the presence of an intervening endothelial cell layer. Scale bar indicates 10 μm.

lumen of tumor vessels, it is formally possible that our observations could be explained by the acquisition of pericyte markers (such as NG2 and PDGF β-receptor) by tumor cells at the vascular lumen. Arguing against this possibility, B16F1, PC3, Lewis lung carcinoma, LNCaP, and U87MG cells were all found to be negative for CD105, CD31, flk-1, NG2 and PDGF β-receptor expression both *in vivo* and *in vitro*. TRAMP and PyMT tumor cells were also negative for NG2 expression (Figures 4b, d and f). Still, this does not preclude the possibility that rare, specialized tumor cells at the vascular lumen might be induced to express NG2 by virtue of the novel environment. Tumor transplantation experiments were performed to address this possibility.

Analysis of breast tumor fragments transplanted from an NG2-positive (MMTV/PyMT) donor into the fat pads of an NG2 knockout host revealed PDGF β-receptor-positive pericytes associated with angiogenic sprouts invading the tumor from the periphery (Figure 4a). These pericytes were invariably NG2-negative (Figure 4b). Likewise, examination of prostate tumor fragments transplanted from an NG2-positive donor (TRAMP) into the cornea of an NG2 knockout host revealed PDGF β-receptor-positive pericytes (Figure 4c) associated with the corneal neovasculature. Once again, these pericytes were always negative for NG2 expression (Figure 4d). If the lumenal NG2-positive cells we have observed in our experiments with NG2-wildtype mice were of tumor origin, we would also expect to find such cells in the tumor vasculature of NG2-null mice. The fact that PDGF β-receptor-positive lumenal cells express NG2 in tumors grown in wildtype mice but not in tumors grown in NG2-null mice argues strongly that lumenal pericytes of the tumor microvasculature are derived from the host rather than from any component of the donor tumor.

Discussion

Two of the observations presented in our study seem especially noteworthy. First, mitotically active pericytes are associated with angiogenic sprouts during the early phases of neovascularization in both pathologic (tumors) and normal (retinal) tissues. Second, pericytes alone can invade tissues in the absence of endothelial cells and can form functional, endothelium-free tubes that may be sub-classified as 'pericyte tubes' under the category of class-5 vessels.

These observations support the idea that activated, mitotic pericytes play an early role in the development of angiogenic sprouts and vessels. Coupled with our previous finding of pericytes associated with angiogenic sprouts in the embryonic central nervous system and in postnatal neovasculature formed in response to ischemia or growth factors [9, 16], these results emphasize the early participation of pericytes in both physiological and pathological angiogenesis. Activated pericytes are present as early as mitotic endothelial cells, and in some instances appear to take the lead in establishing not only pathways of invasion, but also the formation of actual tubes. These findings are not entirely consistent with data suggesting that pericytes have only a late role in angiogenesis [40–42], but instead provide support for reports concerning an early role for pericytes in the formation of angiogenic sprouts [4, 12, 31, 39, 43–47]. Our identification of perfused, endothelium-free pericyte tubes comprising up to 1% of the total number of microvessels in our various preparations may be a reflection of the kinetics of angiogenic development. While pericytes may have a leading role in establishing pathways of invasion and formation of angiogenic tubes, endothelial cell participation cannot lag far behind, and may in fact occur almost simultaneously. Thus in most cases, especially in normal tissues, we observe pericytes and endothelial cells working in concert to form angiogenic microvessels composed of endothelial tubes extensively invested by pericytes. In this sense, pericyte tubes and pericyte-invested endothelial tubes do not represent distinct functional entities, but instead different developmental stages of the same process. In only a small number of instances do we catch a glimpse of pericyte tubes that are not yet fully lined by endothelial cells. It seems possible that sufficient disregulation could occur during tumor angiogenesis to render the early contributions of pericytes more easily detectable.

An alternative mechanism for the formation of pericyte tubes could be the loss of endothelial cells as part of the process of vascular regression/pruning and remodeling. We cannot definitively rule out this possibility. However, it seems the less likely of the two alternatives, based on the following observations. In the developing retina, neovascular remodeling is primarily seen in the central retina, rather than in peripheral areas of the retina that contain the newest angiogenic sprouts [48]. The examples shown in Figure 2 are taken from the peripheral retina at the outermost boundary between the vascular and avascular retina. The structures shown are therefore likely to be nascent sprouts rather than vessels undergoing remodeling. The presence of BrdU-positive endothelial cell nuclei further supports the idea that these are new sprouts rather than regressing vessels. In the tumor studies, it is more difficult to evaluate the ontogeny of vessels in the absence of the stereotypical tissue architecture found in the retina. On the basis of tumor age and the possible existence of hypoxic areas within the tumor, it seems possible that regressing vessels might contribute to the labeling pattern seen in the mature mammary tumors (Figures 1a–c). It seems much less likely that endothelial cell regression can explain the patterns seen in the small, nascent tumor xenografts examined only 12 (d–f) and 7 (g–i) days after tumor cell injection. Endothelial cells from regressing vascular segments usually do not disappear (for example via apoptosis), but instead are re-utilized for the formation of new vessels [49]. Thus, the observation of pericytes invading the seven-day-old PC-3 tumor and

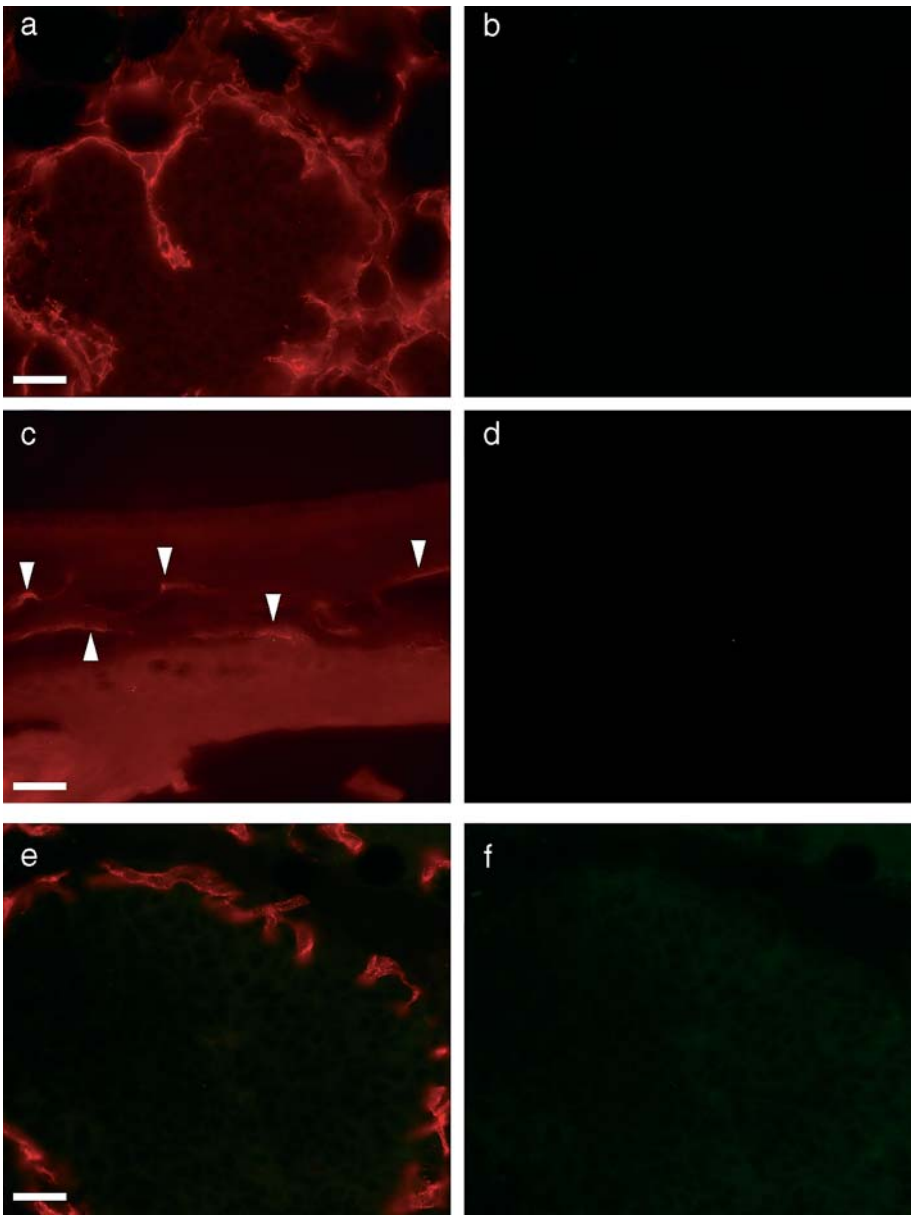

Figure 4. Host origin of pericytes in tumors. (a, b) Section from a PyMT breast tumor fragment transplanted to the fat pad of an NG2 knockout mouse is double-stained for PDGF β-receptor (a) and NG2 (b). Vascular pericytes invading the tumor are immunostained for PDGF β-receptor (a) but not for NG2 (b). (c, d) Section of a TRAMP prostate tumor fragment transplanted to the corneal stroma of an NG2 knockout mouse is double-stained for PDGF β-receptor (c) and NG2 (d). Neovascular pericytes are immunostained for PDGF β-receptor (c) but not for NG2 (d). Arrowheads indicate feeder vessels invading the cornea. (e, f) Section of PyMT breast tumor fragment transplanted to the fat pad of NG2 knockout mouse is double-stained for endothelial markers (CD105 + CD31 + flk1) (e) and NG2 (f). Angiogenic vessels exhibit immunostaining for endothelial markers (e) but not for NG2 (f). Tumor cells are not immunostained for either endothelial markers (e) or NG2 (f). Scale bars indicate 20 μm.

forming tubes in the absence of endothelial cells is more suggestive of the formation of new microvessels than the regression of old ones.

Although pericytes are widely regarded to be the microvascular equivalent of smooth muscle cells, the origin, development, and function of these cells seem to be variable and complex [8, 50, 51]. Reliable identification of pericytes is important for understanding the role of these cells in angiogenic sprout formation and vascular heterogeneity. Our ability to detect the precocious contribution of pericytes to microvascular development depends heavily on the use of PDGF β-receptor and NG2 proteoglycan as markers for these activated mural cells at an early stage of their development [12, 31]. One of the traditional markers for pericyte identification has been the expression of alpha-smooth muscle actin (α-SMA). However, a growing body of evidence suggests that α-SMA is a late marker for differentiated pericytes in rodents and therefore may be poorly expressed in developing angiogenic microvasculature [12, 31]. Since only a fraction of developing pericytes can be identified on the basis of α-SMA expression [4, 12, 52–55], the absence of immunoreactivity for α-SMA does not necessarily indicate the absence of pericytes. By comparison, NG2 is more widely expressed by pericytes, especially during early stages of development. Pericytes

expressing NG2 also express other pericyte markers such as PDGF β-receptor [9, 16, 36, 56–58] and aminopeptidase A [45]. Therefore, NG2 is an established, specific marker for identification of pericytes. It is expressed by pericytes in angiogenic microvasculature during pre- and postnatal development [9, 59], during tumor angiogenesis [43, 44, 60], in granulation tissue [43, 44, 58, 61], and in corneal and retinal angiogenesis models [16].

Our results more firmly establish endothelium-free pericyte tubes as a valid species of angiogenic vessel. Our tumor fragment transplantation experiments support previous results demonstrating a host origin for pericytes in tumor neovasculature [62]. Direct visualization of the invasion of host-derived, GFP-negative cells into GFP-positive tumors has provided additional evidence for the host origin of tumor vasculature [63]. Our combined fluorescein angiography–immunohistochemistry analysis of tumor vasculature is also of interest in this regard, since it provides an additional means of visualizing functional, newly formed pericyte tubes that have recently invaded the tumor.

In summary, our study provides evidence that pericytes contribute to the early phases of angiogenic sprout formation during both neoplastic and non-neoplastic neovascularization. The early participation of pericytes in microvascular development has important implications for therapeutic intervention in the many pathologies in which angiogenesis is a factor. As early players in angiogenesis, pericytes represent an additional target for treatments designed either to up-regulate (for example in ischemic disorders) or down-regulate (for example in cancer) vascularization. Recent studies suggest that dual targeting of pericytes and endothelial cells improves the efficacy of treatments aimed at the destruction of tumor masses [64, 65]. Clearly, the design of improved dual targeting strategies aimed at both pericytes and endothelial cells will depend on further understanding of the role of pericytes in neovascularization.

Acknowledgements

We are indebted to Larry Young, University of California at Davis, for providing the PyMT mammary tumor specimens. This work was supported by postdoctoral fellowship 0120036Y from the American Heart Association Western States Affiliate, New Investigator Grant PC020822 from the US Department of Defense Prostate Cancer Research Program DAMD, and NIH grant RO3 HD044783-01 to Dr Ozerdem, and by NIH grant RO1 CA95287 to Dr Stallcup.

References

1. Folkman J. Angiogenesis in cancer, vascular, rheumatoid and other disease. Nat Med 1995; 1: 27–31.
2. Risau W. Mechanisms of angiogenesis. Nature 1997; 386: 671–4.
3. Sims DE. Recent advances in pericyte biology – implications for health and disease. Can J Cardiol 1991; 7: 431–43.
4. Nehls V, Denzer K, Drenckhahn D. Pericyte involvement in capillary sprouting during angiogenesis *in situ*. Cell Tissue Res 1992; 270: 469–74.
5. Rhodin JA. Ultrastructure of mammalian venous capillaries, venules, and small collecting veins. J Ultrastruct Res 1968; 25: 452–500.
6. Bergers G, Benjamin LE. Tumorigenesis and the angiogenic switch. Nat Rev Cancer 2003; 3: 401–10.
7. Darland DC, D'Amore PA. Blood vessel maturation: Vascular development comes of age. J Clin Invest 1999; 103: 157–8.
8. Sims DE. The pericyte – a review. Tissue Cell 1986; 18: 153–74.
9. Ozerdem U, Grako KA, Dahlin-Huppe K et al. NG2 proteoglycan is expressed exclusively by mural cells during vascular morphogenesis. Dev Dyn 2001; 222: 218–27.
10. Warren BA. The vascular morphology of tumors. In Peterson H-I (ed) Tumor Blood Circulation: Angiogenesis, Vascular Morphology and Blood Flow of Experimental and Human Tumors. Boca Raton, Florida: CRC Press 1979; 31–9.
11. Chang YS, di Tomaso E, McDonald DM et al. Mosaic blood vessels in tumors: Frequency of cancer cells in contact with flowing blood. Proc Natl Acad Sci USA 2000; 97: 14608–13.
12. McDonald DM, Choyke PL. Imaging of angiogenesis: From microscope to clinic. Nat Med 2003; 9: 713–25.
13. Folberg R, Hendrix MJ, Maniotis AJ. Vasculogenic mimicry and tumor angiogenesis. Am J Pathol 2000; 156: 361–81.
14. Hendrix MJ, Seftor EA, Hess AR, Seftor RE. Angiogenesis: Vasculogenic mimicry and tumour-cell plasticity: Lessons from melanoma. Nat Rev Cancer 2003; 3: 411–21.
15. Sood AK, Seftor EA, Fletcher MS et al. Molecular determinants of ovarian cancer plasticity. Am J Pathol 2001; 158: 1279–88.
16. Ozerdem U, Monosov E, Stallcup WB. NG2 proteoglycan expression by pericytes in pathological microvasculature. Microvasc Res 2002; 63: 129–34.
17. O'Reilly MS, Holmgren L, Shing Y et al. Angiostatin: A novel angiogenesis inhibitor that mediates the suppression of metastases by a Lewis lung carcinoma. Cell 1994; 79: 315–28.
18. Fidler IJ. Biological behavior of malignant melanoma cells correlated to their survival *in vivo*. Cancer Res 1975; 35: 218–24.
19. Kaighn ME, Narayan KS, Ohnuki Y et al. Establishment and characterization of a human prostatic carcinoma cell line (PC-3): Invest Urol 1979; 17: 16–23.
20. Horoszewicz JS, Leong SS, Chu TM et al. The LNCaP cell line – a new model for studies on human prostatic carcinoma. Prog Clin Biol Res 1980; 37: 115–32.
21. Ponten J, Macintyre EH. Long term culture of normal and neoplastic human glia. Acta Pathol Microbiol Scand 1968; 74: 465–86.
22. Guy CT, Cardiff RD, Muller WJ. Induction of mammary tumors by expression of polyomavirus middle T oncogene: A transgenic mouse model for metastatic disease. Mol Cell Biol 1992; 12: 954–61.
23. Greenberg NM, DeMayo F, Finegold MJ et al. Prostate cancer in a transgenic mouse. Proc Natl Acad Sci USA 1995; 92: 3439–43.
24. Ozaki H, Seo MS, Ozaki K et al. Blockade of vascular endothelial cell growth factor receptor signaling is sufficient to completely prevent retinal neovascularization. Am J Pathol 2000; 156: 697–707.
25. Campochiaro PA. Retinal and choroidal neovascularization. J Cell Physiol 2000; 184: 301–10.
26. Grako KA, Ochiya T, Barritt D et al. PDGF (alpha)-receptor is unresponsive to PDGF-AA in aortic smooth muscle cells from the NG2 knockout mouse. J Cell Sci 1999; 112: 905–15.
27. Daniel CW, De Ome KB, Young JT et al. The *in vivo* life span of normal and preneoplastic mouse mammary glands: A serial transplantation study. Proc Natl Acad Sci USA 1968; 61: 53–60.
28. Gimbrone Jr, MA, Cotran RS, Leapman SB, Folkman J. Tumor growth and neovascularization: An experimental model using the rabbit cornea. J Natl Cancer Inst 1974; 52: 413–27.

29. Kenyon BM, Voest EE, Chen CC et al. A model of angiogenesis in the mouse cornea. Invest Ophthalmol Vis Sci 1996; 37: 1625–32.
30. Drake CJ, Fleming PA. Vasculogenesis in the day 6.5 to 9.5 mouse embryo. Blood 2000; 95: 1671–9.
31. Gerhardt H, Betsholtz C. Endothelial-pericyte interactions in angiogenesis. Cell Tissue Res 2003; 314: 15–23.
32. Dolbeare F, Gratzner H, Pallavicini MG, Gray JW. Flow cytometric measurement of total DNA content and incorporated bromodeoxyuridine. Proc Natl Acad Sci USA 1983; 80: 5573–7.
33. Dean PN, Dolbeare F, Gratzner H et al. Cell-cycle analysis using a monoclonal antibody to BrdUrd. Cell Tissue Kinet 1984; 17: 427–36.
34. Nowakowski RS, Lewin SB, Miller MW. Bromodeoxyuridine immunohistochemical determination of the lengths of the cell cycle and the DNA-synthetic phase for an anatomically defined population. J Neurocytol 1989; 18: 311–8.
35. Ezaki T, Baluk P, Thurston G et al. Time course of endothelial cell proliferation and microvascular remodeling in chronic inflammation. Am J Pathol 2001; 158: 2043–55.
36. Lindahl P, Johansson BR, Leveen P, Betsholtz C. Pericyte loss and microaneurysm formation in PDGF-B-deficient mice. Science 1997; 277: 242–5.
37. Dawson B, Trapp RG. Basic and Clinical Biostatistics, 3rd ed. New York: McGraw-Hill 2001.
38. D'Amato R, Wesolowski E, Smith LE. Microscopic visualization of the retina by angiography with high- molecular-weight fluorescein-labeled dextrans in the mouse. Microvasc Res 1993; 46: 135–42.
39. Rhodin JA, Fujita H. Capillary growth in the mesentery of normal young rats. Intravital video and electron microscope analyses. J Submicrosc Cytol Pathol 1989; 21: 1–34.
40. Sato Y, Rifkin DB. Inhibition of endothelial cell movement by pericytes and smooth muscle cells: Activation of a latent transforming growth factor-beta 1-like molecule by plasmin during coculture. J Cell Biol 1989; 109: 309–15.
41. Beck Jr, L, D'Amore PA. Vascular development: Cellular and molecular regulation. FASEB J 1997; 11: 365–73.
42. Hirschi KK, Rohovsky SA, Beck LH et al. Endothelial cells modulate the proliferation of mural cell precursors via platelet-derived growth factor-BB and heterotypic cell contact. Circ Res 1999; 84: 298–305.
43. Schlingemann RO, Rietveld FJ, de Waal RM et al. Expression of the high molecular weight melanoma-associated antigen by pericytes during angiogenesis in tumors and in healing wounds. Am J Pathol 1990; 136: 1393–405.
44. Schlingemann RO, Rietveld FJ, Kwaspen F et al. Differential expression of markers for endothelial cells, pericytes, and basal lamina in the microvasculature of tumors and granulation tissue. Am J Pathol 1991; 138: 1335–47.
45. Schlingemann RO, Oosterwijk E, Wesseling P et al. Aminopeptidase a is a constituent of activated pericytes in angiogenesis. J Pathol 1996; 179: 436–42.
46. Wesseling P, Schlingemann RO, Rietveld FJ et al. Early and extensive contribution of pericytes/vascular smooth muscle cells to microvascular proliferation in glioblastoma multiforme: An immuno-light and immuno-electron microscopic study. J Neuropathol Exp Neurol 1995; 54: 304–10.
47. Morikawa S, Baluk P, Kaidoh T et al. Abnormalities in pericytes on blood vessels and endothelial sprouts in tumors. Am J Pathol 2002; 160: 985–1000.
48. Gerhardt H, Golding M, Fruttiger M et al. VEGF guides angiogenic sprouting utilizing endothelial tip cell filopodia. J Cell Biol 2003; 161: 1163–77.
49. Hughes S, Chang-Ling T. Roles of endothelial cell migration and apoptosis in vascular remodeling during development of the central nervous system. Microcirculation 2000; 7: 317–33.
50. Le Lievre CS, Le Douarin NM. Mesenchymal derivatives of the neural crest: Analysis of chimaeric quail and chick embryos. J Embryol Exp Morphol 1975; 34: 125–54.
51. Allt G, Lawrenson JG. Pericytes: Cell biology and pathology. Cells Tissues Organs 2001; 169: 1–11.
52. Nehls V, Drenckhahn D. Heterogeneity of microvascular pericytes for smooth muscle type alpha-actin. J Cell Biol 1991; 113: 147–54.
53. Balabanov R, Dore-Duffy P. Role of the CNS microvascular pericyte in the blood-brain barrier. J Neurosci Res 1998; 53: 637–44.
54. Boado RJ, Pardridge WM. Differential expression of alpha-actin mRNA and immunoreactive protein in brain microvascular pericytes and smooth muscle cells. J Neurosci Res 1994; 39: 430–5.
55. Alliot F, Rutin J, Leenen PJ, Pessac B. Pericytes and periendothelial cells of brain parenchyma vessels co-express aminopeptidase N, aminopeptidase A, and nestin. J Neurosci Res 1999; 58: 367–78.
56. Reuterdahl C, Sundberg C, Rubin K et al. Tissue localization of beta receptors for platelet-derived growth factor and platelet-derived growth factor B chain during wound repair in humans. J Clin Invest 1993; 91: 2065–75.
57. Sundberg C, Ljungstrom M, Lindmark G et al. Microvascular pericytes express platelet-derived growth factor-beta receptors in human healing wounds and colorectal adenocarcinoma. Am J Pathol 1993; 143: 1377–88.
58. Rajkumar VS, Sundberg C, Abraham DJ et al. Activation of microvascular pericytes in autoimmune Raynaud's phenomenon and systemic sclerosis. Arthritis Rheum 1999; 42: 930–41.
59. Grako KA, Stallcup WB. Participation of the NG2 proteoglycan in rat aortic smooth muscle cell responses to platelet-derived growth factor. Exp Cell Res 1995; 221: 231–40.
60. Chekenya M, Enger PO, Thorsen F et al. The glial precursor proteoglycan, NG2, is expressed on tumour neovasculature by vascular pericytes in human malignant brain tumours. Neuropathol Appl Neurobiol 2002; 28: 367–80.
61. Sims DE. Diversity within pericytes. Clin Exp Pharmacol Physiol 2000; 27: 842–6.
62. Abramsson A, Berlin O, Papayan H et al. Analysis of mural cell recruitment to tumor vessels. Circulation 2002; 105: 112–7.
63. Yang M, Baranov E, Wang JW et al. Direct external imaging of nascent cancer, tumor progression, angiogenesis, and metastasis on internal organs in the fluorescent orthotopic model. Proc Natl Acad Sci USA 2002; 99: 3824–9.
64. Bergers G, Song S, Meyer-Morse N et al. Benefits of targeting both pericytes and endothelial cells in the tumor vasculature with kinase inhibitors. J Clin Invest 2003; 111: 1287–95.
65. Saharinen P, Alitalo K. Double target for tumor mass destruction. J Clin Invest 2003; 111: 1277–80.

Angiogenesis **7:** 269–276, 2004.

Pathological angiogenesis is reduced by targeting pericytes via the NG2 proteoglycan

Ugur Ozerdem[1] & William B. Stallcup[2]
[1]*La Jolla Institute for Molecular Medicine, Vascular Biology Division, La Jolla, California, USA;* [2]*The Burnham Institute, Neurobiology Program, La Jolla, California, USA*

Received 12 July 2004; accepted in revised form 23 September 2004

Key words: angiogenesis, cornea, endothelium, model, mural, neovascularization, NG2, pericyte, retina, targeting

Abstract

The NG2 proteoglycan is expressed by nascent pericytes during the early stages of angiogenesis. To investigate the functional role of NG2 in neovascularization, we have compared pathological retinal and corneal angiogenesis in wild type and NG2 null mice. During ischemic retinal neovascularization, ectopic vessels protruding into the vitreous occur twice as frequently in wild type retinas as in NG2 null retinas. In the NG2 knock-out retina, proliferation of both pericytes and endothelial cells is significantly reduced, and the pericyte:endothelial cell ratio falls to 0.24 from the wild type value of 0.86. Similarly, bFGF-induced angiogenesis is reduced more than four-fold in the NG2 null cornea compared to that seen in the wild type retina. Significantly, NG2 antibody is effective in reducing angiogenesis in the wild type cornea, suggesting that the proteoglycan can be an effective target for anti-angiogenic therapy. These experiments therefore demonstrate both the functional importance of NG2 in pericyte development and the feasibility of using pericytes as anti-angiogenic targets.

Abbreviations: BrdU – bromodeoxyuridine; CD31 – PECAM-1; CD105 – endoglin; flk 1 – VEGF receptor-2; NG2 – nerve/glial antigen 2; PBS – phosphate-buffered saline; PDGF β-receptor – platelet-derived growth factor beta receptor

Introduction

Angiogenesis is an essential element of many pathological processes, including tumor growth and metastasis, psoriasis, acne rosacea, rheumatoid arthritis, proliferative diabetic retinopathy, retinopathy of prematurity, and age-related macular degeneration [1, 2–4]. The development of anti-angiogenic therapies for treating these pathologies has therefore become an increasingly important goal of biomedical research. Most of these strategies have focused on targeting endothelial cells, which form the inner lining of the vascular tube and are by far the best understood component of neovasculature. However, the walls of typical angiogenic microvessels have a second cellular component: namely, pericytes (mural cells) which form an outer sheath around the endothelium [2, 5, 6]. Much less is known about these perivascular cells, as evidenced by the 115-fold difference in the number of publications on endothelial cells and pericytes, respectively (revealed by a recent search of the *PUBMED* database). The origin, function, and even reliable identification of pericytes have been elusive [5, 7, 8]. As a result, the benefits of using pericytes as an additional target for anti-angiogenic therapy are just beginning to be explored [9, 10].

The effectiveness of using pericytes as anti-angiogenic targets would be expected to depend heavily on the importance of these cells in the development and function of microvessels: i.e. the more important their function, the greater the impact of targeting them. The functional importance of pericytes during angiogenesis is vividly illustrated by the phenotypes of mice in which pericyte development is disrupted. Ablation of PDGF-B or PDGF β-receptor, critical elements for the recruitment and development of pericytes, gives rise to mice that are pericyte-deficient. Depending on the timing and specificity of the ablations, microvessels in these animals, at the very least, have dramatically altered morphologies [11, 12] and in some cases are subject to lethal microaneurysms [13]. Despite their importance, PDGF β-receptor and PDGF-B do not necessarily represent the only effective means of targeting pericytes. During the process of angiogenesis, extensive cross-talk occurs between pericytes and endothelial cells [2, 14, 15]. Accordingly, other cell surface and soluble components that mediate or modulate this cellular

Correspondence to: Ugur Ozerdem, MD, Assistant Professor, 4570 Executive Drive, Suite 100, La Jolla, CA 92121, USA. Tel: +1-858-857-8788, ext. 128; Fax: +1-858-587-6742; E-mail: ozerdem@ljimm.org

cross-talk are likely to be important candidates for targeting. One such pericyte component is the NG2 chondroitin sulfate proteoglycan, which is expressed on the surfaces of vascular mural cells during both normal and pathological angiogenesis [16–20].

The NG2 proteoglycan binds with high affinity to basic fibroblast growth factor (bFGF), platelet-derived growth factor AA (PDGF-AA), and the kringle domains of plasminogen and angiostatin [21, 22]. In addition, NG2 appears to mediate signal transduction events that lead to increased cell spreading and motility [23–27]. This combination of properties, coupled with the high level of NG2 expression on nascent microvascular pericytes during developmental angiogenesis [19], has led us to investigate the functional role of the proteoglycan in neovascularization. Towards this end, we have utilized well-characterized retinal and corneal models to compare the details of pathological angiogenesis in wild type and NG2 null mice. We have previously demonstrated that NG2 expression is restricted to microvascular pericytes, rather than endothelial cells, in pathological ocular angiogenesis [18] and tumor angiogenesis [17]. The genetic ablation of NG2 can therefore be regarded as a specific "intrinsic" targeting of pericytes in pathological microvasculature. We have also used anti-NG2 antibodies for "extrinsic" targeting of pericyte-expressed NG2. Both types of studies demonstrate the functional importance of NG2 during pathological neovascularization, establishing the potential value of the proteoglycan as a pericyte-specific target for anti-angiogenic therapy.

Materials and methods

Experimental animals

NG2 null mice [28] were generated via a conventional homologous recombination approach [29, 30]. The mice were back-crossed onto a C57Bl/6 genetic background for six generations, and NG2+/− heterozygotes were mated to establish separate NG2 knockout (NG2−/−) and wild type (NG2+/+) colonies.

Animal models

All animal studies were performed in accordance with National Institutes of Health Office of Laboratory Animal Welfare (OLAW) guidelines, and were approved by the authors' institutional animal research committees.

Ischemia-induced retinal angiogenesis

Ischemic retinal angiogenesis was induced by withdrawal of neonatal mice from hyperoxia [31]. Litters of postnatal day 7 (P7) NG2 knockout and wild type mice were placed along with their nursing dams in an environmentally controlled chamber (75% oxygen–25% nitrogen atmosphere) for 5 days. At P12, the animals were returned to room air, and at P17 the mice were sacrificed and the eyes enucleated. In total, five mice of each genotype were utilized, allowing comparison of 10 wild type and 10 knockout eyes. The right and left eyes of each mouse were frozen in the same block and sectioned in a plane oriented sagitally to the optic nerve, so that each section represented complete slices of both eyeballs and retinas. Serial sections were cut through the entire thickness of the eyes, yielding between 85 and 132 sections per pair of eyes. Despite this range in the number of sections obtained, the variation was random, with no statistical difference between the number of sections derived from wild type or knockout eyes ($P = 0.0952$, Mann–Whitney test). The total number of cryosections obtained from each group of mice was 1104.

Using systematic random sampling [32], we selected five sections per mouse to provide a representative sampling of both retinas. The sections were stained using the periodic acid-Schiff (PAS) method, with hematoxylin counterstaining as described [31]. This allowed the identification of the so-called neovascular tufts, or clusters of pathological angiogenic vessels protruding beyond the internal limiting membrane of the retina into the vitreous. Quantification of pathological angiogenesis was accomplished by counting the number of vascular cell nuclei in these tufts. We compiled the data according to the number of angiogenic nuclei per section (with each section representing a pair of eyes). We processed five sections per mouse, and therefore compared 25 wild type sections with 25 knockout sections.

In a separate experiment, mice received daily intraperitoneal injections of BrdU (80 μg/g body weight) on postnatal days 14 through 18 after withdrawal from hyperoxia. This allowed subsequent identification of mitotic cells in the pathological vascular tufts present in the P18 retinas. Right and left eyes from each mouse (one wild type and one NG2 null mouse) were frozen in pairs into OCT blocks and sectioned. Two sets of right and left pairs were mounted on each slide. Systematic random sampling was then used to select five slides for each animal. Thus, each animal was represented by 20 sections (10 left eyes and 10 right eyes). Slides were immunostained for PDGF β-receptor and BrdU and counter-stained with hematoxylin. The percentages of mitotic pericytes and endothelial cells were determined after quantifying the number of BrdU-positive nuclei in each of the two immunohistochemically-defined cell types.

Dual hydron pellet corneal angiogenesis

The surgical procedure for inducing corneal angiogenesis in the mouse [33] was modified for this study to incorporate two pellets in the corneal pocket instead of just a single pellet. Slow-release polyhydroxyethyl methacrylate (hydron) (Hydro Med Sciences, Cranbury, New Jersey) pellets ($0.4 \times 0.4 \times 0.2$ mm) were formulated to contain 45 μg sucrose aluminum sulfate (sucralfate) (Sigma, St. Louis, Missouri) plus one of three experimental additives: 90 ng recombinant bFGF (Life Technologies, Carlsbad, California), 0.8 μg affinity-purified rabbit anti-NG2 antibody [17–19], or PBS (control). Ten-week-old mice were anesthetized with Avertin (0.015–0.017 ml/g body weight), and under an operating microscope two pellets were surgically implanted

into the corneal stroma of one eye at a distance of 0.7 mm from the corneo-scleral limbus. Ten NG2 wild-type mice received pairs of pellets containing bFGF and NG2 antibody. Another 10 NG2 wild type mice received pairs of pellets containing bFGF and PBS. Thirteen NG2 knockout mice received pairs of pellets containing bFGF and PBS. Over an 8 day-period after recovery from surgery, the mice were examined under a Leica GZ6 stereomicroscope (Leica, Allendale, New Jersey) to evaluate the progress of corneal angiogenesis in the operated eyes. On day 8, angiogenesis was quantified by determining the area of vascularization, as described previously [33, 34].

Tissue processing, immunohistochemistry, and imaging

Tissues were fixed in 4% paraformaldehyde for 6 h, cryoprotected in 20% sucrose overnight, and frozen in OCT embedding compound (Miles, Inc., Elkhardt, Indiana). Cryostat sections (40 μm) were air-dried onto Superfrost slides (Fisher Scientific, Pittsburgh, Pennsylvania). Immunohistochemical labeling was carried out as previously described [17–19]. Pericytes were identified by labeling with affinity-purified rabbit polyclonal antibodies against the NG2 proteoglycan or the PDGF β-receptor [13, 17–19, 35]. Both NG2 and PDGF β-receptor are regarded as specific markers for pericytes [36, 37]. An affinity-purified rabbit antibody against the alpha subunit of hypoxia-inducible factor-1 (HIF1α) was a generous gift from Dr. Robert Abraham (The Burnham Institute, La Jolla, California).

Since endothelial cells express different cell surface markers as a function of developmental age [38], we identified them using a cocktail of antibodies against endoglin (CD105), PECAM-1 (CD31), and VEGF receptor-2 (flk-1) (Pharmingen, San Diego, California). This strategy has been previously utilized to maximize labeling of all vascular endothelial cells, both immature and mature [17, 39].

Vascular cells in S (synthesis) phase of the cell cycle were identified by means of BrdU (Sigma, St. Louis, Missouri) incorporation and subsequent labeling with sheep anti-BrdU antibody (Fitzgerald Industries, Concord, Massachusetts) [40–42]. Briefly, frozen sections were digested with 0.005% pepsin (Sigma, St. Louis, Missouri) in 0.01 HCl for 30 min at 37 °C followed by treatment with 4 N HCl for 30 min at room temperature. Sections were then blocked by incubation in 5% goat serum in PBS for 30 min [43] prior to incubation with antibody. Fluorescence microscopic imaging of endothelial (CD31 + CD105 + flk1) [38, 39], pericyte (NG2 or PDGF β-receptor) [13, 18, 19], and nuclear (BrdU) markers [43] was performed according to the published methods.

Statistical analysis

Prism 4.0 software (GraphPad, San Diego, California) was used for statistical analyses. Systematic random sampling of serial histological sections was carried out according to previously described methods [32].

Results

Ischemic angiogenesis is diminished in the NG2 null retina (intrinsic targeting)

The stereotyped laminar architecture of the retina makes it an ideal tissue for quantification of ischemic neovascularization[4, 31]. In the hyperoxia model, the return from exposure to 75% oxygen to a normal atmosphere represents relative hypoxia, resulting in the sprouting of new blood vessels from the primary vascular plexus at the inner face of the retina. Many of these new vessels protrude into the vitreous, where they are easily recognized as pathological angiogenic tufts composed of endothelial cells positive for endoglin (CD105), PECAM-1 (CD31), and VEGF receptor-2 (flk-1) and pericytes positive for PDGF β-receptor. In the wild type mouse retina, the profusion of abnormal vascular protrusions beyond the inner limiting retinal membrane is readily apparent (outlined area in Figure 1b). By contrast, relatively few ectopic vessels are present in the NG2 null retina after parallel hypoxic induction (Figure 1a). The enlargement and morphological distortion of the hypoxic wild type retina are reproducible phenomena caused by edema due to leakage of fluid from the extensive pathological neovasculature. Edema is not apparent in the hypoxic NG2 null retina, presumably due to the relative scarcity of pathological vessels.

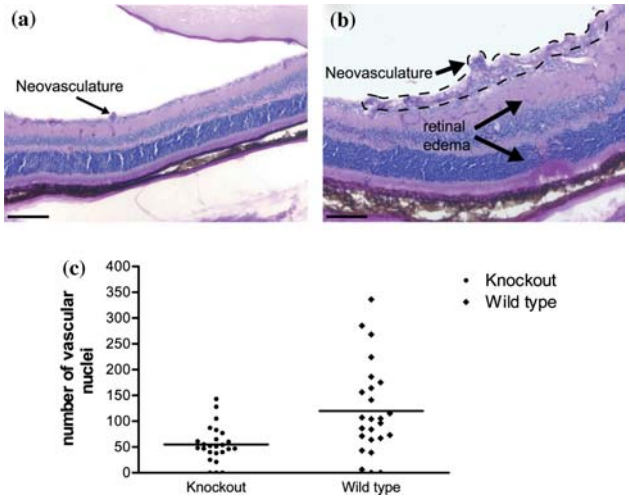

Figure 1. Ischemic retinal neovascularization. Sections of NG2 null (a) and wild type (b) retinas from the ischemia protocol were examined at P17 after PAS/hematoxylin staining. In the wild type retina there is a profusion of vascular tufts protruding past the internal limiting membrane into the vitreous (area enclosed by dashed line). These ectopic vessels are much less common in the NG2 null retina (arrow indicating neovasculature). The wild type retina is also characterized by swelling and distortion from edema caused by leakage from the extensive pathological vasculature. Bars in A and B = 50 μm. (c) Retinal sections from wild type and NG2 knockout mice subjected to the ischemia protocol were analyzed for vascular cell nuclei associated with angiogenic tufts protruding into the vitreous. The number of ectopic vascular nuclei per section (5 mice × 5 sections per mouse = 25 sections) is shown for both genotypes to illustrate the distribution of the data. Wild type mice show a clear trend toward increased ischemic retinal angiogenesis. The average numbers of nuclei per section are shown by the solid bars through each data set (119.8 for wild types vs 54.9 for knockouts. $P = 0.0019$).

Figure 1c presents a quantitative comparison of ischemic neovascularization in the wild type and NG2 null retinas. Each of the data points represents the number of ectopic vascular nuclei (endothelial cells plus pericytes) counted in one of the 25 wild type and 25 knockout slides selected by systematic random sampling from the two sets of serial retinal sections. It is immediately apparent that wild type retinas have an increased tendency towards larger numbers of ectopic vascular nuclei. The averages for the entire data set are 119.8 nuclei per wild type section vs. 54.9 nuclei per NG2 null section (statistically significant by the Mann–Whitney test, $P = 0.0019$). Genetic ablation (intrinsic targeting) of NG2 therefore diminishes the angiogenic response of retinal vasculature to a hypoxic stimulus.

The results of a separate experiment designed to evaluate BrdU labeling suggest that cell proliferation offers at least a partial explanation for the observed difference between the responses of the wild type and NG2 null retinas to hypoxia. In this trial, pathological vascular tufts were again more numerous in wild type than in knockout retinas, confirming the results shown in Figure 1. In addition, BrdU-labeled nuclei were seen more frequently in wild type angiogenic sprouts than in NG2 null counterparts. Double-labeling of hematoxylin-stained sections for BrdU and the pericyte marker PDGF β-receptor allowed us to determine mitotic indices for pericytes in wild type and NG2 null angiogenic tufts. We have previously demonstrated the specific expression of PDGF β-receptor by pericytes in hypoxic retinal tufts [18]. This analysis revealed a large decrease in pericyte proliferation in the ischemic knockout retina. Figure 2a shows that 45.2% of pericytes in angiogenic tufts are labeled with BrdU in the ischemic wild type retina vs. 18.7 % of pericytes in the knockout retina (statistically significant, $P = 0.0068$ Mann–Whitney test). Counting BrdU-positive nuclei in PDGF β-receptor-negative cells also allowed us to compare mitotic indices for endothelial cells. Interestingly, 38.3% of endothelial cells are BrdU-positive in the wild type retina, vs. 22.8% in the NG2 null retina ($P = 0.0147$ Mann–Whitney test).

The validity of these results was confirmed in a separate set of experiments in which BrdU-positive nuclei were counted in conjunction with staining with the endothelial antibody cocktail to identify endothelial cells. The mitotic indices for both endothelial cells and pericytes were reduced in NG2 null retinas. Both types of labeling paradigms (endothelial cocktail and PDGF β-receptor) therefore demonstrate a reduction in proliferation of pericytes and endothelial cells in the NG2 null retina. Reduced proliferation of these cell populations is likely to be an important factor in the sub-normal angiogenic response of the NG2 null retina to hypoxia.

We have previously demonstrated in wild type mice that the extensive investment of ischemic retinal vessels by NG2-positive, PDGF β-receptor-positive pericytes is comparable to the high pericyte:endothelial cell (P/E) ratio normally seen in the central nervous system [18, 19]. An additional important distinction between pathological vessels in the wild type and NG2 null retinas is the relative scarcity of pericytes relative to endothelial cells in the knockout neovasculature. Determination of the respective numbers of pericyte and endothelial cell nuclei associated with the angiogenic tufts allows us to determine the pericyte to endothelial cell investment ratio in these clusters of vessels (Figure 2b). In wild type neovasculature the P/E investment ratio is 0.86 (i.e. close to one pericyte per endothelial cell), while in the knockout retina the P/E value falls to 0.24 (only one pericyte for every four endothelial cells) ($P = 0.0011$ Mann–Whitney test). The observation that pericyte proliferation is more adversely affected than endothelial cell proliferation in knockout retinas may partially account for this difference in P/E investment ratios.

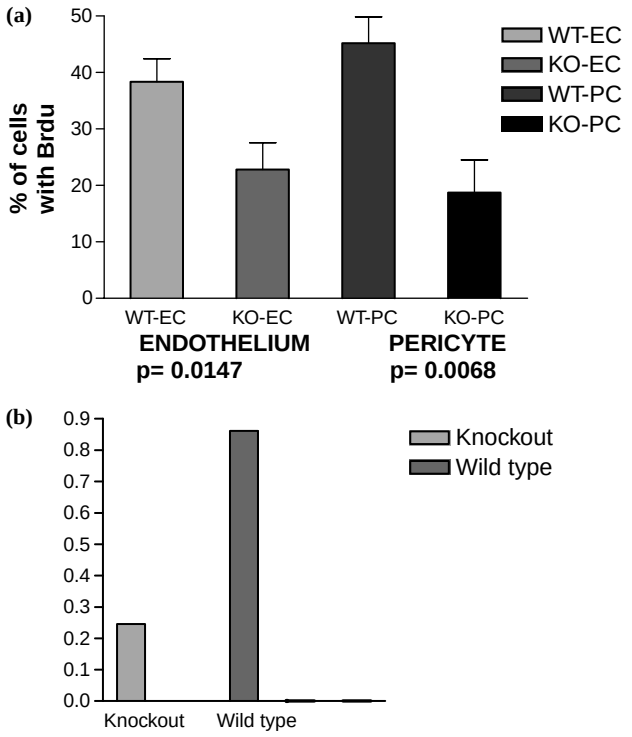

Figure 2. Pericyte/endothelial cell mitotic indices and investment ratios. (a) By combining hematoxylin counter-staining with double staining for PDGF β-receptor and BrdU, we were able to calculate the mitotic index for pericytes and endothelial cells associated with vascular tufts. The number of BrdU-positive pericyte nuclei divided by the total number of hematoxylin-stained pericyte nuclei $\times$ 100 = the percentage of mitotic pericytes. Thus, 45.2% of pericytes are BrdU-positive in the wild type retina (WT-PC) vs. only 18.7% in the knockout retina (KO-PC) ($P = 0.0068$). Total and BrdU-positive nuclei were also counted in PDGF β-receptor negative cells to provide endothelial cell data. In the wild type retina 38.3% of endothelial cells are BrdU-positive (WT-EC), compared to 22.8% in the NG2 null retina (KO-EC) ($P = 0.0147$). (b) The data used to construct (a) were also used to determine the pericyte/endothelial cell investment ratio in ischemic vascular tufts (total number of pericyte nuclei/total number of endothelial cell nuclei). For wild type retinas this ratio was almost one pericyte per endothelial cell (0.86), while in NG2 null retinas the ratio fell to 0.24 ($P = 0.0011$). The high ratio of pericytes to endothelial cells in the wild type retina is characteristic of microvasculature in the central nervous system.

It has been shown that an early step in the angiogenic response of the retinal vasculature to withdrawal from hyperoxia is up-regulation of the HIF-1 transcription factor. HIF-1 plays a critical role in the induction of VEGF expression and subsequent steps in the angiogenic process [44]. Immunostaining for the HIF-1α subunit was used to

evaluate this initial response of wild type and NG2 null retinas to hypoxia. Very low HIF-1α levels were observed in control retinas from P13 wild type and knockout mice. In contrast, 16 h after removal of experimental P13 pups from 75% oxygen, HIF-1α was up-regulated in similar fashion in the inner layers of both the wild type and NG2 null retinas (data not shown). Differences in pathological retinal neovascularization between the two genotypes therefore are not due to the initial response of retinal cells to hypoxia, but to subsequent neovascularization events downstream of HIF-1α expression.

Corneal angiogenesis is reduced by both intrinsic and extrinsic targeting of NG2

Implantation of a bFGF-containing pellet along with a control PBS-containing pellet induces a robust angiogenic response in the wild type mouse cornea (Figure 3a). We have shown that these corneal microvessels are richly invested by NG2-positive, PDGF β-receptor-positive pericytes [18]. If the second pellet contains anti-NG2 antibody instead of PBS, the angiogenic response to bFGF is substantially reduced (Figure 3b). A diminished response to bFGF is also observed in the NG2 null cornea (Figure 3c). These qualitative observations were quantified by measuring the extent of the vascularized areas in each of the three experimental situations (Figure 3d). The mean area of corneal neovascularization was 0.3863 mm^2 in the control group of wild type mice ($n = 10$), compared with 0.087 mm^2 in the NG2 knockout animals ($n = 13$). In the presence of an NG2 antibody-containing pellet, corneal vascularization in wild type mice was reduced to 0.1445 mm^2 ($n = 10$). Both of these differences were statistically significant ($P = 0.0006$ for wild type mice vs. knockout mice, and 0.0039 for control wild type mice vs. antibody treated wild type mice). Thus both intrinsic (genetic ablation) and extrinsic (antibody blocking) targeting of NG2 result in diminished corneal angiogenesis.

Discussion

Since the cellular processes underlying neovascular sprout formation remain incompletely understood [45, 46], increased attention to pericytes and their interaction with endothelial cells will be required not only to attain a better understanding of neovascularization in general, but also to realize the full potential of anti-angiogenic therapy. The critical contribution of pericytes during angiogenesis has been well established by observation of the pathological phenotypes of mice in which pericyte development is blocked [11, 13, 47]. The functional importance of pericytes has been attributed largely to their ability to stabilize and provide structural support to pre-existing endothelial tubes. They are thought to accomplish this by controlling endothelial cell proliferation and motility, and by contributing to the establishment of a permeability barrier and the regulation of blood flow [36, 48–53]. However, it is now becoming clear that pericytes can play a much earlier role in microvascular development than previously realized. The use of NG2 and other markers for nascent pericytes has revealed the participation of these cells in the earliest stages of angiogenesis [6, 36, 16–20, 53–56]. Pericytes may even be important for the stimulation and guidance of nascent vascular tubes. Strategies for targeting pericytes may therefore be able to affect not only existing vessels, but also the formation of new vessels.

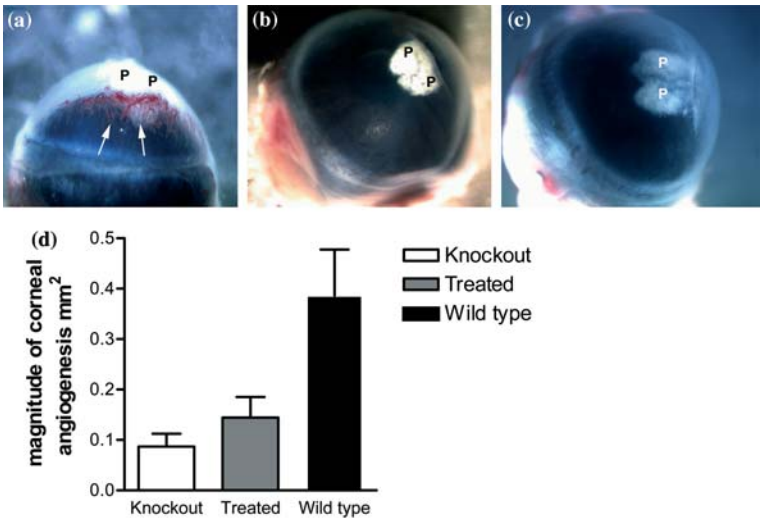

Figure 3. Corneal angiogenesis. Corneal angiogenesis was compared in wild type corneas implanted with a bFGF-containing pellet and a PBS-containing pellet (a), wild type corneas implanted with a bFGF-containing pellet and an NG2 antibody-containing pellet (b), and NG2 null corneas implanted with a bFGF-containing pellet and a PBS-containing pellet (c). Pellets are labeled with the letter P. Invasion of the cornea by new blood vessels in response to bFGF (arrows in a) is greatly reduced in the knockout mouse and by the presence of antibody against NG2 in the wild type mouse. (d) The angiogenic responses shown in (a–c) were quantified by measurement of the area (in mm^2) occupied by new vasculature. Compared to bFGF-induced vascularization of the wild type mouse cornea, vascularization of the NG2 null cornea is reduced by a factor of 4.4 ($P = 0.0006$). Vascularization of the wild type cornea is reduced by a factor of 2.7 by inclusion of anti-NG2 antibody to inhibit invading pericytes ($P = 0.0039$).

Our current studies show that intrinsic targeting of NG2 (by genetic ablation) leads to decreased ischemic angiogenesis in the mouse retina in response to hypoxia. The wild type mouse retina contains more than twice as many pathological vascular tufts as the retina of the NG2 null mouse. Since HIF-1α induction is similar in wild type and knockout retinas, we know that the defect in the null mouse lies not in the initial response of retinal cells to hypoxia, but probably in later stages of vascular cell responsiveness to HIF-1-induced factors such as VEGF. This seems reasonable in light of the fact that NG2 is not expressed by cells of the retina per se, but instead by pericytes in the microvasculature [17–19].

A major factor in the sub-normal angiogenic response of the NG2 null retina appears to be reduced vascular cell proliferation. Only 41% as many mitotic pericytes are present in the ischemic vasculature of the NG2 null retina as in the wild type retina. These data represent the first direct *in vivo* evidence in support of a role for NG2 in cell proliferation. The ability of NG2 to sequester growth factors such as bFGF and PDGF-AA and possibly assist in presentation of these factors to their respective signaling receptors could represent one mechanism by which the proteoglycan promotes cell proliferation [21, 28].

Interestingly, the absence of NG2 and the decreased number of mitotic pericytes is accompanied by a 1.7-fold decrease in the number of mitotic endothelial cells, suggestive of a stimulatory effect of pericytes on endothelial cell proliferation. This idea is somewhat at odds with previous reports that pericytes can inhibit endothelial cell proliferation in cell culture models [48] and that the absence of pericytes is accompanied by endothelial cell hyperplasia *in vivo* [11]. However, the pericyte/endothelial cell relationship is a complex, dynamic one that is likely to vary depending on the specific model under investigation. An excellent example of this is provided by a recent study of the proliferative retinopathy that results from endothelial cell-specific ablation of PDGF-B [47]. The general conclusion from this work was that reduction of pericyte density below 50% of normal, invariably led to the development of proliferative retinopathy. Nevertheless, localized instances were also encountered in the same investigation [47] in which increased pericyte density promoted the formation of chaotic, endothelial cell-rich vasculature, demonstrating that under certain conditions pericytes can have pro-angiogenic properties. The ability to use pericytes as effective anti-angiogenic targets also is suggestive of the pro-angiogenic nature of these cells [9, 10].

Our current data support a pro-angiogenic role for pericytes in the formation of ischemic retinal microvessels. Our results with wild type mice show that endothelial cells are richly invested by NG2-positive, PDGF β-receptor-positive pericytes in this pathological vasculature (see also [18]). Coupled with our documentation of the early participation of NG2-positive pericytes during neovascularization [17], these observations suggest the possibility that pericyte-derived factors or NG2-dependent sequestration of growth factors might act to promote the proliferation of endothelial cells. Alternatively, the ability of NG2 to neutralize the growth-inhibitory effects of angiostatin [22, 57] may promote endothelial cell proliferation in the wild type mouse, an effect that would be absent in the NG2 null mouse.

In addition to the quantitative reduction of ischemic angiogenesis in the NG2 knockout mouse, capillaries in the null mouse also have an altered cellular composition. The pericyte:endothelial cell investment ratio in ischemic vessels of the wild type retina is 0.86, or almost one pericyte per endothelial cell. This high investment ratio is characteristic of capillaries in the central nervous system in general, and the retina in particular, possibly contributing to the integrity of the blood–brain barrier and the high metabolic needs of neural tissues [5, 36]. This investment ratio falls to 0.24 in the ischemic neovasculature of the NG2 null retina. The relative changes in pericyte and endothelial cell proliferation in the NG2 knockout mouse would not appear to account for the magnitude of this decrease. Thus other factors that we have not yet investigated, such as decreased cell motility or increased apoptosis, may contribute to the large decrease in pericyte number relative to that of endothelial cells. While a specific role for NG2 in apoptosis has not been explored, there are numerous indications of NG2 involvement in cytoskeletal reorganization and cell motility [23–28]. In future work it will therefore be important for us to investigate the impact of NG2 on these processes in the context of neovascularization.

Intrinsic targeting of NG2 by genetic ablation leads to an even more pronounced decrease in bFGF-induced corneal angiogenesis. Neovasculature covers a 4.4-fold greater surface area in the wild type cornea than in the NG2 null cornea, once again supporting the idea that NG2 plays a role in pericyte development and/or function, and in the development of new vasculature. Interestingly, extrinsic targeting of NG2 through the use of a neutralizing antibody also produces a significant decrease in corneal angiogenesis (2.7-fold). While our data do not allow us to determine which aspects of pericyte function are blocked by the antibody, previous studies have shown that anti-NG2 antibodies are capable of blocking growth factor-induced cell proliferation [58] and both growth factor-induced and extracellular matrix-induced cell motility [27, 59] in cell culture models.

Our demonstration of the functional importance of NG2 during pathological ocular angiogenesis logically raises the question of the proteoglycan's function during normal developmental neovascularization. How can we rationalize the observation that the NG2 knockout mouse possesses functional vasculature? More than one answer is possible. First, pathological angiogenesis may differ in some respects from normal angiogenesis. During pathological angiogenesis, the vasculature may be responding to combinations of signals that are not normally experienced during development or else are occurring out of their normal sequence (multiple factors released by tumor cells would be a good example). The role of NG2 may be magnified under these abnormal circumstances. Additional experiments with wild type and NG2 knockout mice are planned in order to examine NG2-dependent aspects of angiogenesis in other types of pathological models such as tumor progression and

wound healing. Second, both of our pathological angiogenesis models have utilized postnatal animals, whereas the bulk of developmental neovascularization takes place during embryogenesis. It seems possible that embryonic development involves a higher degree of plasticity than events that occur postnatally. In other words, the ability to compensate for the loss of NG2 may be greater during embryogenesis. In response to postnatal challenges, such compensatory mechanisms may not be available, thus facilitating our ability to detect the contribution of NG2. Examination of normal angiogenic events that occur postnatally (for example in normal retinal development) may therefore reveal the effects of NG2 ablation. It has required detailed and careful experimentation to detect changes in pathological retinal and corneal angiogenesis in the NG2 null mouse. The same type of painstaking analysis may be required to detect subtle deficiencies in developmental neovascularization in the knockout mouse. Such studies remain to be undertaken, but in light of our current results would appear to offer great promise.

Acknowledgements

This work has been supported by grants from NIH (National Institute Of Child Health and Human Development) RO3 HD044783, the US Department of Defense Prostate Cancer Research Program PC020822 and, Tobacco-Related Disease Research Program (TRDRP 13IT-0067) to Dr Ozerdem, and by NIH Grant RO1 CA95287 to Dr Stallcup.

References

1. Folkman J. Angiogenesis in cancer, vascular, rheumatoid and other disease. Nat Med 1995; 1(1): 27–31.
2. Risau W. Mechanisms of angiogenesis. Nature 1997; 386(6626): 671–4.
3. Neumann E, Frithz A. Capillaropathy and capillaroneogenesis in the pathogenesis of rosacea. Int J Dermatol 1998; 37(4): 263–6.
4. Campochiaro PA. Retinal and choroidal neovascularization. J Cell Physiol 2000; 184(3): 301–10.
5. Sims DE. Recent advances in pericyte biology – implications for health and disease. Can J Cardiol 1991; 7(10): 431–43.
6. Nehls V, Denzer K, Drenckhahn D. Pericyte involvement in capillary sprouting during angiogenesis in situ. Cell Tissue Res 1992; 270(3): 469–74.
7. Sims DE. Diversity within pericytes. Clin Exp Pharmacol Physiol 2000; 27(10): 842–6.
8. Allt G, Lawrenson JG. Pericytes: Cell biology and pathology. Cells Tissues Organs 2001; 169(1): 1–11.
9. Bergers G, Song S, Meyer-Morse N et al. Benefits of targeting both pericytes and endothelial cells in the tumor vasculature with kinase inhibitors. J Clin Invest 2003; 111(9): 1287–95.
10. Saharinen P, Alitalo K. Double target for tumor mass destruction. J Clin Invest 2003; 111(9): 1277–80.
11. Hellstrom M, Gerhardt H, Kalen M et al. Lack of pericytes leads to endothelial hyperplasia and abnormal vascular morphogenesis. J Cell Biol 2001; 153(3): 543–53.
12. Abramsson A, Berlin O, Papayan H et al. Analysis of mural cell recruitment to tumor vessels. Circulation 2002; 105(1): 112–7.
13. Lindahl P, Johansson BR, Leveen P, Betsholtz C. Pericyte loss and microaneurysm formation in PDGF-B-deficient mice. Science 1997; 277(5323): 242–5.
14. Folkman J, D'Amore PA. Blood vessel formation: What is its molecular basis? Cell 1996; 87(7): 1153–5.
15. Beck L, Jr., D'Amore PA. Vascular development: Cellular and molecular regulation. Faseb J 1997; 11(5): 365–73.
16. Schlingemann RO, Rietveld FJ, de Waal RM et al. Expression of the high molecular weight melanoma-associated antigen by pericytes during angiogenesis in tumors and in healing wounds. Am J Pathol 1990; 136(6): 1393–405.
17. Ozerdem U, Stallcup WB. Early contribution of pericytes to angiogenic sprouting and tube formation. Angiogenesis 2003; 6(3): 241–249.
18. Ozerdem U, Monosov E, Stallcup WB. NG2 proteoglycan expression by pericytes in pathological microvasculature. Microvasc Res 2002; 63(1): 129–34.
19. Ozerdem U, Grako KA, Dahlin-Huppe K et al. NG2 proteoglycan is expressed exclusively by mural cells during vascular morphogenesis. Dev Dyn 2001; 222(2): 218–27.
20. Rajantie I, Ilmonen M, Aluminaite A et al. Adult bone marrow-derived cells recruited during angiogenesis comprise precursors for periendothelial vascular mural cells. Blood 2004; 104(7): 2084–86.
21. Goretzki L, Burg MA, Grako KA, Stallcup WB. High-affinity binding of basic fibroblast growth factor and platelet-derived growth factor-AA to the core protein of the NG2 proteoglycan. J Biol Chem 1999; 274(24): 16831–7.
22. Goretzki L, Lombardo CR, Stallcup WB. Binding of the NG2 proteoglycan to kringle domains modulates the functional properties of angiostatin and plasmin(ogen). J Biol Chem 2000; 275(37): 28625–33.
23. Majumdar M, Vuori K, Stallcup WB. Engagement of the NG2 proteoglycan triggers cell spreading via rac and p130cas. Cell Signal 2003; 15(1): 79–84.
24. Tillet E, Gential B, Garrone R, Stallcup WB. NG2 proteoglycan mediates beta1 integrin-independent cell adhesion and spreading on collagen VI. J Cell Biochem 2002; 86(4): 726–36.
25. Stallcup WB, Dahlin-Huppe K. Chondroitin sulfate and cytoplasmic domain-dependent membrane targeting of the NG2 proteoglycan promotes retraction fiber formation and cell polarization. J Cell Sci 2001; 114(Pt 12): 2315–25.
26. Fang X, Burg MA, Barritt D et al. Cytoskeletal reorganization induced by engagement of the NG2 proteoglycan leads to cell spreading and migration. Mol Biol Cell 1999; 10(10): 3373–87.
27. Burg MA, Nishiyama A, Stallcup WB. A central segment of the NG2 proteoglycan is critical for the ability of glioma cells to bind and migrate toward type VI collagen. Exp Cell Res 1997; 235(1): 254–64.
28. Grako KA, Ochiya T, Barritt D et al. PDGF (alpha)-receptor is unresponsive to PDGF-AA in aortic smooth muscle cells from the NG2 knockout mouse. J Cell Sci 1999; 112(Pt 6): 905–15.
29. Mansour SL, Thomas KR, Capecchi MR. Disruption of the proto-oncogene int-2 in mouse embryo-derived stem cells: a general strategy for targeting mutations to non-selectable genes. Nature 1988; 336(6197): 348–52.
30. Capecchi MR. Altering the genome by homologous recombination. Science 1989; 244(4910): 1288–92.
31. Smith LE, Wesolowski E, McLellan A et al. Oxygen-induced retinopathy in the mouse. Invest Ophthalmol Vis Sci 1994; 35(1): 101–11.
32. Dawson B, Trapp RG. Basic and Clinical Biostatistics, 3rd edition, New York: McGraw-Hill 2001.
33. Kenyon BM, Voest EE, Chen CC et al. A model of angiogenesis in the mouse cornea. Invest Ophthalmol Vis Sci 1996; 37(8): 1625–32.
34. Kenyon BM, Browne F, D'Amato RJ. Effects of thalidomide and related metabolites in a mouse corneal model of neovascularization. Exp Eye Res 1997; 64(6): 971–8.
35. Sundberg C, Ljungstrom M, Lindmark G et al. Microvascular pericytes express platelet-derived growth factor-beta receptors in human healing wounds and colorectal adenocarcinoma. Am J Pathol 1993; 143(5): 1377–88.
36. Gerhardt H, Betsholtz C. Endothelial–pericyte interactions in angiogenesis. Cell Tissue Res 2003; 314(1): 15–23.
37. McDonald DM, Choyke PL. Imaging of angiogenesis: from microscope to clinic. Nat Med 2003; 9(6): 713–25.

38. Drake CJ, Fleming PA. Vasculogenesis in the day 6.5 to 9.5 mouse embryo. Blood 2000; 95(5): 1671–9.
39. Chang YS, di Tomaso E, McDonald DM et al. Mosaic blood vessels in tumors: frequency of cancer cells in contact with flowing blood. Proc Natl Acad Sci USA 2000; 97(26): 14608–13.
40. Dolbeare F, Gratzner H, Pallavicini MG, Gray JW. Flow cytometric measurement of total DNA content and incorporated bromodeoxyuridine. Proc Natl Acad Sci USA 1983; 80(18): 5573–7.
41. Dean PN, Dolbeare F, Gratzner H et al. Cell-cycle analysis using a monoclonal antibody to BrdUrd. Cell Tissue Kinet 1984; 17(4): 427–36.
42. Nowakowski RS, Lewin SB, Miller MW. Bromodeoxyuridine immunohistochemical determination of the lengths of the cell cycle and the DNA-synthetic phase for an anatomically defined population. J Neurocytol 1989; 18(3): 311–8.
43. Ezaki T, Baluk P, Thurston G et al. Time course of endothelial cell proliferation and microvascular remodeling in chronic inflammation. Am J Pathol 2001; 158(6): 2043–55.
44. Ozaki H, Yu AY, Della N et al. Hypoxia inducible factor-1alpha is increased in ischemic retina: Temporal and spatial correlation with VEGF expression. Invest Ophthalmol Vis Sci 1999; 40(1): 182–9.
45. Bergers G, Benjamin LE. Tumorigenesis and the angiogenic switch. Nat Rev Cancer 2003; 3(6): 401–10.
46. Darland DC, D'Amore PA. Blood vessel maturation: Vascular development comes of age. J Clin Invest 1999; 103(2): 157–8.
47. Enge M, Bjarnegard M, Gerhardt H et al. Endothelium-specific platelet-derived growth factor-B ablation mimics diabetic retinopathy. Embo J 2002; 21(16): 4307–16.
48. Orlidge A, D'Amore PA. Inhibition of capillary endothelial cell growth by pericytes and smooth muscle cells. J Cell Biol 1987; 105(3): 1455–62.
49. Shepro D, Morel NM. Pericyte physiology. Faseb J 1993; 7(11): 1031–8.
50. Sato Y, Rifkin DB. Inhibition of endothelial cell movement by pericytes and smooth muscle cells: Activation of a latent transforming growth factor-beta 1-like molecule by plasmin during co-culture. J Cell Biol 1989; 109(1): 309–15.
51. Benjamin LE, Hemo I, Keshet E. A plasticity window for blood vessel remodelling is defined by pericyte coverage of the preformed endothelial network and is regulated by PDGF-B and VEGF. Development 1998; 125(9): 1591–8.
52. Hirschi KK, Rohovsky SA, Beck LH et al. Endothelial cells modulate the proliferation of mural cell precursors via platelet-derived growth factor-BB and heterotypic cell contact. Circ Res 1999; 84(3): 298–305.
53. Wesseling P, Schlingemann RO, Rietveld FJ et al. Early and extensive contribution of pericytes/vascular smooth muscle cells to microvascular proliferation in glioblastoma multiforme: An immuno-light and immuno-electron microscopic study. J Neuropathol Exp Neurol 1995; 54(3): 304–10.
54. Schlingemann RO, Oosterwijk E, Wesseling P et al. Aminopeptidase a is a constituent of activated pericytes in angiogenesis. J Pathol 1996; 179(4): 436–42.
55. Amselgruber WM, Schafer M, Sinowatz F. Angiogenesis in the bovine corpus luteum: An immunocytochemical and ultrastructural study. Anat Histol Embryol 1999; 28(3): 157–66.
56. Redmer DA, Doraiswamy V, Bortnem BJ et al. Evidence for a role of capillary pericytes in vascular growth of the developing ovine corpus luteum. Biol Reprod 2001; 65(3): 879–89.
57. Chekenya M, Enger PO, Thorsen F et al. The glial precursor proteoglycan, NG2, is expressed on tumour neovasculature by vascular pericytes in human malignant brain tumours. Neuropathol Appl Neurobiol 2002; 28(5): 367–80.
58. Nishiyama A, Lin XH, Giese N et al. Co-localization of NG2 proteoglycan and PDGF alpha-receptor on O2A progenitor cells in the developing rat brain. J Neurosci Res 1996; 43(3): 299–314.
59. Grako KA, Stallcup WB. Participation of the NG2 proteoglycan in rat aortic smooth muscle cell responses to platelet-derived growth factor. Exp Cell Res 1995; 221(1): 231–40.